

ACTA MYOLOGICA

(Myopathies, Cardiomyopathies and Neuromyopathies)

Vol. XXXVII - September 2018

Official Journal of
Mediterranean Society of Myology
and
Associazione Italiana di Miologia

Founders: Giovanni Nigro and Lucia Ines Comi

Three-monthly

EDITOR-IN-CHIEF

Luisa Politano

ASSISTANT EDITOR

Vincenzo Nigro

CO-EDITORS

Valerie Askanas

Giuseppe Novelli

Lefkos Middleton

Reinhardt Rüdel



Established in 1982 as *Cardiomyology*

ACTA MYOLOGICA

(Myopathies, Cardiomyopathies and Neuromyopathies)

Official Journal of
Mediterranean Society of Myology
and
Associazione Italiana di Miologia

Founders: Giovanni Nigro and Lucia Ines Comi

Three-monthly

EDITORIAL BOARD

Corrado Angelini, Padova
Enrico Bertini, Roma
Serge Braun, Paris
Kevin P. Campbell, Iowa City
Marinos Dalakas, Athens
Feza Deymeer, Istanbul
Salvatore Di Mauro, New York
Denis Duboc, Paris
Victor Dubowitz, London
Massimiliano Filosto, Brescia
Fayçal Hentati, Tunis
Michelangelo Mancuso, Pisa
Giovanni Meola, Milano
Eugenio Mercuri, Roma
Carlo Minetti, Genova
Clemens Müller, Würzburg
Francesco Muntoni, London

Carmen Navarro, Vigo
Luís Negrão, Coimbra
Gerardo Nigro, Napoli
Anders Oldfors, Göteborg
Elena Pegoraro, Padova
Heinz Reichmann, Dresden
Filippo Maria Santorelli, Pisa
Serenella Servidei, Roma
Piraye Serdaroglu, Istanbul
Yeuda Shapira, Jerusalem
Osman I. Sinanovic, Tuzla
Michael Sinnreich, Montreal
Andoni J. Urtizberea, Hendaye
Gert-Jan van Ommen, Leiden
Steve Wilton, Perth
Massimo Zeviani, London
Janez Zidar, Ljubljana



EDITOR-IN-CHIEF

Luisa Politano, Napoli

ASSISTANT EDITOR

Vincenzo Nigro, Napoli

EDITORIAL STAFF

Chiara Fiorillo

Lorenzo Maggi

Giulia Ricci

Vincenzo Russo

CO-EDITORS

Lefkos Middleton, Nicosia

Giuseppe Novelli, Roma

Reinhardt Rüdell, Ulm

Gabriele Siciliano, Pisa

Haluk Topaloglu, Ankara

Antonio Toscano, Messina

BOARD OF THE MEDITERRANEAN SOCIETY OF MYOLOGY

V. Nigro, *President*

H. Topaloglu, *Past President*

L.T. Middleton, G. Siciliano, *Vice Presidents*

K. Christodoulou, *Secretary*

L. Politano, *Treasurer*

E. Abdel-Salam, M. Dalakas, F. Deymeer, F. Hentati, G. Meola, Y. Shapira, E. Tizzano, A. Toscano,

J. Zidar

Co-opted Members: V. Askanas, S. Di Mauro, R. Rüdell

Acta Myologica publishes 4 issues per year in March, June, September, December. The Journal is available in OPEN ACCESS at: www.actamyologica.it

Acta Myologica is cited in Index Medicus/MEDLINE, Medicine, Excerpta Medica Database (EMBASE), Index Copernicus and monitored for coverage in Chemical Abstracts Service. The Journal is available on PubMed Central (<http://www.ncbi.nlm.nih.gov/pmc/journals/1221/>).

All correspondence should be addressed to: Mediterranean Society of Myology - Cardiomyology and Medical Genetics - Primo Policlinico - Piazza Miraglia - 80138 Naples, Italy - Tel. +39 081 566 5300 - Fax +39 081 566 5101.

Editor in Chief: Luisa Politano

Tribunal Authorization, Napoli N. 3827, January 10, 1989 - Journal registered at "Registro pubblico degli Operatori della Comunicazione" (Pacini Editore srl registration n. 6269 - 29/8/2001).

The editor remains at the complete disposal of those with rights whom it was impossible to contact, and for any omissions.

© 1981 Gaetano Conte Academy. All rights reserved.

The Journal and the individual contributions contained in it are protected by the copyright of Gaetano Conte Academy and the following terms and conditions apply to their use:

Photocopies, for personal use, are permitted within the limits of 15% of each publication by following payment to SIAE of the charge due, article 68, paragraphs 4 and 5 of the Law April 22, 1941, No 633.

Reproductions for professional or commercial use or for any other other purpose other than personal use can be made following a written request and specific authorization in writing from AIDRO, Corso di Porta Romana, 108, 20122 Milan, Italy, E-mail: segreteria@aidro.org and web site: www.aidro.org.

Publisher

Pacini
Editore

Via A. Gherardesca - 56121 Pisa, Italy

Published by Pacini Editore Srl, Pisa, Italy, November 2018

CONTENTS

ORIGINAL ARTICLES

- Kir2.2 p.Thr140Met: a genetic susceptibility to sporadic periodic paralysis*
Chunxiang Fan, Marius Kuhn, Alexander Pepler MBiol, James Groome, Vern Winston, Saskia Biskup, Frank Lehmann-Horn and Karin Jurkat-Rott 193
- Prevalence of metabolic syndrome and non-alcoholic fatty liver disease in a cohort of Italian patients with spinal-bulbar muscular atrophy*
Francesco Francini-Pesenti, Giorgia Querin, Cristina Martini, Sara Mareso and David Sacerdoti 204
- Childhood onset limb-girdle muscular dystrophies in Aegean part of Turkey*
Uluç Yiş, Gülten Diniz, Filiz Hazan, Hülya Sevcan Daimagüler, Bahar Toklu Baysal, Figen Baydan, Gülçin Akinci, Ayca Ünalp, Gül Aktan, Erhan Bayram, Semra Hiz, Cem Paketçi, Derya Okur, Erdener Özer, Ayça Ersen Danyeli, Muzaffer Polat, Gökhan Uyanik and Sebahattin Çirak 210
- LGMD1D myopathy with cytoplasmic and nuclear inclusions in a Saudi family due to DNAJB6 mutation*
Saeed A Bohlega, Sarah Alfawaz, Hussam Abou-Al-Shaar, Hindi N. Al-Hindi, Hatem N. Murad, Mohamed S. Bohlega, Brian F. Meyer and Dorota Monies 221

CASE REPORT

- Myotonic dystrophy type 1 and pulmonary embolism: successful thrombus resolution with dabigatran etexilate therapy*
Emanuele Gallinoro, Andrea Antonio Papa, Anna Rago, Simona Sperlongano, Antonio Cassese, Nadia Della Cioppa, Maria Cristina Giada Magliocca, Giovanni Cimmino, Paolo Golino 227

OBITUARY

- Professor Frank Lehmann-Horn (1948-2018)*
Reinhardt Rüdell 232

NEWS FROM AROUND THE WORLD

- AIM 233
MSM 234
WMS 235

FORTHCOMING MEETINGS 236

- Instructions for Authors 240

ORIGINAL ARTICLES

Kir2.2 p.Thr140Met: a genetic susceptibility to sporadic periodic paralysis

CHUNXIANG FAN^{1*}, MARIUS KUHN^{2*}, ALEXANDER PEPLER MBIOL³, JAMES GROOME⁴, VERN WINSTON⁴, SASKIA BISKUP³, FRANK LEHMANN-HORN^{1**} AND KARIN JURKAT-ROTT¹

¹Division of Neurophysiology, Ulm University, Germany; ²Genetikum, Neu-Ulm, Germany; ³CeGaT GmbH, Tübingen, Germany; ⁴Department of Biological Sciences, Idaho State University, Pocatello, USA

Introduction. Periodic paralyses (PP) are recurrent episodes of flaccid limb muscle weakness. Next to autosomal dominant forms, sporadic PP (SPP) cases are known but their genetics are unclear.

Methods. In a patient with hypokalemic SPP, we performed exome sequencing to identify a candidate gene. We sequenced this gene in 263 unrelated PP patients without any known causative mutations. Then we performed functional analysis of all variants found and molecular modelling for interpretation.

Results. Exome sequencing in the proband yielded three heterozygous variants predicted to be linked to disease. These encoded p.Thr140Met in the Kir2.2 potassium channel, p.Asp229Asn in protein kinase C theta, and p.Thr15943Ile in titin. Since all hitherto known causative PP genes code for ion channels, we studied the Kir2.2-encoding gene, *KCNJ12*, for involvement in PP pathogenesis. *KCNJ12* screening in 263 PP patients revealed three further variants, each in a single individual and coding for p.Gly419Ser, p.Cys75Tyr, and p.Ile283Val. All four Kir2.2 variants were functionally expressed. Only p.Thr140Met displayed relevant functional alterations, i.e. homo-tetrameric channels produced almost no current, and hetero-tetrameric channels suppressed co-expressed wildtype Kir2.1 in a dominant-negative manner. Molecular modelling showed Kir2.2 p.Thr140Met to reduce movement of potassium ions towards binding sites in the hetero-tetramer pore compatible with a reduced maximal current. MD simulations revealed loss of hydrogen bonding with the p.Thr140Met substitution.

Discussion. The electrophysiological findings of p.Thr140Met are similar to those found in thyrotoxic PP caused by Kir2.6 mutations. Also, the homologous Thr140 residue is mutated in Kir2.6. This supports the idea that Kir2.2 p.Thr140Met conveys susceptibility to SPP and should be included in genetic screening.

Key words: periodic paralysis, susceptibility gene, Kir2.2 channel, Kir2.1 channel, hetero-tetramer

Introduction

The periodic paralyses (PPs) are characterised by recurrent bouts of flaccid limb muscle weakness often accompanied by alteration in serum potassium level (1). PP can be divided into familial PP (FPP), thyrotoxic PP (TPP), and sporadic PP (SPP) based on relative genotype-phenotype correlations. Fully penetrant dominant mutations are observed in FPP, incomplete penetrance exacerbated by thyrotoxicosis is characteristic of TPP, and incomplete penetrance with an unknown exacerbation factor or multifactorial causes underlies SPP.

With respect to pathogenesis, PPs result from sustained muscular depolarization that abolishes action potentials (APs). Causative mutations are located in the *SCN4A* gene encoding the sodium channel Nav1.4 initiating the AP, the *CACNA1S* gene encoding the calcium channel Cav1.1 coupling the AP to contraction, or the *KCNJ2* and *KCNJ18* genes encoding the potassium channels Kir2.1 and Kir2.6 that maintain the resting potential (2). Underlying mechanisms of these mutations include i) disruption of channel inactivation of Nav1.4 resulting in persistent currents, ii) leaky S4 voltage sensor domains of Nav1.4 and Cav1.1 resulting in short-circuit inward cation currents, and iii) reduced conductance of the inwardly rectifying Kir potassium currents (2-5). The goal of our study was to look for a putative additional genetic cause in a single individual with hypokalemic SPP, an SPP form with ictal drop of serum potassium.

* Equal contribution to first author

**Dedicated to the late Prof. Dr. Frank Lehmann-Horn who faithfully contributed to this work until his death on May 8th, 2018. We hereby thank him for his constant support and his continued optimism in the research field of ion channelopathies.

Address for correspondence: Marius Kuhn, Genetikum, Wegenerstraße 15, 89231 Neu-Ulm, Germany. E-mail: Kuhn@genetikum.de

Patients and methods

Patients

Informed consent was obtained from the proband with hypokalemic PP, and was already given for an additional 263 PP patients who were referred earlier for genetic consultation. Of the latter, 29 had FPP, 25 had TPP, and 209 had SPP. Clinical diagnosis was based on patient history provided by the referring physician. PP was diagnosed if the patient had at least two episodes of flaccid quadriplegia. FPP was diagnosed if, additionally, a parent, a sibling, or an offspring of the patient were clinically affected. TPP was diagnosed if there was concomitant hyperthyroidism present, and SPP was diagnosed for isolated cases. All patients had been tested negative for known pathogenic variants in *SCN4A*, *CACNA1S*, *KCNJ2*, and *KCNJ18* genes. All procedures were approved by the Ethics Committee of Ulm University.

Exome sequencing

To determine the genetic cause of hypokalemic SPP in the proband, DNA was enriched with the SureSelectXT V5 exome kit (Agilent Technologies) and sequenced on a HiSeq 2500 Illumina sequencer. About 195 million paired reads of 100 bp length were produced. Reads were de-multiplexed with Casava version 1.8.2 (Illumina) and adapter sequences removed with Skewer version 0.1.116. Trimmed reads were mapped with Burrows-Wheeler Aligner version 0.7.2 (6) against the human reference genome hg19 (UCSC), yielding an average coverage of 155. Variant calling was performed using VarScan version 2.3.5 and Samtools version 0.1.18 (7). Calls were annotated using the Database of Single-Nucleotide Polymorphisms (dbSNP, www.ncbi.nlm.nih.gov/snp).

Variants potentially changing the protein were analysed further, i.e. non-synonymous SNPs, changes of initiation or stop codons, splicing variants, and in-frame or frameshifting insertions or deletions. Filtering was performed by excluding all variants more frequent than 0.5% as listed in dbSNP or UCSC Table Browser (www.genome.ucsc.edu) and requiring expression in skeletal muscle according to the Human Protein Atlas (320 genes, www.proteinatlas.org). The resulting variants were preliminarily interpreted using the protein prediction tools Polyphen-2 (www.genetics.bwh.harvard.edu/pph2), MutationTaster (www.mutationtaster.org), and Sift (www.sift.jcvi.org).

Sanger sequencing

To confirm the presence of the identified *KCNJ12* variant in the proband sample, the coding region of *KCNJ12*

was sequenced. Subsequently, *KCNJ12* was sequenced in the remaining 263 DNA samples to check for recurrence in PP. The coding region of *KCNJ12* was amplified using a gene-specific nested polymerase chain reaction (PCR) with two specific primers (forward: CCAGACATGCTGTCGTCTCTGTTG; reverse: GGGCCTCTCC-CAGCCG). The resulting products were sequenced using the forward-primers (CCAGACATGCTGTCGTCTCTGTTG/CTGGCGGTACATGCTGCTCATC/CGC-CGTGGTGGCCCTGCGTGAC/GCCAATGAGATCCTGTGGGGTCAC). Potential pathogenicity of the variants was preliminarily interpreted using the prediction tools Polyphen-2, Mutation Taster, and Sift. Additionally, to exclude mapping problems of the exome sequencing in the proband sample, the coding region of the known PP gene *KCNJ18* was sequenced in the proband sample using the gene-specific nested PCR technique previously described (8).

Electrophysiological study

For functional expression of the identified variants, the human *KCNJ12* subunit was sub-cloned into the pcDNA3.1 vector and site-directed mutagenesis of base changes coding for p.Thr140Met, p.Gly419Ser, p.Cys75Tyr, and p.Ile283Val variants was performed by an external lab (GATC Biotech). The human *KCNJ2* subunit was cloned into the pcDNA3.1 vector by the same external lab. Whole-cell patch clamp recordings were performed after transient transfection of human tsA201 cells with *KCNJ12* (0.2 µg) and pEGFP (0.05 µg) or, in co-expression studies, *KCNJ12* (0.1 µg) with *KCNJ2* (0.1 µg) and pEGFP (0.05 µg). Transfected cells were identified by GFP fluorescence. Potassium currents were recorded without leak subtraction after partial series resistance compensation (~85%) using an Axopatch 200B amplifier (Molecular Devices). The pipette resistance was approximately 1.5 MΩ after filling with internal solution containing (in mM): Potassium gluconate 110, KCl 20, HEPES 10, EGTA 10, MgCl₂·6H₂O 1, Na₂ATP 5, glucose 5. The external solution contained (in mM): NaCl 117, KCl 30, CaCl₂·2H₂O 2, MgCl₂·6H₂O 1, glucose 5, NaHCO₃ 2, HEPES 10. In some experiments, external KCl was reduced to 5mM and NaCl increased to 142 mM. The pH was adjusted to 7.3 and 7.4 for external and internal solutions, respectively, and osmolarity was ~300 mOsm. Data are presented as mean ± standard error of the mean (SEM). Student's t-tests were applied for statistical evaluation with significance levels set to p < 0.05.

Fluorescence imaging

To compare trafficking of wildtype channels to the p.Thr140Met variant, coding Kir2.2 regions were

sub-cloned into pEGFP vectors whereby EGFP was fused to the N-terminus of the region by an external lab (GATC Biotech). Transfected tsA cells cultured on 11 mm glass cover slips were fixed with paraffin, images were taken with fixed exposure time on an Axioskop 2 microscope with AxioCamMR3 and EC Plan-Neofluar 40x/1.30 oil lens (Zeiss), and the GFP detection was filtered as for Alexa 488. Membrane areas over the cytoplasm of the cells and background were analyzed as mean gray values with ImageJ. For quantification, background values were subtracted from the membrane values for each cell.

Molecular modelling

The crystal structure of a prokaryotic inwardly rectifying Kir channel (KirBac 3.1) was used as template for homology modelling of mammalian *KCNJ12* and *KCNJ2* (9). Clustal amino acid alignment of mammalian Kir channels encoded by *KCNJ1-15*, the *Gallus gallus* Kir2.2 channel, and KirBac3.1 channels was used in the production of homology models of human wildtype (WT) Kir2.1, WT Kir2.2, and variant p.Thr140Met Kir2.2. For these models, we used the structure file 4lp8.pdb (KirBac3.1)9 as template in MODELLER. Potassium ion coordinates were saved for the A chain in the Kir2.2 model, and tetramers of Kir2.2-Kir2.1 were constructed. Tetrameric models were then equilibrated to relieve subunit clashes and allowed to reach an energy minimum, with Chimera (10). The energy minimized tetramers were used to visualize the distribution of potassium ions with respect to the selectivity filter.

The quantitative impact of the p.Thr140Met variant was assessed with molecular dynamics (MD) simulations. Equilibrated models of KirWT2.2-KirWT2.1 or KirT140M2.2-KirWT2.1 (equimolar ratio of Kir2.2 and Kir2.1) were incorporated into POPC (1-palmitoyl 2-oleoyl-sn-glycero-3-phosphocholine) lipid bilayers, solvated with TIPW water molecules and 0.2M KCl, and equilibrated for lipid and protein minimization, using VMD (visual molecular dynamics). Simulations were run in NAMD (not another molecular dynamics) with application of a CHARMM force field with Langevin dynamics at -600 mV. Trajectories of distance between the carboxyl of Glu139 and Thr140 (WT) or Met140 (variant) were calculated using the PLUMED plug-in, and trajectories of hydrogen bonding between Glu139 and Ile144 of the selectivity filter motif (TIGYG) were calculated using the H-bonding plug-in of VMD. Hydrogen bonding between analogous pairs is a critical step in early permeation of K⁺ ions through the selectivity filter in KcsA (11).

Results

Proband phenotype

The phenotype description of the proband is based on the medical file excerpts sent by the referring physician with the patient's consent. The proband did not volunteer further information and denied additional examination and biopsy. He experienced only two documented episodes of quadriplegic weakness in his life, at age 18 and 30 years, both lasting 12 hours. During the second, serum potassium level was 1.88 mmol/L and potassium administration relieved the symptoms. Thyroid hormones levels were normal. The patient reported no cardiac arrhythmia and no dysmorphic features as would be typical for Andersen-Tawil syndrome. No relatives were known to be affected by PP. We classified the phenotype as very mild, hypokalemic SPP.

Exome sequencing

Altogether, 83,246 variants were detected in the sample of the proband, including redundant listings of the same variant in different splice isoforms. Elimination of intronic and synonymous changes reduced the number of variants including redundancies down to 17,880. Filtering by allele frequencies for variants more rare than 0.5% reduced the number of variants to 2,685. Filtering for muscle-specific expression (i.e. the 320 muscle specific genes according the Human Protein Atlas) and eliminating the redundant listings left 31 variants. These were preliminarily interpreted using Polyphen2, MutationTaster, and Sift (Table 1). Since these programs cannot interpret consequences of splicing variants, the two identified splice variants could not be analysed further. Of the remaining variants, only three were predicted to be linked to disease by at least two of the prediction programs: a *KCNJ12* variant c.419C > T coding for p.Thr140Met in the Kir2.2 channel, a *PRKCQ* variant c.685G > A coding for p.Asp229Asn in protein kinase C theta, and a *TTN* variant c.47828C > T coding for p.Thr15943Ile in titin. All three of these variants were present in a heterozygous state. None of the three variants have been, to our knowledge, reported to be associated to disease in the literature. Since all hitherto known causative PP genes encode ion channels, we opted to further study only the *KCNJ12* variant.

Sanger sequencing

The presence of the heterozygous c.419C > T base change in *KCNJ12* coding for p.Thr140Met in Kir2.2 was confirmed using Sanger sequencing (Fig. 1, top). Since a homologous p.Thr140Met in Kir2.6 encoded by *KCNJ18* was reported previously (12), we confirmed absence of

Table 1. Exome sequencing proband.

Gene	Base change	Protein change	SNP	Allele frequency	Poly-phen2	Mutation taster	Sift
<i>ACTN3</i>	c.2385C > G	p.Asp795Glu	n.a.	n.a.	Benign	Pseudogene	n.a.
<i>AGBL1</i>	c.774_779dupAGATGA	p.Glu258_Asp259dup	rs775629809	0.000017	n.a.	Polymorphism	n.a.
<i>CLIC5</i>	c.237A > T	p.Arg79Ser	rs41271277	0.002805	Benign	Polymorphism	Tolerated
<i>FHL3</i>	c.331 + 7G > C	splice variant	rs4570384	0.000594	n.a.	n.a.	n.a.
<i>HRC</i>	c.1001G > A	p.Gly334Asp	rs796956072	n.a.	Benign	Polymorphism	Tolerated
<i>HRC</i>	c.992C > A	p.Ala331Asp	rs763482766	0.000017	Benign	Polymorphism	Tolerated
<i>HRC</i>	c.986T > A	p.Val329Asp	rs138152757	0.000042	Benign	Polymorphism	Tolerated
<i>HRC</i>	c.744T > A	p.Asp248Glu	n.a.	n.a.	Benign	Polymorphism	Tolerated
<i>HRC</i>	c.738T > A	p.Asp246Glu	n.a.	n.a.	Benign	Polymorphism	Tolerated
<i>HRC</i>	c.730G > A	p.Glu244Lys	rs775263588	0.000817	Benign	Polymorphism	Tolerated
<i>HRC</i>	c.722A > G	p.Gln241Arg	rs773435857	0.000784	Benign	Polymorphism	Tolerated
<i>HRC</i>	c.703G > A	p.Gly235Ser	rs760105084	0.000746	Benign	Polymorphism	Tolerated
<i>HRC</i>	c.689G > A	p.Gly230Glu	rs756913154	0.000690	Benign	Polymorphism	Tolerated
<i>IGFN1</i>	c.4646C > G	p.Thr1549Arg	rs199718718	n.a.	n.a.	Polymorphism	Tolerated
<i>IGFN1</i>	c.4715C > T	p.Ala1572Val	rs201241861	0.000090	n.a.	Polymorphism	Tolerated
<i>IGFN1</i>	c.4728G > A	p.Met1576Ile	n.a.	n.a.	n.a.	Polymorphism	Tolerated
<i>IGFN1</i>	c.4747A > G	p.Ser1583Gly	rs199574248	n.a.	n.a.	Polymorphism	Tolerated
<i>IGFN1</i>	c.4823T > C	p.Val1608Ala	rs201505263	n.a.	n.a.	Polymorphism	Tolerated
<i>IGFN1</i>	c.4828G > A	p.Glu1610Lys	rs71524455	0.000962	n.a.	Polymorphism	Tolerated
<i>IGFN1</i>	c.4855G > A	p.Gly1619Ser	rs189258058	n.a.	n.a.	Polymorphism	Tolerated
<i>IGFN1</i>	c.5160G > A	p.Met1720Ile	rs200673977	0.000787	n.a.	Polymorphism	Tolerated
<i>IGFN1</i>	c.6016G > A	p.Glu2006Lys	rs12729404	0.000116	Benign	Polymorphism	Tolerated
<i>IGFN1</i>	c.6024A > G	p.Ile2008Met	rs12728986	0.000114	Benign	Polymorphism	Tolerated
<i>IGFN1</i>	c.6043G > A	p.Gly2015Ser	rs796090138	n.a.	Benign	Polymorphism	Tolerated
<i>KCNJ12</i>	c.419C > T	p.Thr140Met	rs536297311	0.000056	Probably damaging	Disease causing	Damaging
<i>LRRC14B</i>	c.310C > T	p.Arg104Cys	n.a.	n.a.	Benign	Polymorphism	Tolerated
<i>MAFA</i>	c.621_623delCCA	p.His208del	rs141816879	n.a.	n.a.	Polymorphism	n.a.
<i>PPP1R3A</i>	c.1428T > A	p.Asn476Lys	rs2974944	0.001129	Benign	Polymorphism	Tolerated
<i>PRKCG</i>	c.685G > A	p.Asp229Asn	rs34524148	0.001052	Probably damaging	Disease causing	Tolerated
<i>TTN</i>	c.47828C > T	p.Thr1594Ile	rs776113556	0.000008	Probably damaging	Disease causing	n.a.
<i>TTN</i>	c.10361-5delT	Splice variant	rs58651353	n.a.	n.a.	n.a.	n.a.

n.a. = not available.

the corresponding homologous c.419C > T base change in the *KCNJ18* gene by Sanger Sequencing to exclude mapping problems of the exome analysis (Fig. 1, bottom). To test the possibility of the *KCNJ12* gene being generally linked to PP, we sequenced 263 PP samples in *KCNJ12* using the Sanger technique. No changes were detected in 249 samples; eleven samples had synonymous SNP (coding for 1x p.Arg214Arg, 8x p.Asp61Asp 1x p.Ser266Ser, 1x p.Asp291Asp), and three samples each had a different non-synonymous base change. The latter were: c.1255G > A coding for p.Gly419Ser (rs77266866) with an allele frequency of 0.00077 (consistently predicted to be benign), the not yet described c.224G > A coding

for p.Cys75Tyr (consistently predicted to be pathogenic), and c.847A > G coding for p.Ile283Val (1x predicted to be pathogenic, 2x predicted to be benign) (Table 2).

The phenotypes for the three SPP cases with non-synonymous variants were briefly: i) for the p.Cys75Tyr carrier: onset at age 18, yearly quadriplegic episodes, ictal potassium of 1.5mM, episodes triggered by diarrhoea, fever, and sports, ii) for the p.Ile283Val carrier: onset at age 52, small fibre neuropathy, muscle jerking, cramps, myalgia, intermittent hypokalaemia with morning weakness lasting minutes, and iii) for the p.Gly419Ser carrier: two episodes in lifetime at age 22 and 28 lasting three hours, having concomitant myalgia, and being triggered by cortisol administration.

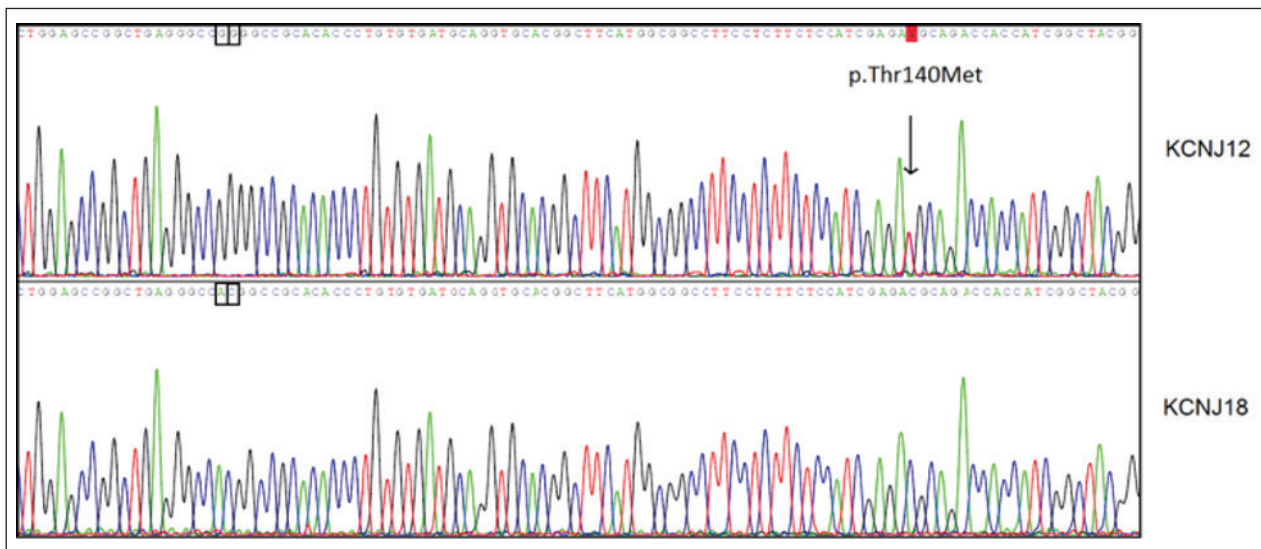


Figure 1. Sanger sequencing proband. Electropherogram of both genes, *KCNJ12* (top) and *KCNJ18* (bottom). The presence of a heterozygous c.419C > T base change coding for p.Thr140Met in the coding region of *KCNJ12* was confirmed using Sanger sequencing (red box). In *KCNJ18*, no base change was identified at this position. Additionally, two positions were marked (black boxes) to highlight the differences in wildtype sequences of these two genes in this highly homologous region proving the specificity of our amplification.

Table 2. Sanger sequencing *KCNJ12* in PP.

Base change	Protein change	SNP	Allele frequency	Poly-Phen2	Mutatio taster	Sift
c.224G > A	p.Cys75Tyr	n.a.	n.a.	Probably damaging	Disease causing	Damaging
c.847A > G	p.Ile283Val	n.a.	n.a.	Benign	Disease causing	Tolerated
c.1255G > A	p.Gly419Ser	rs77266866	0.00077	Benign	Polymorphism	Tolerated

n.a. = not available

The prediction results (Tables 1, 2) suggest i) that p.Gly419Ser would not be expected to cause any effects, ii) that the expectation for p.Ile283Val is unclear, and iii) that p.Cys75Tyr and p.Thr140Met would be expected to produce relevant changes in channel function. To test whether the prediction programs correctly assessed the disease-causing potency of the variants and, more specifically, to test whether p.Thr140Met may contribute to the SPP phenotype in the proband, we performed whole cell patch clamp studies on the four non-synonymous Kir2.2 variants.

Electrophysiology and fluorescence imaging

Kir currents were elicited from a holding potential of 0 mV in 10 mV-voltage steps of 100ms duration from hyperpolarized potentials – 80 mV to + 40 mV. In 30 mM external KCl, typical rectifier Kir currents were recorded from expression of Kir2.2-WT and the three variants

p.Cys75Tyr, p.Ile283Val, and p.Gly419Ser. In contrast, no endogenous Kir currents were detected in untransfected cells or in cells expressing p.Thr140Met. However, when WT was co-expressed with p.Thr140Met, typical Kir currents could be observed (Fig. 2A).

These findings could indicate, among other possibilities, that p.Thr140Met channels are not synthesized, not inserted into the membrane, or not functional. To assess the subcellular localization of the p.Thr140Met channels in comparison with Kir2.2-WT, we performed fluorescence imaging. Both channel types were expressed uniformly on the plasma membrane, with gray levels of WT vs p.Thr140Met being 16.17 ± 0.95 vs 13.49 ± 1.11 ($p = 0.08$, $n = 18-19$) (Fig. 2B). This finding indicates that p.Thr140Met channels are observed at levels similar to WT in the plasma membrane 24 hours post-transfection which means that protein synthesis, trafficking, and membrane insertion are intact. Therefore, the effect of p.Thr140Met is more likely to be

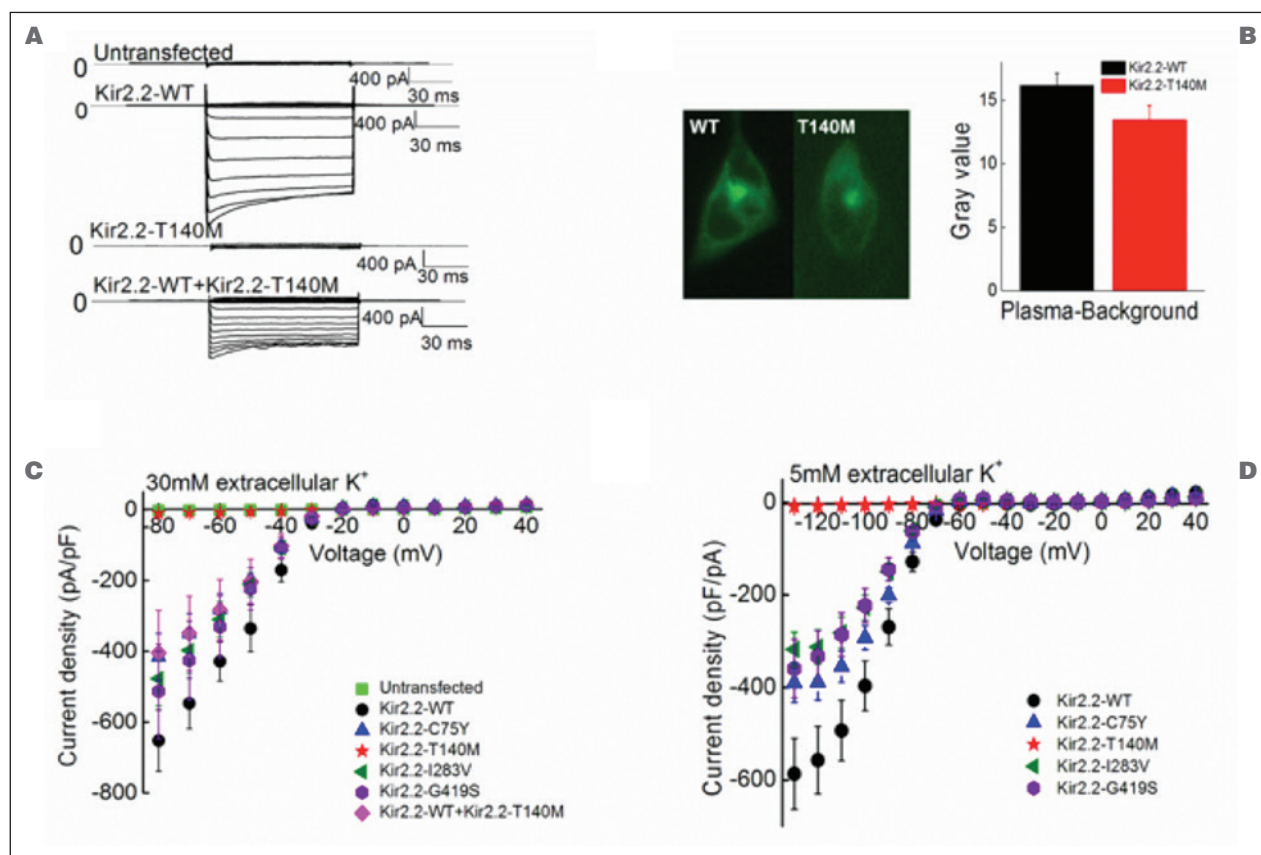


Figure 2. Functional expression. Functional characterization of Kir2.2-WT and four missense variants expressed in tsA 201 cells. **A**) Representative current traces. Note that p.Thr140Met channels do not produce a current. **B**) Fluorescence image of the tsA 201 cell expressing WT and p.Thr140Met Kir2.2 fusion proteins with GFP (Left). Mean gray values from the membrane areas after subtraction of background showed comparable signal intensity between WT ($n = 18$) and p.Thr140Met ($n = 19$) (Right). **C**) Normalized current-voltage relationships for untransfected cells ($n = 9$), WT ($n = 19$), p.Cys75Tyr ($n = 15$), p.Thr140Met ($n = 16$), p.Ile283Val ($n = 15$), p.Gly419Ser ($n = 8$) and Kir2.2-WT+Kir2.2-p.Thr140Met ($n = 10$) recorded in 30mM external K⁺. **D**) Normalized current-voltage relationships for WT ($n = 10$), p.Cys75Tyr ($n = 11$), p.Thr140Met ($n = 15$), p.Ile283Val ($n = 11$) and p.Gly419Ser ($n = 11$) recorded in 5mM external K⁺. Data are shown as means \pm SEM.

due to a direct effect on channel function, a possibility that we focused further on using electrophysiology.

Plotting of the obtained current peaks against the voltage revealed almost linear current-voltage relationships (Fig. 2C). Conductances were calculated from the steepness of the current-voltage relationship in the voltage range from -70 mV to -40 mV. Conductances for the inward currents were 288.28 ± 49.11 nS/pF for WT ($n = 19$), 308.49 ± 77.84 nS/pF for p.Gly419Ser ($n = 8$, $p = 0.82$), 275.36 ± 44.47 nS/pF for p.Ile283Val ($n = 15$, $p = 0.85$), 220.76 ± 37.39 nS/pF for p.Cys75Tyr ($n = 15$, $p = 0.3$), 2.67 ± 0.79 nS/pF for p.Thr140Met ($n = 16$, $p < 0.001$), and 216.47 ± 64.36 for Kir2.2-WT-Kir2.2-p.Thr140Met ($n = 10$, $p = 0.39$). Of these, only the conductance of p.Thr140Met alone differed from WT significantly.

To further study the voltage range around the resting membrane potential of skeletal muscle, extracellular KCl was decreased to 5 mM and the starting potential adjusted to -140 mV. Plotting of these current peaks against the voltage revealed linear to saturated current-voltage relationships and reduced current densities compared to WT (Fig. 2D). Conductances for the inward current were 840.48 ± 98.62 nS/pF for WT ($n = 10$), 530.26 ± 82.47 nS/pF for p.Gly419Ser ($n = 11$, $p = 0.19$), 523.08 ± 62.29 nS/pF for p.Ile283Val ($n = 11$, $p = 0.06$), 614.29 ± 73.16 nS/pF for p.Cys75Tyr ($n = 11$, $p = 0.18$), and 1.51 ± 0.43 nS/pF for p.Thr140Met ($n = 15$, $p < 0.001$). This suggests that only p.Thr140Met reduced channel function.

Since the homologous Kir2.1 is the main skeletal muscle potassium channel maintaining the resting

membrane potential, along with Kir2.2 (13) we investigated the effects of the variants on heteromeric Kir2.2-Kir2.1 channels by co-transfecting the two plasmids at an equimolar ratio. As expected by the literature (14), WT Kir2.1/WT Kir2.2 co-expression showed a significantly higher current density at 5 mM extracellular KCl at -130 mV (-737.06 ± 113.27 pA/pF, $n = 14$) compared with expression of WT Kir2.1 alone (-491.82 ± 48.18 pA/pF, $n = 17$, $p = 0.04$) which indicates formation of functional hetero-tetramers in our experimental conditions (Fig. 3A). Plotting of the obtained current peaks against the voltage revealed linear to saturated current-voltage relationships (Fig. 3B). Conductances for the inward current were 1036.91 ± 151.97 nS/pF for WT ($n = 14$), 529.66 ± 75.37 nS/pF for p.Gly419Ser ($n = 16$, $p = 0.01$), 624.91 ± 110.25 nS/pF for p.Ile283Val ($n = 17$, $p = 0.03$), 552.36 ± 92.89 nS/pF for p.Cys75Tyr ($n = 17$, $p = 0.01$), and 134.11 ± 48.99 nS/pF for p.Thr140Met ($n = 19$, $p < 0.001$). This suggests that all variants reduced co-expressed Kir2.1 function to some degree with p.Thr140Met being the most potent which may elicit a so-called dominant-negative effect on Kir2.1 by reducing conductance by 87% in our experiment.

Molecular modelling

To confirm a dominant negative effect of Kir2.2 with p.Thr140Met on WT Kir2.1, we created three-dimensional models of Kir2.2-Kir2.1 hetero-tetramers (Fig. 4A, B). These were equilibrated for energy minimization using Chimera, and compared for the WT Kir2.2-Kir2.1 tetramer, p.Thr140Met Kir2.2-WT Kir2.1 tetramer (2:2) and for

p.Thr140Met Kir2.2-WT Kir2.1 (3:1), p.Thr140Met Kir2.2 chains. For the Kir WT 2.2-2.1 tetramer in equimolar model ratio, energy minimization resulted in a re-distribution of potassium ions towards the putative binding sites in the pore helix of Kir 2.2 compatible with a higher maximal current of the hetero-tetramer (Fig. 4C). For the Kir p.Thr140Met 2.2-Kir WT2.1 tetramer in equimolar model ratio, re-distribution of potassium ion was minimal (Fig. 4D), and this effect was even more pronounced when 3 Kir p.Thr140Met 2.2 chains were used in construction of the tetramer (Fig. 4E). These findings support the functional results showing that p.Thr140Met reduces the maximal current of the hetero-tetramer.

In order to quantify the effect of the variant, molecular dynamics simulations for the WT Kir2.2-Kir2.1 tetramer *versus* p.Thr140Met Kir2.2-WT Kir2.1 tetramer (2:2) were performed. They revealed two significant differences between the WT Kir2.2-Kir2.1 model (Fig. 5A) and Thr140Met Kir2.2-WT Kir2.1 model (Fig. 5B). The first was that the distance between center of mass at the distal carbon for adjacent residues in the pore helix of Glu139 and Thr140 (WT) or Met140 (variant) was significantly greater for the WT model (8.09 ± 0.43 Å) compared to the Thr140Met model (5.39 ± 0.52 Å, $p \leq 0.05$, Fig. 5C). The second was that the H-bonding between Glu139 and Ile144 of the TIGYG selectivity filter was observed in 37.2% of frames for the WT model, but in no frames at all for the Thr140Met model (Fig. 5D). It is quite possible that the shorter distance between side chains of the Glu139 and Met140 compared to that for Glu139 and Thr140 may contribute to the loss of hydrogen bonding in the Thr140Met model.

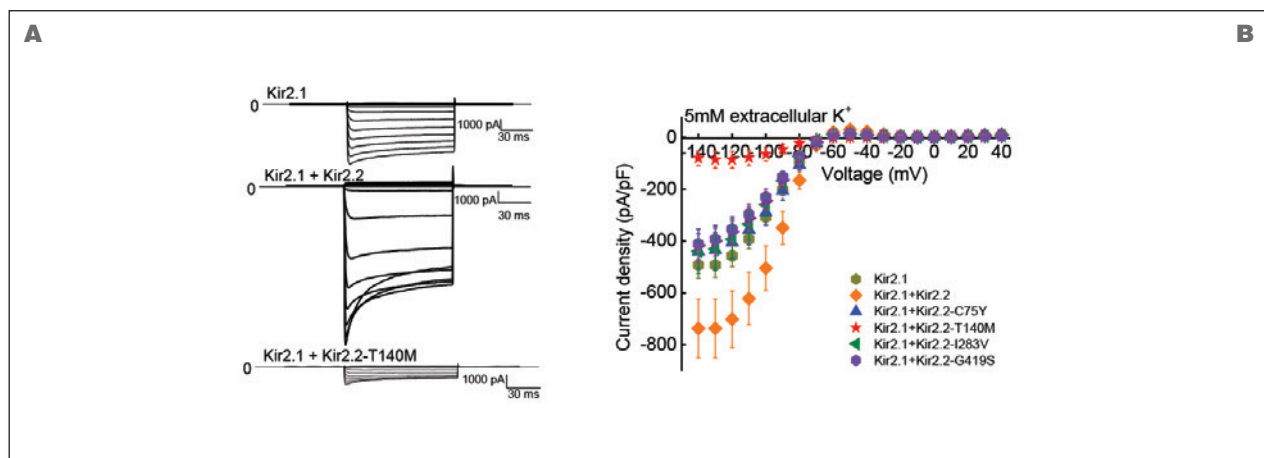


Figure 3. Co-expression of Kir2.1. Functional characterization of hetero-tetramers between Kir2.1 and Kir2.2-WT and four missense variants expressed in tsA 201 cells. **A)** Representative current traces. **B)** Normalized current-voltage relationships for WT Kir2.1 ($n = 17$), WT/WT Kir2.1 + Kir2.2 ($n = 14$), WT Kir2.1 + Kir2.2-p.Cys75Tyr ($n = 17$), WT Kir2.1 + Kir2.2-p.Thr140Met ($n = 19$), WT Kir2.1 + Kir2.2-p.Ile283Val ($n = 17$) and WT Kir2.1 + Kir2.2- p.Gly419Ser ($n = 16$) recorded in 5mM external K⁺. Data are shown as means \pm SEM.

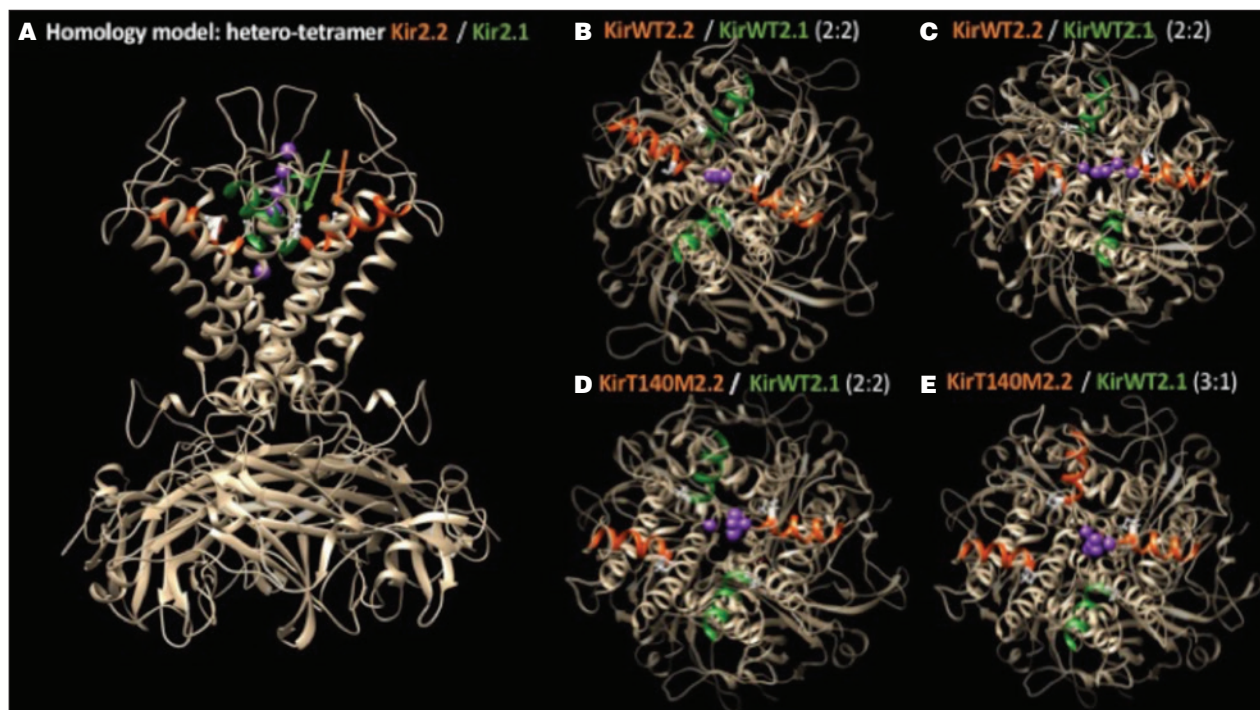


Figure 4. Homology models. Homology models of Kir2.2 and Kir2.1 incorporated into a tetramer of equimolar ratio **A**). Pore helical regions are colored orange (Kir2.2) or green (Kir2.1), with homologous pore helix residues Thr140 (Kir2.2) and Thr139 (Kir2.1) shown in white with corresponding arrows; potassium ions are included with chain A (Kir2.2, right) from the original 4lp8 pdb coordinates. Top view of same prior to equilibration is shown in **B**). After equilibration for energy minimization, top views show relative re-distribution of potassium ions for the WT equimolar heterotetramer **C**), and with variant p.Thr140Met incorporated into 2 Kir2.2 chains **D**) or 3 Kir2.2 chains **E**). The Kir2.2 p.Thr140Met variant resulted in less movement of the potassium ions towards binding sites in the pore helix.

Discussion

Based on the Sanger sequencing data, it is clear that non-synonymous Kir2.2 variants are infrequent; we found 4 in 264 patient samples (1.5%) a frequency similar to a previous study of the homologous channel Kir2.6 which detected 10 variants in 263 patient samples (3.8%) (8). Three of the variants, p.Gly419Ser, p.Ile283Val, and p.Cys75Tyr, are all located in cytoplasmic regions of the Kir2.2 channel. p.Gly419Ser is a known benign polymorphism named rs77266866 (dbSNP database, www.ncbi.nlm.nih.gov/snp/) which slightly depressed co-expressed Kir2.1. The two novel variants, p.Ile283Val, and p.Cys75Tyr, presented with functional effects of a similar degree. Therefore, all three variants may be interpreted as benign functional polymorphisms according to Jurkat-Rott and Lehmann-Horn 2005 (15). In contrast, p.Thr140Met is located in a transmembrane pore-forming alpha helix close to the selectivity filter (amino acid residues 143-148). It produced a loss of Kir2.2 function and suppressed co-expressed WT Kir2.1. This may indicate a susceptibility or potentially pathogenic variant.

The prediction programs were not reliable in determining the functional effects since of the two variants which both were consistently predicted to be pathogenic, p.Cys75Tyr and p.Thr140Met, only one had significant functional effects. In contrast, three variants had comparable function but very different prediction results: p.Gly419Ser which was consistently predicted to be benign and the two novel variants, p.Ile283Val and p.Cys75Tyr, one of which was consistently predicted to be pathogenic. This assessment is in agreement with previous studies on the quality of prediction programs in ion channelopathies which found reasonable sensitivities ranging from ~ 70-90% but low specificities of ~ 15-50% depending on channel type and protein regions within the channels (16, 17).

Our data show that the loss of function of p.Thr140Met Kir2.2 is not due to a trafficking defect but results from an alteration of the ion pore conductance. Together with the dominant negative effect on the main skeletal muscle rectifying potassium channel, Kir2.1, the functional effects are very similar to those of the PP Mutations in Kir2.6 which also display a loss of function and suppress co-

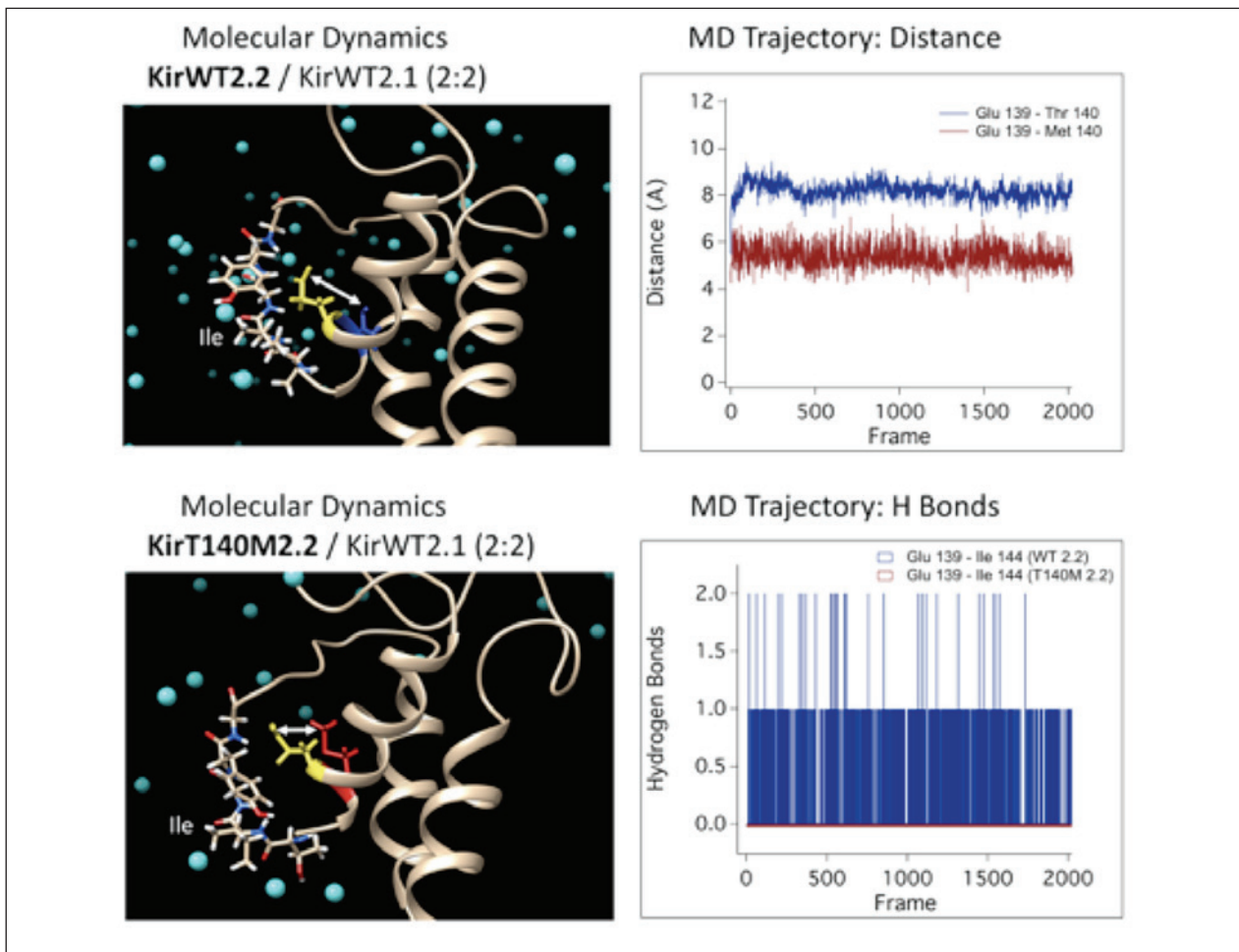


Figure 5. *Molecular dynamics simulations.* Models of equimolar Kir2.2 and Kir2.1 were incorporated into a POPC membrane, solvated and ionized, and subjected to an electric field for molecular dynamics simulations. The pore helix of one Kir2.2 chain and the TIGYG selectivity filter are shown in panels **A**) (WT 2.2) and **B**) (Thr140M 2.2), along with potassium ions (cyan). Distance measurements between the pore helix Glu139 (yellow) and Thr140 (blue, panel **A**) or Met140 (red, panel **B**) are depicted by the white arrows, and are calculated from MD trajectories shown in panel **C**). Hydrogen bonding between Glu139 and the Ile144 of the selectivity filter are calculated from trajectories shown in panel **D**). Reduced distance between pore helix residues Glu139/Met140 in the variant compared to Glu139/Thr140 in WT is correlated with an absence of hydrogen bonding between Glu139 and the target Ile144 of the selectivity filter.

expressed Kir2.1. (12, 18). Additionally, the same amino acid change, i.e. p.Thr140Met, in the highly homologous Kir2.6 channel has been shown to cause a similar phenotype, TPP (12), which supports the notion of susceptibility or potential pathogenicity of p.Thr140Met in Kir2.2.

As to the dominant negative effect on Kir2.1, loss of function mutations in the encoding *KCNJ2* gene are known to cause Andersen-Tawil Syndrome, a PP phenotype with the additional features cardiac arrhythmia and facial dysmorphism (5). However, our patient did not have such symptoms nor did the TPP patients with Kir2.6 mutations described previously (12). To clarify this conundrum, we compared public data of quantitative tissue-specific ex-

pression patterns. According to the Genotype Tissue Expression Consortium (www.gtexportal.org), the following RNA expression levels in reads per kilobase per million mapped reads have been found for *KCNJ12* vs *KCNJ2*: for skeletal muscle 12.3 vs 1.0, for heart 2.9 vs 2.3, and for skin 3.6 vs 0.9. Data from another source, the Human Protein Atlas (www.proteinatlas.org), lists the following transcripts per million: for skeletal muscle 23.1 vs 3.3., for heart 3.9 vs 6.3, and for skin 2.1 vs 5.6. The Fantom5 Consortium (www.fantom.gsc.riken.jp) has published the following expression levels in tags per million: for skeletal muscle 19.1 vs 8.1, for heart 7.4 vs 23.9, and for skin no data is available. All three sources agree that *KCNJ12* ex-

pression in skeletal muscle is at least two times larger than *KCNJ2*. This is not the case for heart and skin.

Possible phenotypes may be suggested by knockouts. While *KCNJ2* knockout mice die within hours after birth due to severe dysmorphia (cleft palate) and show no Kir currents in arterial myocytes, *KCNJ12* knockouts are viable and fertile and without dysmorphia (19). Suppression of Kir2.1 in heart leads to reduction of the cardiac Kir current by 95% (20). Taken together, expression levels and knockout data suggest that Kir2.2 mutations are most likely, if not exclusively, to cause muscle symptoms and not dysmorphia or cardiac arrhythmia.

Assuming a relative abundance of *KCNJ12* to *KCNJ2* of 2:1, there would be an equimolar ratio of WT Kir2.2 to p.Thr140Met Kir 2:2 to WT Kir2.1, i.e. of 1:1:1. Heterotetramers with none, one, or several p.Thr140Met may be present. Our molecular modelling demonstrated that the incorporation of an increasing number of Kir2.2 p.Thr140 in heterotetramers with Kir2.1 decreased the movement of potassium ions towards their binding sites in the pore helix which directly results in current reduction. Quantification by molecular dynamics simulations demonstrated that the incorporation of Kir2.2 p.Thr140 in heterotetramers with Kir2.1 resulted in loss of formation of hydrogen bonding between Glu139 and Ile144 of the selectivity filter. This interaction is important in early permeation steps in KcsA channels (11), supporting the hypothesis that current reduction in heterotetramers containing the p.Thr140Met Kir 2:2 variant may be, at least partly, the consequence of the observed reduction in hydrogen bonding. Whether or not the current reduction is enough to reduce the total inward Kir current sufficiently to cause PP determines the difference between pathogenic variant and susceptibility (15).

Additionally, there may be genetic background factors to take into account. In the proband with p.Thr140Met in Kir2.2, there were two additional, unknown, non-synonymous, possibly pathogenic, heterozygous variants: one in *PRKCQ* encoding protein kinase C theta (*PKCθ*) and one in *TTN* encoding titin. Both have previously not been linked to PP, but may still contribute to the phenotype of the proband. Titin mutations are known to cause multiple other diseases of heart and skeletal muscle; namely several cardiomyopathies, limb-girdle dystrophy type 2, proximal myopathy with respiratory involvement, Salih myopathy, and tardive tibial muscular dystrophy (21, 22) and, therefore, titin variants could contribute to the manifestation of muscle weakness. For *PKCθ*, even though it has not been associated to disease at all, it is quite important for regulation of skeletal muscle function. *PKCθ* phosphorylates and thereby reduces the current amplitude of the muscular chloride channel CIC-1 (23) which helps muscle to uphold muscle excitability during exer-

cise (24). An increased *PKCθ* could mimic the pathogenic mechanism underlying the skeletal muscle disorder of myotonia congenita which is caused by muscle hyperexcitability due to decreased CIC-1 current (25). Alternatively, an inhibition of Protein kinase C – which may be expected to a. o. increase CIC-1 current – improves muscle regeneration in a mouse model of Duchenne muscular dystrophy (26) and could lessen the severity of a PP phenotype.

Taken together, the sporadic occurrence of SPP suggests that the pathogenic potency of Kir2.2 variants may be dependent on additional factors such as individual genetic background (i.e. co-existing variants in *PRKCQ* and *TTN*) or epigenetic phenomena. Therefore, we conclude that Kir2.2 p.Thr140Met may be most safely interpreted as a SPP susceptibility variant and it should be included in the genetic testing scheme for diagnosing SPP.

Acknowledgements

This study was supported by the non-profit Hertie Foundation, the German Federal Ministry of Research (BMBF IonNeurONet), the DGM German Muscle Disease Society, Taro Pharma, and NIH R15 NS09357901-A1. We thank Landon Bayless-Edwards (ISU) for invaluable assistance with computations from MD simulations.

References

1. Matthews E, Silwal A, Sud R, et al. Skeletal muscle channelopathies: rare disorders with common pediatric symptoms. *J Pediatr* 2017;188:181-5.
2. Cannon SC. Channelopathies of skeletal muscle excitability. *Compr Physiol* 2015;5:761-90.
3. Jurkat-Rott K, Groome JR, Lehmann-Horn F. Pathophysiological role of omega pore current in channelopathies. *Front Neuropharmacol* 2012;3:1-15.
4. Spillane J, Kullmann DM, Hanna MG. Genetic neurological channelopathies: molecular genetics and clinical phenotypes. *J Neurol Neurosurg Psychiatry* 2016;87:37-48.
5. Statland JM, Tawil R, Venance SL. Andersen-Tawil syndrome. In: Adam MP, Ardinger HH, Pagon RA, et al., Eds. *GeneReviews*®. Seattle (WA): University of Washington, 1993-2018.
6. Li H, Durbin R. Fast and accurate short read alignment with Burrows-Wheeler transform. *Bioinformatics* 2009;25:1754-60.
7. Li H, Handsaker B, Wysoker A, et al. 1000 genome project data processing subgroup. The sequence alignment/map format and SAMtools. *Bioinformatics* 2009;25:2078-9.
8. Kuhn M, Jurkat-Rott K, Lehmann-Horn F. Rare *KCNJ18* variants do not explain hypokalaemic periodic paralysis in 263 unrelated patients. *J Neurol Neurosurg Psychiatry* 2016;87:49-52.

9. Zubcevic L, Bavro VN, Muniz JRC, et al. Control of KirBac3.1 potassium channel gating at the interface between cytoplasmic domains. *J Biol Chem* 2014;289:143-51.
10. Pettersen EF, Goddard TD, Huang CC, et al. UCSF Chimera – a visualization system for exploratory research and analysis. *J Comput Chem* 2004;25:1605-12.
11. Berneche S, Roux B. A gate in the selectivity filter of potassium channels. *Structure* 2005;13:591-600.
12. Ryan DP, da Silva MR, Soong TW, et al. Mutations in potassium channel Kir2.6 cause susceptibility to thyrotoxic hypokalemic periodic paralysis. *Cell* 2010;140:88-98.
13. DiFranco M, Yu C, Quiñonez M, et al. Inward rectifier potassium currents in mammalian skeletal muscle fibres. *J Physiol* 2015;593:1213-38.
14. Panama BK, McLerie M, Lopatin AN. Functional consequences of Kir2.1/Kir2.2 subunit heteromerization. *Pflugers Arch* 2010;460:839-49.
15. Jurkat-Rott K, Lehmann-Horn F. Muscle channelopathies and critical points in functional and genetic studies. *J Clin Invest* 2005;115:2000-9.
16. Leong IU, Stuckey A, Lai D, et al. Assessment of the predictive accuracy of five in silico prediction tools, alone or in combination, and two metaservers to classify long QT syndrome gene mutations. *BMC Med Genet* 2015;16:34.
17. Flanagan SE, Patch AM, Ellard S. Using SIFT and PolyPhen to predict loss-of-function and gain-of-function mutations. *Genet Test Mol Biomarkers* 2010;14:533-7.
18. Cheng CJ, Lin SH, Lo YF, et al. Identification and functional characterization of Kir2.6 mutations associated with non-familial hypokalemic periodic paralysis. *J Biol Chem* 2011;286:27425-35.
19. Zaritsky JJ, Eckman DM, Wellman GC, et al. Targeted disruption of Kir2.1 and Kir2.2 genes reveals the essential role of the inwardly rectifying K(+) current in K(+)-mediated vasodilation. *Circ Res* 2000;87:160-6.
20. McLerie M, Lopatin AN. Dominant-negative suppression of I(K1) in the mouse heart leads to altered cardiac excitability. *J Mol Cell Cardiol* 2003;35:367-78.
21. Chauveau C, Rowell J, Ferreira A. A rising titan: TTN review and mutation update. *Hum Mutat* 2014;35:1046-59.
22. Savarese M, Sarparanta J, Vihola A, et al. Increasing role of Titin mutations in neuromuscular disorders. *J Neuromuscul Dis* 2016;3:293-308.
23. Camerino GM, Bouchè M, De Bellis M, et al. Protein kinase C theta (PKC θ) modulates the ClC-1 chloride channel activity and skeletal muscle phenotype: a biophysical and gene expression study in mouse models lacking the PKC θ . *Pflugers Arch* 2014;466:2215-28.
24. Riisager A, de Paoli FV, Yu WP, et al. Protein kinase C-dependent regulation of ClC-1 channels in active human muscle and its effect on fast and slow gating. *J Physiol* 2016;594:3391-406.
25. Imbrici P, Altamura C, Pessia M, et al. ClC-1 chloride channels: state-of-the-art research and future challenges. *Front Cell Neurosci* 2015;9:156.
26. Marrocco V, Fiore P, Benedetti A, et al. Pharmacological Inhibition of PKC θ counteracts muscle disease in a mouse model of Duchenne muscular dystrophy. *EBioMedicine* 2017;16:150-61.

Prevalence of metabolic syndrome and non-alcoholic fatty liver disease in a cohort of Italian patients with spinal-bulbar muscular atrophy

FRANCESCO FRANCCINI-PESENTI¹, GIORGIA QUERIN², CRISTINA MARTINI¹, SARA MARESO¹
AND DAVID SACERDOTI¹

¹ Department of Medicine, University of Padua, Italy; ² Department of Neurosciences, University of Padua, Italy

Spinal-bulbar muscular atrophy (SBMA), is an X-linked motor neuron disease caused by a CAG-repeat expansion in the first exon of the androgen receptor gene (AR) on chromosome X. In SBMA, non-neural clinical phenotype includes disorders of glucose and lipid metabolism. We investigated the prevalence of metabolic syndrome (MS), insulin resistance (IR) and non alcoholic fatty liver disease (NAFLD) in a group of SBMA patients. Forty-seven consecutive patients genetically diagnosed with SBMA underwent biochemical analyses. In 24 patients abdominal sonography examination was performed. Twenty-three (49%) patients had fasting glucose above reference values and 31 (66%) patients had a homeostatic model assessment (HOMA-IR) ≥ 2.6 . High levels of total cholesterol were found in 24 (51%) patients, of LDL-cholesterol in 18 (38%) and of triglycerides in 18 (38%). HDL-cholesterol was decreased in 36 (77%) patients. Twenty-four (55%) subjects had 3 or more criteria of MS. A positive correlation ($r = 0.52$; $p < 0.01$) was observed between HOMA-IR and AR-CAG repeat length. AST and ALT were above the reference values respectively in 29 (62%) and 18 (38%) patients. At ultrasound examination increased liver echogenicity was found in 22 patients (92%). In one patient liver cirrhosis was diagnosed. Liver/kidney ratio of grey-scale intensity, a semi-quantitative parameter of severity of steatosis, strongly correlated with BMI ($r = 0.68$; $p < 0.005$). Our study shows a high prevalence of IR, MS and NAFLD in SBMA patients, conditions that increase the cardiovascular risk and can lead to serious liver damage, warranting pharmacological and non-pharmacological treatment.

Key words: muscular atrophy, spinal-bulbar muscular atrophy, metabolic syndrome, insulin resistance, non alcoholic fatty liver disease

Introduction

Kennedy's disease, also known as spinal-bulbar muscular atrophy (SBMA), is a rare, late-onset, X-linked motor neuron disease. It is caused by a CAG trinucleotide-repeat expansion in the first exon of the androgen receptor gene (AR) on chromosome X. The CAG sequence encodes a polyglutamine tract (polyQ), with more than 38 repeats considered to be pathogenetic (1).

SBMA affects adult males with onset usually between 30 and 50 years, and is characterized by selective motor neuron degeneration occurring in brainstem and spinal cord, leading to progressive bulbar and limb muscle weakness and atrophy (2). Besides the well-known neurological phenotype, non-neurological symptoms are common in SBMA. These include features belonging to the cluster of metabolic syndrome (MS), a condition of increased cardiovascular risk characterized by insulin resistance (IR), abdominal obesity, dyslipidemia and glucose intolerance (3). In man, hypogonadism is associated with MS, which seems to be improved by treatment with testosterone (4). Several molecular mechanisms mediated by AR signaling can lead to the development of MS (5). IR is a key pathogenic factor in both MS and non-alcoholic fatty liver disease (NAFLD), a clinicopathologic entity that includes a spectrum of liver damage ranging from simple steatosis to nonalcoholic steatohepatitis (NASH) (6). As MS and NAFLD may lead to worse outcomes in patients with chronic diseases and benefit from pharmacological and non-pharmacological treatment, we investigated the prevalence of MS, IR and NAFLD in a group of SBMA subjects.

Patients and methods

Forty-seven consecutive patients genetically diagnosed with Kennedy's disease, undergoing no specific treatment for SBMA, were recruited after obtaining written informed consent. They were all Italian and followed-up in the Department of Neurosciences, University of Padua. No patients was under statin or metabolic treatment at the time of evaluation. One hundred twenty-three age-matched healthy males served as controls. For all participants, anthropometric parameters, systolic blood pressure (SBP), diastolic blood pressure (DBP) and laboratory data were collected. Body weight was assessed with a calibrated standard beam balance, height was measured by a standard height bar, and Body Mass Index (BMI) was calculated as weight (kg) divided by height (m²). Waist circumference was measured at the midway between lower rib and crista iliaca, according to WHO recommendations (7).

Blood pressure was measured using the method recommended by the Seventh Report of the Joint National Committee on Prevention, Detection, Evaluation, and Treatment of High Blood Pressure (8). Laboratory tests, measured after an overnight fast, included: fasting plasma glucose, immuno-reactive insulin, serum triglycerides (TG), total cholesterol, high-density lipoprotein cholesterol (HDL-C), low-density lipoprotein cholesterol (LDL-C), alanine aminotransferase (ALT), aspartate aminotransferase (AST), and total serum testosterone.

To evaluate IR, homeostatic model assessment (HOMA-IR) was calculated using the formula: $\text{HOMA-IR} = [\text{glucose (mmol/L)} * \text{insulin } (\mu\text{U/mL})/22.5]$, using fasting values (9). IR was defined as $\text{HOMA-IR} \geq 2.5$. According to NHLBI/AHA criteria (10), MS was diagnosed when three or more of the following risk factors were present: abdominal obesity (waist circumference > 102 cm), hypertension (blood pressure $\geq 130/ \geq 85$ mmHg) or specific medication, level of triglycerides ≥ 150 mg/dl (1.7 mmol/L) or specific medication, low HDL cholesterol < 40 mg/dl (1.03 mmol/L) or specific medication, and fasting plasma glucose ≥ 100 mg/dl (5.6 mmol/L) or history of diabetes mellitus or taking antidiabetic medications.

Genomic DNA was extracted from peripheral blood leucocytes using the standard salting out procedure. CAG repeats were amplified by PCR as previously described (11) and repeats fragment sizing was performed on an ABI PRISM 3,700 DNA Sequencer (Applied Biosystems, Foster City, California, USA). The specific length of CAG repeats was further verified via Sanger sequencing.

We assessed motor functions using the revised version of amyotrophic lateral sclerosis functional rating

scale (ALSFRS-R). Although this scale was not developed for SBMA, all items in this rating scale are applicable to the disease (12).

Abdominal sonography was performed in 24 subjects with SBMA, randomly chosen within the group. The exam was performed by a single skilled operator with an Hitachi HI VISION Ascendus equipment (Hitachi Medical Corporation, Tokyo, Japan) and a convex phased array transducer (5-1 MHz) after at least an 8-hours fast. All images were obtained with the same presetting of the sonographic equipment that is, imaging probe, gain, focus, and depth range. Liver steatosis was graded as follows (13):

- grade I (mild): slightly increased liver brightness relative to that of the kidney with normal visualization of the diaphragm and intrahepatic vessel borders;
- grade II (moderate): increased liver brightness relative to that of the kidney with slightly impaired visualization of the intrahepatic vessels and diaphragm;
- grade III (severe): markedly increased liver brightness relative to that of the kidney with poor or no visualization of the intrahepatic vessel borders, diaphragm and posterior portion of the right lobe of the liver.

A semiquantitative estimate of steatosis was also obtained based on comparative analysis of digital sonographic images of the liver and right kidney (14). Briefly, US images of both organs were acquired and the grey-scale intensity of selected regions of interest was measured, and a liver/kidney (L/K) ratio was calculated, which has been shown to display direct correlation with the degree of steatosis measured by histology.

The diagnosis of NAFLD was established by ultrasonography followed by the exclusion of the secondary causes of hepatic steatosis: alcohol intake of 30 g/day or more, ingestion of drugs known to produce hepatic steatosis, a positive serology for hepatitis B or C virus, a history of another known liver disease.

Continuous variables were described as means plus or minus one standard deviation. Student's *t* test was used to measure the statistical significance of the mean differences, and the relationship between two continuous variables was analyzed using Spearman's correlation coefficients. The significance level was set at $p < 0.05$.

Results

The baseline characteristics, anthropometric and biochemical parameters of the SBMA patients and the healthy control subjects are summarized in Table I. Mean SBMA duration since its onset was 14.9 ± 7.0 years (range 4-30). The SBMA patients had higher waist circumference, SBP, DBP, glycate haemoglobin, IRI,

Table 1. Anthropometric and biochemical profile of patients with SBMA and control subjects.

	SBMA (n. 47)	Control (n. 124)	p value
Age (years)	57.7 ± 7.0	55.3 ± 8.4	n.s.
BMI (kg/m ²)	25.5 ± 3.7	24.8 ± 3.4	n.s.
Waist circumference (cm)	101 ± 7.5	98 ± 8.1	< 0.05
SBP (mmHg)	138 ± 18	129 ± 13	< 0.001
DBP (mmHg)	90 ± 10	86 ± 9	< 0.01
Fasting glucose (mmol/l)	115 ± 34	108 ± 21	n.s.
Glycate haemoglobin (mmol/mol)	41 ± 13	37 ± 11	< 0.05
IRI (μU/ml)	15.0 ± 10.7	8.8 ± 7.2	< 0.001
HOMA-IR	4.1 ± 2.5	2.1 ± 2.0	< 0.001
Total cholesterol (mmol/l)	5.36 ± 0.84	5.21 ± 0.76	n.s.
HDL-cholesterol (mmol/l)	1.38 ± 0.42	1.43 ± 0.39	n.s.
Triglycerides (mmol/L)	1.98 ± 1.26	1.72 ± 1.11	n.s.
AST (U/L)	47 ± 21	25 ± 11	< 0.001
ALT (U/L)	57 ± 27	27 ± 15	< 0.001

BMI: body mass index; SBP: systolic blood pressure; DBP: diastolic blood pressure; IRI: immunoreactive insulin; HOMA-IR: insulin resistance homeostatic model assessment; HDL: high-density lipoprotein; AST: aspartate transaminase; ALT: alanine transaminase.

HOMA-IR, AST and ALT than the controls. Twenty-four (55%) patients with SBMA had 3 or more criteria of MS.

In SBMA patients a positive correlation was observed between HOMA-IR and AR-CAG repeat length (Fig. 1A). No correlation was observed between HOMA-IR and BMI, between HOMA-IR and disease duration and between HOMA-IR and ALSFRS-R. No difference in BMI was found between patients with normal and high HOMA-IR.

AST and ALT were above the references values respectively in 29 (62%) and 18 (38%) cases. Twenty-six patients with hypertransaminasemia had an AST/ALT ratio < 1. Total serum testosterone was elevated in five patients (10%) and decreased in three (6%).

At ultrasound examination increased liver echogenicity was found in 22/24 SBMA patients. Eleven patients showed grade I, 7 patients grade II and 4 patients grade III steatosis (Table 2). One patient was diagnosed with liver cirrhosis. L/K ratio strongly correlated with BMI (Fig. 1B). AR-CAG repeat length and disease duration did not correlate with L/K ratio All patients with grade III steatosis and the subject with liver cirrhosis

were obese (BMI ≥ 30 kg/m²). Dividing patients based on the steatosis grading, the group with higher degree had a BMI significantly greater than those with a lower degree. On the contrary, no differences were observed in the AR-CAG repeat length and in the disease duration (Table 2). No significant correlation was found between total serum testosterone and other parameters.

Discussion

This study evidenced that SBMA patients had higher prevalence of MS criteria, IR and hypertransaminasemia than the controls. Many mechanisms related to IR and MS, such as hyperglycemia, dyslipidemia, high blood pressure and inflammation, can accelerate atherosclerosis and increase the risk of vascular complications (15).

Recently, a high prevalence of IR in SBMA patients was reported by Nakatsuji et al. (16). The authors described a correlation between motor function, evaluated with ALSFRS-R, and HOMA-IR that in our patients was not found. This discrepancy can be partly due to ethnic differences in insulin sensitivity observed between Caucasian and Asian peoples (17).

Hypertransaminasemia was frequently observed in our SBMA patients. Both AST and ALT are present in skeletal muscle, with ALT being more specific to the liver (18). These data suggest a liver involvement in SBMA patients. To characterize this, NAFLD was found in 92% of SBMA patients undergoing abdominal sonography. NAFLD is strictly related to IR, and linked to MS. Its global prevalence is 25% (19). Even if NAFLD is frequently a benign condition, it can progress to non-alcoholic steatohepatitis, liver cirrhosis and hepatocellular carcinoma (20). Although most of studied subjects had a mild or moderate steatosis, 4 patients had a severe fatty liver and in one patient hepatic involvement had evolved to micronodular cirrhosis. In this patient, MS and liver abnormalities were diagnosed several years before the onset of Kennedy's disease. In SBMA, as well as in the general population (21), obesity seems to worsen the severity of NAFLD, which can occur also in lean subjects. On the contrary, the severity of NAFLD does not appear to be related to the disease duration.

An evidence of NAFLD was recently reported by Gruber et al. (22) in nearly all SBMA patients evaluated with magnetic resonance spectroscopy.

IR is a key pathogenic factor in both NAFLD and MS. Increased adipose tissue results in increased FFA flux to tissues, including the liver, triglyceride storage and IR (23). In fatty liver, glucose uptake and insulin-mediated suppression of glucose production are impaired, exacerbating the IR.

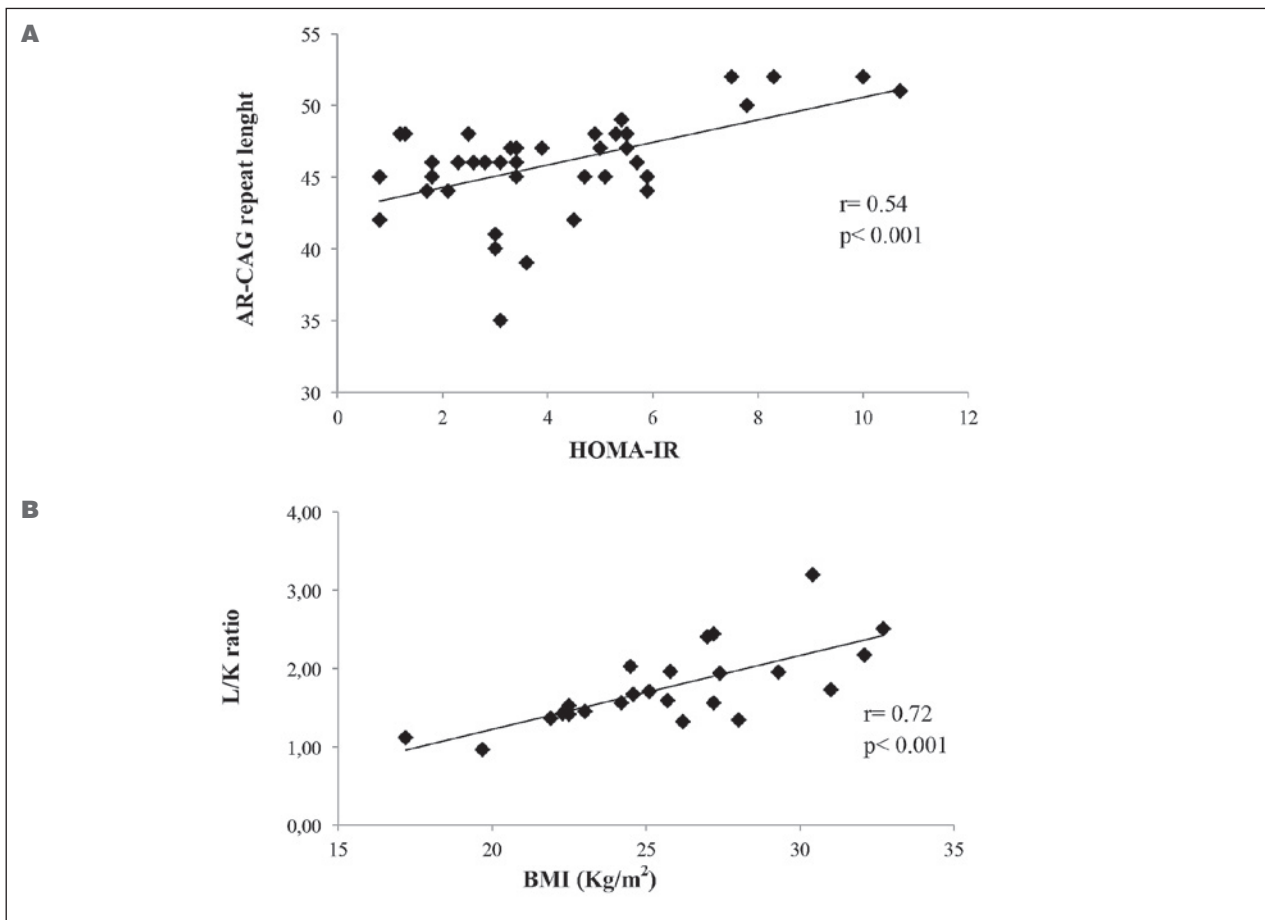


Figure 1. Correlations between AR-CAG repeat length and HOMA-IR (**A**) and between L/K ratio and BMI (**B**).

AR: androgen receptor; BMI: body mass index; HOMA-IR: homeostatic model of assessment insulin resistance

Testosterone and androgen receptors play a pivotal role in the regulation of insulin signaling and in several aspects of MS. Epidemiological studies demonstrate an association between low levels of testosterone in men and obesity, MS and type 2 diabetes mellitus (24). In prostate cancer, androgen-deprivation therapy improves survival but it leads to severe hypogonadism with different adverse effects, including increase of fat mass and circulating insulin levels (25). Clinical studies showed that testosterone replacement can improve insulin sensitivity in hypogonadal men (26) and reduce markers of MS and inflammation in hypogonadal men with MS (27).

The CAG repeat polymorphism within the AR gene can also play a role in development of MS (28). The polymorphism of AR-CAG repeats influences insulin sensitivity and the components of MS in men (29). Evidence suggests that CAG number is inversely correlated to the transcriptional activity of AR (30). According to these data, in SBMA patients IR, evaluated by HOMA-IR, positively correlated with AR-CAG repeat length.

The mechanisms through which testosterone acts on metabolism control in man are complex. An increasing body of evidence shows that testosterone modulates the expression of important regulatory proteins involved in glycolysis, glycogen synthesis and lipid metabolism in liver, muscle and adipose tissues. The molecular basis of deficiency in AR signaling has been investigated using animal models. Male mice with global deletion of AR (GARKO) show central obesity, fasting hyperglycemia, glucose intolerance, and IR (31). In the GARKO mouse model, the ability of insulin to activate the phosphatidylinositol-3 kinase, was reduced by 60% in skeletal muscle and liver, resulting in impairment of insulin signaling (32). In the selective hepatocyte deleted AR mouse (LARKO), a high-fat diet induced development of obesity, hepatic steatosis, fasting hyperglycemia and insulin resistance (32). Reduced insulin sensitivity in fat-fed LARKO mice was associated with decreased phosphoinositide-3 kinase activity and increased phosphoenolpyruvate carboxykinase expression, features

Table 2. BMI and AR-CAG repeat length in patients with spinal and bulbar muscular atrophy sorted by sonographic echogenicity.

	Grade of liver echogenicity: 0-1	Grade of liver echogenicity: > 1	P-value
N.	12	12	
BMI (kg/m ²)	24.2 ± 3.5	28.3 ± 3.5	< 0.01
AR-CAG repeat length	46 ± 4	49 ± 7	n.s.
Disease duration (years)	12.8 ± 3.3	12.6 ± 3.5	n.s.

BMI: body mass index; AR: androgen receptor.

which can explain the impaired insulin signaling and increased hepatic glucose production (31). In testicular feminized mice, which have a non-functional *AR*, an elevated expression of key regulatory enzymes of fatty acid synthesis, acetyl-CoA carboxylase alpha (ACACA) and fatty acid synthase, was found, explaining the increased hepatic lipid deposition compared to controls (32). Taken together, IR and elevated lipid synthesis observed in the liver of animal models with *AR* defect can explain the very high prevalence of NAFLD in SBMA subjects. NAFLD severity was correlated with BMI, but not with AR-CAG repeat length, suggesting that, although *AR* deficiency can lead to NAFLD, its severity, and, maybe, progression, is related to obesity, warranting pharmacological and non-pharmacological treatment. An attenuation of expression of insulin receptors in the skeletal muscle of SBMA patients has been recently reported by Nakatsuji et al., providing another possible pathomechanism of metabolic alterations (16). Instead, this study failed to find a valid association between HOMA-IR and androgen insensitivity in SBMA patients. In contrast, Guber et al. reported an increased retinol binding protein 4 (RBP4) expression in their SBMA patients, consistent with a loss of androgen stimulation (22). The increase of RBP4 plasma levels contributes to insulin-resistance and its expression is significantly increased in *AR* knock-out mice (33). In conclusion, this study confirm both metabolic and hepatic involvement in the SBMA patients. These alterations can be explained mainly by the reduction of testosterone activity because of polyQ expansion in *AR* gene and must be considered as a main characteristic of Kennedy disease. Metabolic alterations in SBMA are a suggestive model of androgen deprivation in male and require a multidisciplinary approach to disease. However, considering the conflicting data on the role of androgen stimulation in the metabolic involvement, further studies are needed to understand the pathogenesis of NAFLD and IR in SBMA patients and the possible detrimental consequences of anti-androgen approaches to disease.

References

1. La Spada AR, Wilson EM, Lubahn DB, et al. Androgen receptor gene mutations in X-linked spinal and bulbar muscular atrophy. *Nature* 1991;352:77-9.
2. Katsuno M, Tanaka F, Adachi H, et al. Pathogenesis and therapy of spinal and bulbar muscular atrophy (SBMA). *Prog Neurobiol* 2012;99:246-56.
3. Querin G, Bertolin C, Da Re E, et al. Non-neural phenotype of spinal and bulbar muscular atrophy: results from a large cohort of Italian patients. *J Neurol Neurosurg Psychiatry* 2016;87:810-6.
4. Wespes E. Metabolic syndrome and hypogonadism. *Eur Urol Suppl* 2013;12:2-6.
5. Yu IC, Lin HY, Sparks JD, et al. Androgen receptor roles in insulin resistance and obesity in males: the linkage of androgen-deprivation therapy to metabolic syndrome. *Diabetes* 2014;63:3180-8.
6. Yki-Järvinen H. Non-alcoholic fatty liver disease as a cause and a consequence of metabolic syndrome. *Lancet Diabetes Endocrinol* 2014;2:901-10.
7. World Health Organization. Obesity: preventing and managing the global epidemic. Geneva: WHO 1998.
8. Chobanian AV, Bakris GL, Black HR, et al. Joint national committee on prevention, detection, evaluation, and treatment of high blood pressure, national heart and blood institute; national high blood pressure education program coordinating committee: seventh report of the joint national committee on prevention, detection, evaluation, and treatment of high blood pressure. *Hypertension* 2003;42:1206-52.
9. Matthews DR, Hosker JP, Rudenski AS, et al. Homeostasis model assessment: insulin resistance and beta-cell function from fasting plasma glucose and insulin concentrations in man. *Diabetologia* 1985;28:412-9.
10. Grundy SM, Cleeman JI, Daniels SR, et al. Diagnosis and management of the metabolic syndrome. An American heart association/national heart, lung, and blood institute scientific statement. *Circulation* 2005;112:2735-52.
11. Fratta P, Nirmalanathan N, Masset L, et al. Correlation of clinical and molecular features in spinal bulbar muscular atrophy. *Neurology* 2014;82:2077-84.
12. Hashizume A, Katsuno M, Banno H, et al. Longitudinal changes

- of outcome measures in spinal and bulbar muscular atrophy. *Brain* 2012;135(Pt 9):2838-48.
13. Gerstenmaier IF, Gibson RN. Ultrasound in chronic liver disease. *Insights Imaging* 2014;5:441-55.
 14. Gaiani S, Avogaro A, Bombonato GC, et al. Nonalcoholic fatty liver disease (NAFLD) in nonobese patients with diabetes: prevalence and relationships with hemodynamic alterations detected with doppler sonography. *J Ultrasound* 2009;12:1-515.
 15. Mottillo S, Filio KB, Genest J, et al. The metabolic syndrome and cardiovascular risk a systematic review and meta-analysis. *J Am Coll Cardiol* 2010; 56:1113-1.
 16. Nakatsuji H, Araki A, Hashizume A, et al. Correlation of insulin resistance and motor function in spinal and bulbar muscular atrophy. *J Neurol* 2017;264:839-47.
 17. Kodama K, Tojjar D, Yamada S, et al. Ethnic differences in the relationship between insulin sensitivity and insulin response. A systematic review and meta-analysis. *Diabetes Care* 2013;36:1789-96.
 18. Weibrecht K, Dayno M, Darling C, et al. Liver aminotransferases are elevated with rhabdomyolysis in the absence of significant liver injury. *J Med Toxicol* 2010;6:294-300.
 19. Younossi ZM, Koenig AB, Abdelatif D, et al. Global epidemiology of nonalcoholic fatty liver disease-Meta-analytic assessment of prevalence, incidence, and outcomes. *Hepatology* 2016;64:73-84.
 20. Adams LA, Lymp JF, St Sauver J, et al. The natural history of non-alcoholic fatty liver disease: a population-based cohort study. *Gastroenterology* 2005;129:113-21.
 21. Lomonaco R, Bril F, Portillo-Sanchez P, et al. Metabolic impact of nonalcoholic steatohepatitis in obese patients with type 2 diabetes. *Diabetes Care* 2016;39:632-8.
 22. Guber RD, Takyar V, Kokkinis A, et al. Nonalcoholic fatty liver disease in spinal and bulbar muscular atrophy. *Neurology* 2017;89:2481-90.
 23. Grundy SM. Metabolic syndrome update. *Trends Cardiovasc Med* 2016;26:364-73.
 24. Allan CA, McLachlan RI. Androgens and obesity. *Curr Opin Endocrinol Diabetes Obes* 2010;17:224-32.
 25. Smith JC, Bennett S, Evans LM, et al. The effects of induced hypogonadism on arterial stiffness, body composition, and metabolic parameters in males with prostate cancer. *J Clin Endocrinol Metab* 2001;86:4261-7.
 26. Wang C, Jackson G, Jones TH, et al. Low testosterone associated with obesity and the metabolic syndrome contributes to sexual dysfunction and cardiovascular disease risk in men with type 2 diabetes. *Diabetes Care* 2011;34:1669-75.
 27. Kalinchenko SY, Tishova YA, Mskhalaya GJ, et al. Effects of testosterone supplementation on markers of the metabolic syndrome and inflammation in hypogonadal men with the metabolic syndrome: the double-blinded placebo-controlled Moscow study. *Clin Endocrinol (Oxf)* 2010;73:602-12.
 28. Zitzmann M, Gromoll J, von Eckardstein A, et al. The CAG repeat polymorphism in the androgen receptor gene modulates body fat mass and serum concentrations of leptin and insulin in men. *Diabetologia* 2003;46:31-9.
 29. Möhlig M, Arafat AM, Osterhoff MA, et al. Androgen receptor CAG repeat length polymorphism modifies the impact of testosterone on insulin sensitivity in men. *Eur J Endocrinol* 2011;164:1013-8.
 30. Lin HY, Xu Q, Yeh S, et al. Insulin and leptin resistance with hyperleptinemia in mice lacking androgen receptor. *Diabetes* 2005;54:1717-25.
 31. Lin HY, Yu IC, Wang RS, et al. Increased hepatic steatosis and insulin resistance in mice lacking hepatic androgen receptor. *Hepatology* 2008;47:1924-35.
 32. Kelly DM, Nettleship JE, Akhtar S, et al. Testosterone suppresses the expression of regulatory enzymes of fatty acid synthesis and protects against hepatic steatosis in cholesterol-fed androgen deficient mice. *Life Sci* 2014;109:95-103.
 33. McInnes KJ, Smiths LB, Hunger NI, et al. Deletion of the androgen receptor in adipose tissue in male mice elevates retinol binding protein 4 and reveals independent effects on visceral fat mass and on glucose homeostasis. *Diabetes* 2012;61:1072-81.

Childhood onset limb-girdle muscular dystrophies in the Aegean part of Turkey

ULUÇ YIŞ¹, GÜLDEN DİNİZ², FİLİZ HAZAN³, HÜLYA SEVCAN DAİMAGÜLER^{4,5},
BAHAR TOKLU BAYSAL⁶, FIGEN BAYDAN², GÜLÇİN AKINCI⁶, AYCAN ÜNALP⁶, GÜL AKTAN⁷,
ERHAN BAYRAM¹, SEMRA HIZ¹, CEM PAKETÇİ¹, DERYA OKUR¹, ERDENER ÖZER⁸,
AYÇA ERSEN DANYELİ⁸, MUZAFFER POLAT⁹, GÖKHAN UYANIK^{10,11} AND SEBAHATTİN ÇIRAK^{4,5}

¹ Dokuz Eylül University, School of Medicine, Department of Pediatrics, Division of Child Neurology, İzmir, Turkey; ² Neuromuscular Disease Center, Tepecik Research Hospital, İzmir, Turkey; ³ Dr Behçet Uz Children's Research Hospital, Department of Medical Genetics, İzmir, Turkey; ⁴ University Hospital Cologne, Department of Pediatrics, Cologne, Germany; ⁵ Center for Molecular Medicine Cologne (CMMC), University of Cologne, Cologne, Germany; ⁶ Dr Behçet Uz Children's Research Hospital, Department of Pediatric Neurology, İzmir, Turkey; ⁷ Ege University, School of Medicine, Department of Pediatrics, Division of Child Neurology, İzmir, Turkey; ⁸ Dokuz Eylül University, School of Medicine, Department of Pathology, İzmir, Turkey; ⁹ Celal Bayar University, School of Medicine, Department of Pediatrics, Division of Child Neurology, Manisa, Turkey; ¹⁰ Center for Medical Genetics, Hanusch Hospital, Vienna, Austria; ¹¹ Medical Faculty, Sigmund Freud Private University, Vienna, Austria

The aim of this study is to analyze the epidemiology of the clinical and genetic features of childhood-onset limb-girdle muscular dystrophies (LGMD) in the Aegean part of Turkey. In total fifty-six pediatric cases with LGMD followed in four different pediatric neurology departments in the Aegean region of Turkey were evaluated. Among them, LGMD2C was the most common followed by LGMD2A, LGMD2D, and LGMD2F with equal frequencies. In twenty-eight patients (50%) the diagnosis could be confirmed by genetic analysis, where *SGCG* proved to be disease-causing in most of the cases. About half of the patients were diagnosed with whole exome or targeted gene sequencing. A positive correlation between muscle biopsy and genetic findings were observed in 11% of the patients. We report one novel frameshifting mutation in *TTN*. Knowledge on frequencies of childhood-onset limb-girdle muscular dystrophies and related genes in Turkey will lead to a prompt diagnosis of these neuromuscular disorders.

Key words: limb-girdle muscular dystrophy, genetic diagnosis, childhood, Turkey

Introduction

Limb-girdle muscular dystrophies (LGMD) are clinically and genetically heterogeneous muscle disorders.

They are inherited in an autosomal recessive or dominant manner. Thirty-three recessively and dominantly inherited forms have currently been identified. The prevalence is about 4-7 per 100.000. They may have childhood, teenage or adulthood onsets. They are clinically characterized by symmetrical weakness of pelvic, scapular and trunk muscles, raised serum creatine kinase levels and dystrophic changes on muscle biopsy (1).

Autosomal recessive muscle disorders like LGMD and congenital muscular dystrophies are common in Turkey due to high rates of consanguineous marriages. Unfortunately, the distribution of subgroups is not well known. The Aegean region is one of seven regions found in Turkey. It is situated in the western part of the country. The region includes 8 provinces and over nine million inhabitants. Having knowledge of specific subgroups of a muscle disease, their related genes and clinical findings in a specific geographic region should alert physicians for prompt disease identification. The aim of this study is to document the clinical findings and related mutations in proven cases of childhood-onset LGMD in the Aegean part of Turkey.

Material and methods

Patients

Patients with childhood onset LGMD clinical features plus confirmed histologic, genetic or histologic plus genetic diagnosis of LGMD of four different child neurology departments (Dokuz Eylül University, Ege University, Izmir Dr. Behçet Uz Children's Hospital, Tepecik Research, and Education Hospital) were included in the study. The individual database was reviewed in all cases. Clinical information including age, gender, family history and consanguinity was recorded. Serum creatine kinase levels, nerve conduction times and electromyographic examinations were also evaluated.

Muscle biopsy

Most of the patients underwent a diagnostic muscle biopsy after written informed consent was obtained. Muscle biopsies were obtained from gastrocnemius or vastus lateralis muscles. The morphological and immunohistochemistry analyses were performed in accordance with standard procedures (Supplement 1).

Genetic analysis

Genomic DNAs were extracted from the remnant muscle tissues or blood samples using available DNA extraction kits (Qiagen, US) following the manufacturer's standard protocol. The exon regions and flanking short intronic sequences of the 4 SGCs genes were amplified using the polymerase chain reaction (PCR), followed by direct sequencing of the PCR products (ABI, US). In addition, the multiplex ligation-dependent probe amplification (MLPA) technique was used for deletion and duplication analysis for patient 13 (2). Patients with nonspecific muscle biopsy findings underwent either whole exome sequencing (WES) (Table 1: patient 7, 8, 11, 12, 14, 21, and 26) or for patient 6, 9, 20, 22-25, 27 and 28 Mendeliome sequencing, which solved 54% of the genetically confirmed cases. For WES, we used the Nimblegen enrichment (SeqCap EZ Human Exome Library v2.00) kit and sequenced on the Illumina HiSeq 2000 with an average mean coverage of 103 fold or we used Agilent SureSelect V6 enrichment kit with an average mean coverage of 82 fold. For the other 10% of the patients, we used targeted gene sequencing on the Illumina TruSight One panel (Mendeliome, Illumina, San Diego, CA, USA) with an average mean coverage of 97 fold. The Cologne Center for Genomics VARBANK pipeline v.2.12 (<https://varbank.ccg.uni-koeln.de/>) was used for genomic data analysis (3-5). All patients were also investigated for dystrophin deletion/duplications by MLPA analysis. If parental or family members were available, we performed co-

segregation studies by using Sanger Sequencing applying standard techniques.

Frequency and descriptive analyses were performed using the statistical software SPSS 9.05 for Windows.

Results

Clinical findings

The study was approved by Dokuz Eylül University School of Medicine Institute's Ethics Committee (No: 24/05/2018; 2018/13-38). Fifty-six patients were evaluated in total. The mean age of patients was 7.92 years (1 to 17). There were 31 boys (55%) and 25 girls (45%). The consanguinity rate was 38%. Patients with *LMNA* and *MYOT* mutations showed the lowest and patients with *SGCG* mutations the highest serum creatine kinase levels. Our patient collective was drawn up out of patients with the following mutations: 24 LGMD2C (43%), 7 LGMD2A (13%), 7 LGMD2E (13%), 6 LGMD2D (11%), 3 LGMD2J (5%), 3 LGMD2K (5%), 1 LGMD1B (2%), 1 LGMD1A (2%), 1 LGMD2B (2%), and 3 unclassified (4%). Difficulty in rising from the floor, delay in motor milestones, muscle weakness and HyperCKemia detected in routine laboratory tests were notable findings. Patients with LGMD2C had a similar disease course as Duchenne muscular dystrophy and all of them had calf hypertrophy. Most of the patients with LGMD2C were non-ambulatory after age 15. HyperCKemia detected in routine laboratory tests and mild proximal muscle weakness were the most common findings in LGMD2A, LGMD2D, and LGMD2E groups. Scapular winging, atrophy in hamstring muscles and Achilles contractures were important clinical clues in advanced stages of LGMD2A patients. Patients with LGMD2K had mild microcephaly, intellectual disability, and generalized muscle hypertrophy. They were slower than their peers. Brain magnetic resonance imaging of these patients was normal. Patients with LGMD2J and LGMD2B presented with HyperCKemia identified during routine laboratory examinations. A fifteen-year-old girl (patient no: 21) with LGMD1B presented with a new onset generalized weakness and she had frequent syncope attacks since early childhood. She had a positive Gower's sign and proximal muscle strength was 4/5 in lower extremities. She had mild pes cavus deformity and deep tendon reflexes were negative. Her serum creatine kinase level was normal but the electromyography recording was myopathic. A first degree atrioventricular block was determined as a cause of syncope attacks. Her mother and aunt were also treated for cardiac arrhythmia. A patient with LGMD1A (patient no: 22) presented mild increased serum creatine kinase level with no clinical findings. However, her mother and uncle had scapulo-

humeral weakness and a Gowers sign. They had a distinctive nasal, dysarthric pattern of speech. They also had reduced deep tendon reflexes. Their electromyography recording showed signs of myopathy. We could not make a subgroup classification in two patients due to lack of all sarcoglycans in one patient and combined deficiency of gamma and alpha deficiency in the other patient. Nerve conduction velocities were normal and electromyography showed myopathic motor unit potentials in all tested patients.

Muscle biopsy findings

52 patients (93%) had a muscle biopsy. 48 of these biopsies (92%) showed dystrophic findings including alteration of myofiber size and shape, splitting, increase in the number of internal nuclei, fiber type disproportions, regeneration and fibrosis. In the remaining four patients, muscle biopsy findings were unremarkable. The diagnosis of these patients with unremarkable biopsy finding were LGMD2C (two patients), LGMD2D (one patient) and LGMD1B (one patient). Three of these patients (LGMD2C and 2D) were asymptomatic at the time of muscle biopsy and muscle biopsy was done due to HyperCKemia (Fig. 1). However, the patient with LGMD1B was symptomatic at the time of muscle biopsy. Genetically, these patients were diagnosed with whole exome sequencing. Expression defects of sarcoglycan staining were as follows: 21 gamma (40%), 6 combined alpha and gamma (12%), 5 calpain (10%), 4 beta (8%), 3 all sarcoglycans (6%), 2 dysferlin (4%) and 1 alpha-dystroglycan (2%). Ten patients (20%) showed normal staining for

sarcoglycans. We could compare muscle biopsy and genetic findings in 27 patients. In terms of dystrophic changes without immunohistochemistry, genetic diagnosis was obtained in 23 of 27 patients. However, the correlation between immunohistochemistry and genetic diagnosis was poor. There was a correlation between genetic diagnosis and immunohistochemistry findings in only 5/27 patients (patient numbers: 1-5). All of these patients had a diagnosis of LGMD2C.

Genetic analysis

In twenty-eight patients (50%) the clinical diagnosis could be confirmed by genetic analysis. 15 of these patients were diagnosed by whole exome sequencing (WES) or targeted gene sequencing. Results of genetic analysis were as follows, given the number of patients: 9 *SGCG* homozygous, 6 *SGCA* (5 homozygous missense mutation and 1 homozygous 7bp-deletion of exon 3), 3 *SGCB* (2 homozygous and 1 whole gene deletion), 3 sibling with a novel *TTN* homozygous, 3 *POMT1* homozygous, 1 *LMNA* heterozygous, 2 *CAPN3* homozygous and 1 *MYOT* heterozygous (Table 1). The mutation c.107163_107167delTACTT (NM_001267550.1) in *TTN* was listed in ClinVar, however, detailed clinical descriptions were not given (www.ncbi.nlm.nih.gov/clinvar/variation/196657/) and there are no scientific publications describing this mutation in *TTN* before, this will be the first report to be published patients with this *TTN* mutation (Fig. 2). MLPA analysis for the detection of deletions, duplications and complex rearrangements in the dystrophin gene were performed and reported as normal for each case.

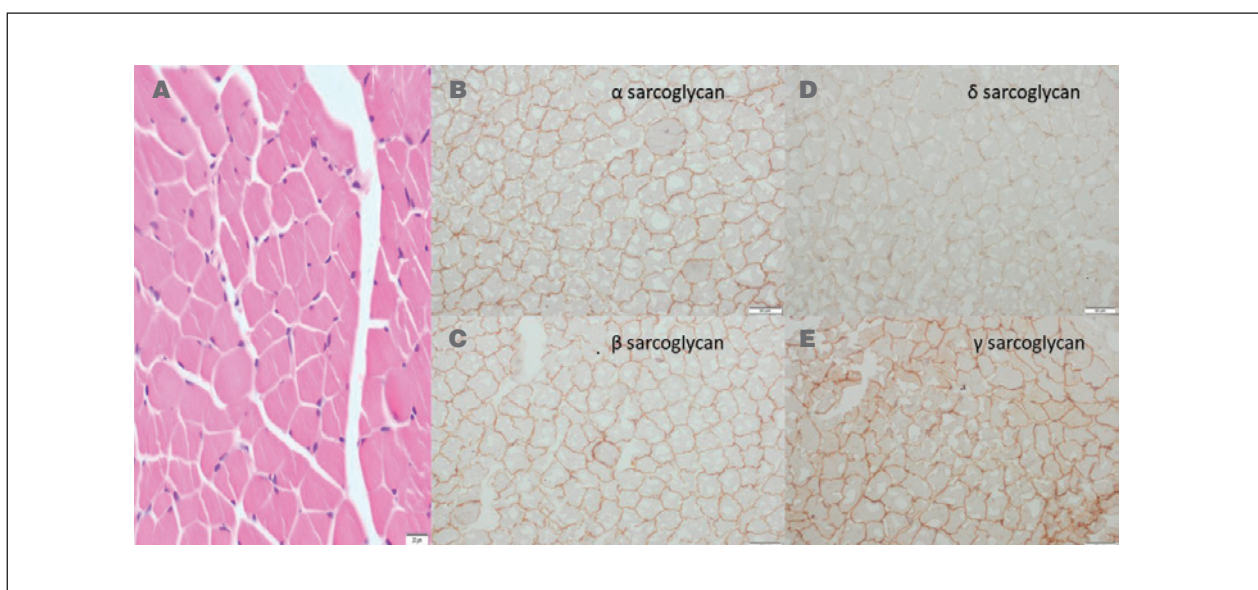


Figure 1. The muscle biopsy of the patient with the genetically confirmed LGMD2D showing no sign of dystrophy (A) and normal expression of all sarcoglycans (B, C, D, E). The biopsy was taken at the age of 8 years.

Discussion

LGMDs are non-syndromic hereditary muscle disorders limited to skeletal muscle. Protein testing by immunostaining or immunoblotting on a muscle biopsy or demonstration of complete or partial deficiencies for a particular protein followed by mutation studies of the corresponding gene(s) may establish the diagnosis in most of the cases (1). However, about 50% of currently identified LGMD would have no molecular diagnosis although all known genes of LGMD were sequenced by traditionally Sanger Sequencing (1). Turkey is a rich genetic pool for neuromuscular disorders. In Turkey, 50% of pediatric muscular disorders consist of patients with Duchenne/Becker muscular dystrophy, which is followed by LGMD2 (20%) and congenital muscular dystrophy (15%) (6). In a large adult neurology clinic in Istanbul, 46% of the patients are diagnosed with Duchenne/Becker muscular dystrophy, followed by facioscapulohumeral dystrophy (FSHD) (18%), myotonic dystrophy (16%) and LGMD2 (14%) (6). Evaluation of 38 LGMD2 families from Turkey showed that calpainopathy and beta-sarcoglycanopathy were the most common subtypes. Gamma sarcoglycanopathy was the third common (7). In our cohort, gamma-sarcoglycanopathy was the most common (44%) followed by calpainopathy, beta- and alpha-sarcoglycanopathy. In this cohort, gamma-sarcoglycanopathy was clinically the most severe group as a whole, whereas dysferlinopathy was the mildest.

Patients with gamma-sarcoglycanopathy had early onset of symptoms resembling Duchenne muscular dystrophy and a progressive decline in motor functions as becoming wheelchair-bound after age 15. All of them also had gastrocnemius hypertrophy as in Duchenne muscular dystrophy.

Mild proximal muscle weakness and increased serum creatine kinase levels incidentally detected during routine laboratory tests were the main presenting findings in calpainopathy, alpha- and beta- sarcoglycanopathy patients. A typical appearance for calpainopathy including generalized atrophy, scapular winging and selective involvement of hamstring muscles were observed in one of the seven patients in our cohort. This was related to his advanced age (17 years old). Patients with dysferlinopathy and LGMD2J were also diagnosed by idiopathic HyperCKemia because symptoms dominantly involving distal muscles occur after adolescence. Mutations of *POMT1* gene typically lead to Walker Warburg syndrome characterized by severe muscle, brain and eye involvement. In 2005, Balci et al. described a form of LGMD2 due to common mutation of *POMT1* gene (p.A200P) characterized by mild mental retardation, microcephaly, and normal brain magnetic resonance imaging, highly elevated serum creatine kinase levels and reduced glycosylation of alpha-dystroglycan in muscle biopsy (8). Our patients with LGMD2K (patient numbers: 26-28) also

had the same clinical findings but we could not show an alpha-dystroglycan deficiency in muscle biopsy due to the lack of antibody at the time of diagnosis. The patients were diagnosed by whole exome sequencing.

We only had two patients in the autosomal dominant group. The patients were clinically asymptomatic only with mildly increased serum creatine kinase levels. They also had a family history of cardiac arrhythmia and cardiomyopathy as expected in LGMD1B. The mother and uncle of the LGMD1A patient had typical scapulohumeral weakness and myopathic electromyography. The cases with LGMD1A and LGMD1B show the importance of family history and examination of other family members in neuromuscular disorders.

Reduced or absent sarcolemmal expression of one of the four sarcoglycans can be found in patients with any type of sarcoglycanopathies and dystrophinopathies. Different patterns of sarcoglycan expression could predict the primary defect but residual sarcoglycan expression could be highly variable and accurate prediction of the genotype could not be achieved in most of the cases. Our study also showed that some patients had combined or total deficiencies of sarcoglycans in muscle biopsies. We reached a certain diagnosis in these patients (patient numbers: 10, 13, 15, 16, 17, 18, 19) with genetic studies but could not classify two patients in a particular group due to lack of genetic studies. Although there was a good correlation between dystrophic findings and genetic analysis, this was not valid for immunohistochemistry findings. All patients with genetic-histologic correlations were in the gamma-sarcoglycanopathy group (patient numbers: 1-5). However, there were also patients with normal immunostaining for gamma-sarcoglycan, but mutations in the *SGCG* gene (patient numbers: 6, 7, 9). On the other hand, there were also patients with all defective sarcoglycans in muscle biopsy and single gene mutation (patient numbers: 8, 10, 13, 15-19). This finding suggests that muscle biopsy is helpful in terms of dystrophy but defective sarcoglycan in muscle biopsy should be confirmed genetically. Interestingly, the muscle biopsy of the index patient with LGMD2J showed dysferlin deficiency. Histologically, the muscle biopsy of this patient only revealed a focus with degenerative and regenerative fibers. In this focus there were macrophages showing myophagia (Fig. 3) However, in the rest of the biopsy there was no prominent difference between the sizes of myofibers. Although the absence of calpain-3 has been documented in association with C-terminal titin mutations due to the loss of calpain-3 binding site in the titin C-terminus, dysferlin deficiency has not been reported before (9). This novel finding reminds us that patients with tibial muscular dystrophy who have dysferlin deficiency in their muscle biopsy but negative genetic analysis results for dysferlin gene should be checked for *TTN* mutations. However, this novel finding should be supported with additional

Table 1. Pathologic findings and mutations of patients with a genetic diagnosis. Following reference sequences have been used for the mutation nomenclature: SGCG NM_000231.2, SGCB NM_000232.4, CAPN3 NM_000070.2; LMNA NM_170707.3, MYOT NM_006790.2, POMT1 NM_007171.3, TTN NM_001267550.1; NA = not applicable, ROH = Regions of Homozygosity are calculated via data analysis pipeline from next-generation sequencing data (<https://varbank.ccg.uni-koeln.de/>), ROH > 200 indicated certain consanguinity of parents.

Patient n.	Dystrophy in muscle biopsy	Defective sarcoglycan in muscle biopsy	Gene	Mutation	Final diagnosis
1/2	Yes	Gamma	<i>SGCG</i>	c.525delT (p.F175Lfs*20)	LGMD2C
3	Yes	Gamma	<i>SGCG</i>	c.848G > A (p.C283Y)	LGMD2C
4/5	Yes	Gamma	<i>SGCG</i>	c.800_801delGT (p.Cys267Serfs*51)	LGMD2C
6	No	Normal	<i>SGCG</i>	c.525delT (p.F175Lfs*20)	LGMD2C
7	Yes	Normal	<i>SGCG</i>	c.525delT (p.F175Lfs*20)	LGMD2C
8	Yes	Normal	<i>SGCG</i>	c.525delT (p.F175Lfs*20)	LGMD2C
9	No	Normal	<i>SGCG</i>	c.101G > A (p.R34H)	LGMD2C
10	Yes	All sarcoglycans	<i>SGCB</i>	c.265G > A (p.V89M)	LGMD2E
11/12	Yes	Normal	<i>CAPN3</i>	c.2243G > A (p.R748Q)	LGMD2A
13	Yes	All sarcoglycans	<i>SGCB</i>	Homozygous whole gene deletion	LGMD2E
14	NA	NA	<i>SGCB</i>	c.919T > C (p.C307R)	LGMD2E
15	Yes	Alpha and gamma	<i>SGCA</i>	c.232_238delTACACCC	LGMD2D
16/17	Yes	Alpha and gamma	<i>SGCA</i>	c.226C > T (p.L76F)	LGMD2D
18/19	Yes	Alpha and gamma	<i>SGCA</i>	c.101G > A (p.R34H)	LGMD2D
20	No	Normal	<i>SGCA</i>	c.850C > T (p.R284C)	LGMD2D
21	No	Normal	<i>LMNA</i>	c.734T > C (p.L245P)	LGMD1B
22	NA	NA	<i>MYOT</i>	c.163T > C (p.S55P)	LGMD1A
23/24/25	Yes	Normal	<i>TTN</i>	c.107163_107167delTACTT (p.F35721Lfs*)	LGMD2J
26	Yes	Normal	<i>POMT1</i>	c.1939G > A (p.A647T)	LGMD2K
27/28	Yes	Normal	<i>POMT1</i>	c.1939G > A (p.A647T)	LGMD2K

	Correlation between gene defect and muscle biopsy	Previously described mutation	Genetic methodology	ClinVar	Allele status of parents (ROH)
	Yes	Yes, reference 10	Sanger sequencing	189243 (Pathogenic)	NA
	Yes	Yes, reference 16	Sanger sequencing	2006 (Pathogenic)	NA
	Yes	Yes, reference 2	Sanger sequencing	Not included	NA
	No	Yes, reference 10	Mendeliome	189243 (Pathogenic)	NA (115)
	No	Yes, reference 10	Whole exome sequencing (Agilent V6r2)	189243 (Pathogenic)	NA (356)
	No	Yes, reference 10	Whole exome sequencing (NimbleGenV2)	189243 (Pathogenic)	Heterozygous (270)
	No	Yes, reference 27	Mendeliome	Not included	Heterozygous (430)
	No	Yes, reference 23	Sanger sequencing	Not included	NA
	No	Yes, references 11,12	Whole exome sequencing (Illumina Nextera)	128670 (Pathogenic-likely pathogenic)	NA
	No	Yes, reference 24	MLPA	NA	NA
	NA	Yes, reference 25	Whole Exome Sequencing (NimbleGenV2)	Not included	Heterozygous (502)
	No	Yes, reference 20	Sanger sequencing	NA	NA
	No	Yes, reference 19	Sanger sequencing	432007 (Pathogenic)	NA
	No	Yes, reference 17	Sanger sequencing	92301 (Likely pathogenic)	NA
	No	Yes, reference 20	Mendeliome	9439 (Pathogenic/likely pathogenic)	Heterozygous (184)
	No	Yes, reference 41	Whole exome sequencing (Agilent V6r2)	Not included	NA (95)
	NA	Yes, reference 43	Mendeliome	Not included	Co-segregation (56)
	No	Novel	Mendeliome	196657 (Pathogenic/likely pathogenic)	NA (385)
	No	Yes, reference 32	Whole exome sequencing (NimbleGenV2)	Not included	Heterozygous (350)
	No	Yes, reference 32	Mendeliome	Not included	Heterozygous (592)

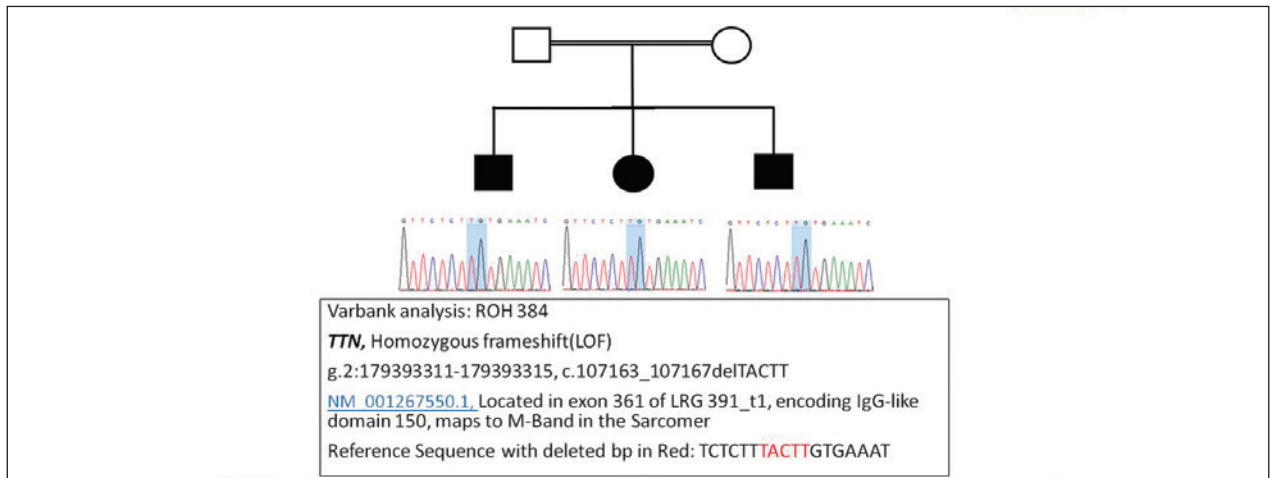


Figure 2. Pedigree of the family with TTN mutation. Homozygous frameshift mutation, g.2:179393311-179393315, c.107163_107167delTACTT, NM_001267550.1, Located in exon 361 of LRG 391_t1, encoding IgG-like domain 150, maps to M-Band in the Sarcomer, reference Sequence with deleted bp kursiv: TCTCTTACTTGTGAAAT.

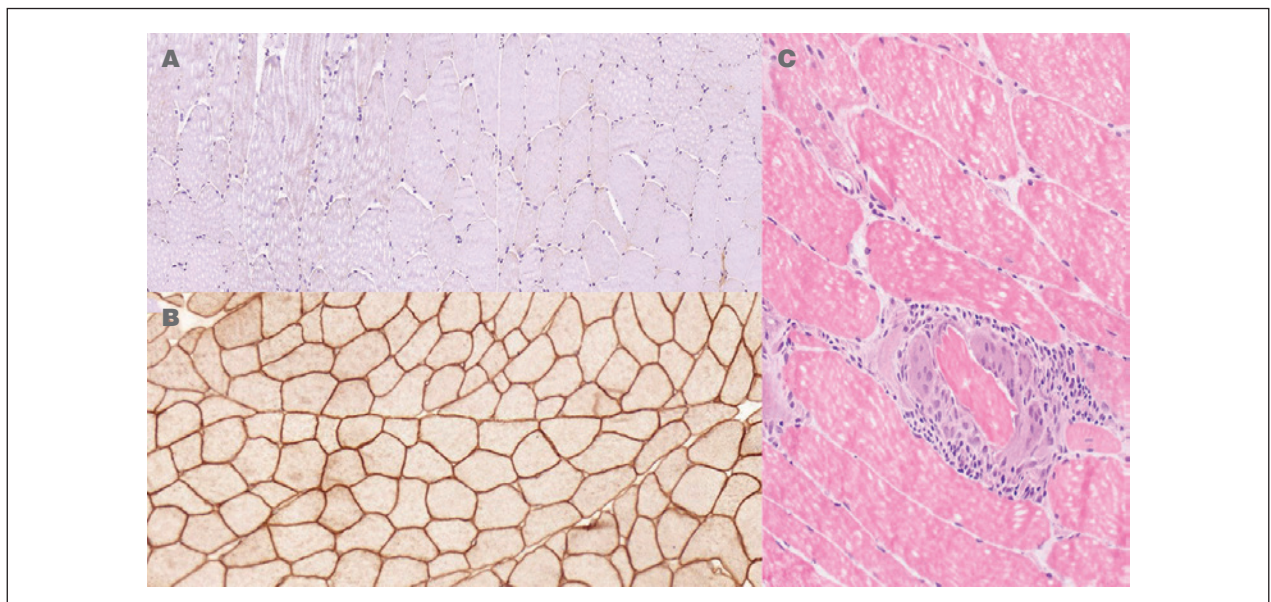


Figure 3. The muscle biopsy of the index patient showed a complete deficiency of dysferlin immunohistochemically **(A)**. The positive simultaneously stained control slide of another patient's biopsy reveals a complete sarcolemmal staining of the dysferlin antibody **(B)**. There was only one focus with degenerative and regenerative fibers. In this focus, there were also macrophages showing myophagia **(C)**. The muscle biopsy was taken at the age of 17 years from the left quadriceps femoris.

cases and functional studies in muscle biopsy. So it remains speculative if this is correct or not.

The autosomal recessive forms represent more than 90% of all LGMDs. LGMD2A or calpainopathy is considered to be the most common form of recessive LGMD in most populations, accounting for about 30-40% of the patients (10). The c.550delA is the most common mutation

among patients from different European populations (11). A founder effect for the c.550delA has been reported in some populations like Russia, Croatia, Bulgaria, Northern Italy and Turkey (10, 12). In 1997, the CAPN3 mutation was detected in 10 families from Turkey with LGMD2A. The c.550delA mutation was detected in the half of the families (13). In 2006, Balci et al. revealed 93 Turkish LGMD2

families and detected *CAPN3* mutations in 29 patients from 21 families (10). In this study, c.550delA mutation was the most common followed by c.1469G>A (p.R490Q) mutation. In our study, we detected c.2243G>A (p.R748Q) mutation in two siblings. This mutation had been reported in several Spanish patients and also previously in one patient from Turkey (13, 14).

The four common types of LGMD are called sarcoglycanopathies; LGMD2C (*SGCG*), LGMD2D (*SGCA*), LGMD2E (*SGCB*) and LGMD2F (*SGCD*) (15). The frequencies of mutations in *SGCA* and *SGCD* are respectively the highest and lowest in most populations. A clinical study from Iran evaluating 25 sarcoglycanopathy patients showed that more than the half of the patients had *SGCB* mutations followed by *SGCG* (28%), *SGCD* (12%) and *SGCA* (4%) mutations (16). In India, mutation frequencies regarding sarcoglycanopathies were reported as *SGCG* 44.4%, *SGCD* 27.8% and *SGCB* 5.6% (12). In our study *SGCG* mutation (9 patients, 31%) was the most common. The frequencies of *SGCA* and *SGCB* mutations were 20% (6 patients) and 10% (3 patients), respectively. Mutations in sarcoglycan genes are commonly small defects, such as short deletions/insertions or single nucleotide substitutions (17). The majority of sarcoglycanopathies are associated with missense mutations but large deletions had also been reported (18, 19). More than 70 pathogenic mutations had been described in *SGCA* (20). The most common mutation of this gene is p.R77C which has a founder effect in Finland and Magdalen (12). This mutation was also reported as a founder mutation in several LGMD2D patients from Europe and also Brazil (20). Other founder mutations are p.R34L in Taiwan and p.R192* in Egypt (10). In our LGMD2D patients, we found five different mutations in 6 patients. These mutations had previously been described (2, 19, 21-23). LGMD2E is a clinically heterogeneous disorder associated with missense, truncating and deletion mutations in *SGCB* located on the 4q12 chromosomal region. Large homozygous microdeletion of chromosome 4q11-q12 and isolated exon deletion had also been reported (24). The founder mutations of *SGCB* are c.377_384dup in Northern Italy and p.T151R in Amish population. The p.M1L, p.Q11*, p.V89M, p.I92T, p.I92S and c.739insA mutations had been reported from Turkey (25). In this study, the patient with whole gene deletion (patient no: 13) had previously been reported by Diniz et al. (26). The p.V89M mutation (1 patient) had been reported in the Turkish population and p.C307R mutation (1 patient) had been presented as a poster presentation in 1st National Neuromuscular Disease Congress in Ankara, 2017 (25, 27). The reported founder mutations of *SGCG* are c.525delT in North Africans, p.C283Y in Roma Gypsies and c.87insT in Northern Italy. Especially the high prevalence of the c.525delT mutation, which is also called the Maghrebian form (formerly name delta521T) present as a founder

mutation in North Africa and Spain, can be an indicator of the migratory movement in Mediterranean Sea. (6). The frameshift mutation c.800_801GT (formerly 923-924TG) in the (TG) 4 repeat in the 3' coding area and deletion of exon 5 of the *SGCG* gene (formerly described as 510del120) had been reported from Turkey (13, 28). Another study evaluating 20 LGMD2C patients from Turkey showed most patients had silent homozygous or heterozygous mutations (2). In our study, 5 mutations were found in 9 patients. The most common mutation was c.525delT which was found in 5/9 patients. Patients with c.800_801delGT mutations had been reported previously (2). Additionally, p.C283Y (1 patient) and p.R34H (1 patient) mutations had also been described previously (18, 29).

Titin is a giant muscle protein expressed in cardiac and striated muscles. It spans half of the sarcomere from Z line to M line. It plays major functions in muscle assembly, force transmission and maintenance of resting tension. Its gene is located on 2q31.2 and encodes the largest protein of the human genome (15). More than 230 mutations of *TTN* have been reported in human gene mutation database (HGMD) (30). Mutations of this gene cause tibial muscular dystrophy, dilated cardiomyopathy 1G, familial hypertrophic cardiomyopathy 9, early onset myopathy with fatal cardiomyopathy, proximal myopathy with early respiratory muscle involvement and LGMD2J (15). Symptoms in LGMD2J start in the first or second decade and progresses over the next 20 years to wheelchair confinement. We detected a novel homozygous mutation c.107163_107167delTACTT (NM_001267550.2) in three siblings (patient number: 23-25). The index patient was diagnosed due to idiopathic HyperCKemia. She is currently 17 years old. The symptoms started at the age of 14 years. She has symmetric weakness prominent in distal lower extremity muscle and she has difficulty while walking on heels. Upper extremity, axial and facial muscles are not involved. There are no signs of cardiac and respiratory dysfunctions. Serum creatine kinase level is 2939 IU/L. Her younger siblings are asymptomatic.

Mutations in *POMT1*, which mapped to chromosome 9q34.13, are related to autosomal recessive muscular dystrophies which include three subgroups as MDDGA1, MDDGB1 and MDDGC1 (also known as LGMD2K) (31). The Walker-Warburg syndrome (WWS) is the most severe phenotype but patients with milder mutations in *POMT1* might present with milder forms of LGMD (31). While there is not any clear genotype-phenotype correlation, the variable phenotypic severity can be related to the type and location of the mutations (31). The *POMT1* protein has loops within the lumen (loops 1, 3 and 5) and within the cytoplasm (loops 2, 4 and 6). Patients with mutations only affecting the loops within the cytoplasm are more likely to show the milder phenotype of LGMD. Mutations affecting the transmembrane domains, loop 1 and loop 5 within the lumen of the

endoplasmic reticulum are associated with the more severe clinical presentation of congenital muscular dystrophy (32). Two *POMT1* mutations had been reported from Turkey. One of them was a p.R514* mutation in a patient with Walker-Warburg syndrome. This mutation affects the loop of protein within the lumen of the endoplasmic reticulum (33). The other reported mutation was p.A200P mutation leading to a significantly milder clinical phenotype with predominant muscular dystrophy and mild intellectual disability, but without obvious brain malformations (8). The second reported mutation affects the part of protein within the cytoplasm. Herein we reported three patients (patient number: 26-28) with a previously reported homozygous p.A647T mutation which affects loop 6 (34). They shared a similar phenotype with patients reported by Balci et al. in 2005 (8).

LGMD1B is caused by *LMNA* which is located on 1q22.15. Mutations of this gene are associated with a wide range of disease phenotypes, ranging from cardiac, neuromuscular and metabolic disorders to premature aging syndromes. Muscular dystrophies associated with *LMNA* are autosomal dominant Emery-Dreifuss muscular dystrophy, a form of congenital muscular dystrophy and LGMD1B. It is difficult to establish a correlation between phenotype and genotype (35). However, these clinical entities can be determined by the same *LMNA* mutation and coexist in the context of the same family (36). Some *LMNA* mutations had been reported from Turkey before. The p.Glu31del mutation had been reported in a patient with *LMNA*-CMD and others including p.D47N, p.R349W, p.R482W, p.A527H, and p.A529V had been reported in patients with lipodystrophy mandibuloacral dysplasia (37-42). Herein we reported *LMNA* mutations in a patient with LGMD1B for the first time from Turkey (patient number: 21). The mutations p.L245P been reported as a poster presentation in 12th European Pediatric Neurology Congress in Lyon/France. The phenotype of this patient included proximal muscle weakness with normal serum creatine kinase, pes cavus, foot-drop gait, absent deep tendon reflexes and first degree A-V block (43).

LGMD1A is caused by mutations in *MYOT* gene localized on the 5q31.2 chromosomal region. Mutation of *MYOT* also causes myofibrillar myopathy (44). We detected p.S55F mutation in one patient (patient number: 22). This young girl had mild serum creatine kinase elevation but had no clinical findings of a muscle disease yet. However, her mother and uncle had typical findings of LGMD1A. This mutation had also previously been reported in an Argentinian family with LGMD1A (45). The clinical findings in the Argentinian family started by 42-58 years of age with proximal leg and arm weakness which later progressed to distal weak-

ness. Half of the patients had dysarthric speech and serum CK levels were elevated to 5-fold to 15-fold. The clinical findings of the index case's mother and uncle were similar in this family, however, symptoms started in the second decade. Their serum CK never exceeded 1000 IU/l.

Gamma sarcoglycanopathies were the most common LGMD in Aegean part of Turkey like Spain and North Africa. For example in Tunisia, the frequency of LGMD2 is higher than for dystrophinopathies and LGMD2C is the most common type (6). About 90% of the cases with LGMD2C carry c.525delT exon 6 founder mutation. In the Catalan part of Spain, LGMD2C is the most common type of LGMD2 and interestingly 50% of their gamma-sarcoglycan mutations is the Maghrebian form as c.525delT (6). In our study, 55% of our cases with LGMD2C also carried c.525delT mutation. These findings suggest that the Aegean part of the Turkey has probably been influenced by migrations in the Mediterranean sea from a genetic epidemiologic point of view.

SGCA, *SGCB*, *SGCD*, *SGCG*, *CAPN3*, *LMNA*, and *POMT1* mutations have been reported in LGMD patients from Turkey (2, 7, 8, 10, 13, 20, 21, 26-28). Rare types of childhood-onset LGMD2 due to mutations of *TRAPPC11*, *POMK*, and *PLEC* were also reported from Turkey (46-48). Molecular genetic diagnosis of LGMD remains challenging. Recently, clinicians consider multi-gene panels or whole exome sequencing (WES) for genetic diagnosis of LGMD. The diagnostic rate of WES ranges between 34% and 45% (49). Next-generation sequencing has the advantage of detecting a mutation in a very large gene like *TTN* (50). In our cohort, more than half of the cases with the genetic diagnosis had been solved by WES.

In conclusion, LGMD2C is the most common LGMD2 in the Aegean part of Turkey. Most of the childhood cases present with mild proximal muscle weakness and increased serum creatine kinase levels detected during routine laboratory examinations. Results of immunostaining of muscle biopsies should be confirmed with molecular genetic testing because there is a very limited correlation between immunohistochemical and genetic findings. Whole exome sequencing confirms the diagnosis in most of the cases with nonspecific clinical and muscle biopsy findings.

Acknowledgments

SC received funding from Muscular Dystrophy Association (Developmental Grant) and the Deutsche Forschungsgemeinschaft Emmy Noether Grant (CI 218/1-1).

Supplement 1

Details of muscle biopsy

Samples were frozen in isopentane cooled in liquid nitrogen and 8 to 12 micron sections were cut using the cryostat. Slides were stained with hematoxylin&eosin, Gomori's trichrome, modified Gomori's trichrome (Engel-Cunningham modification), oil red-O, Periodic Acid Schiff (PAS), d-PAS, crystal violet stains. For enzyme histochemical techniques we used nicotinamide adenine dinucleotide tetrazolium reductase (NADH-TR), succinate dehydrogenase (SDH), cytochrome oxidase (COX) and combined COX-SDH stains. Spectrin (Novo-castra, UK, NCL-spec1), dystrophin N-terminus (Novo-castra, UK, NCL-dys3), adhalin (Novocastra, UK, NCL-a-sarc), other sarcoglycans (beta, delta, gamma; Novo-castra, UK, NCL-b-d-g-sarc), laminin alpha-2 chain (Novo-castra, UK, NCL-merosin), myotilin (Novo-castra, UK, NCL-myotilin), collagen VI (Novocastra, UK, NCL-

COLL-vI), β -dystroglycan (Novocastra, UK, NCL-b-DG), HLA Class I (Novo-castra, UK, NCL-HLA-ABC), NCAM (ThermoScientific, CA, USA, CD56), nitric oxide synthase-1 (Novo-castra, UK, NCLNOS-1), emerin (Novo-castra, UK, NCL-emerin), caveolin 3 (Novus Biologicals, CA, USA, NB110-5029), calpain 3 (Abcam, Cambridge, UK, ab103250) and dysferlin (Novo-castra, UK, NCL-Hamlet-2) antibodies were used by standard techniques for immunohistochemical analyses. Myosin heavy chain fast (Novo-castra, UK, NCL-MHCf) antibody was used for discriminating between fiber types, and myosin heavy chain neonatal (Novo-castra, UK, NCL-MHCn) antibody was used for identification of immature fibers. Monoclonal antibodies against T-cells (CD3), B-cells (CD 20), macrophages (CD68), suppressor T cells (CD8) and helper T cells (CD4) were used in selected cases for the identification of the inflammatory cell spectrum (2).

References

- Vissing J. Limb girdle muscular dystrophies: classification, clinical spectrum and emerging therapies. *Curr Opin Neurol* 2016;29:635-41.
- Diniz G, Hazan F, Yildirim HT, et al. Histopathological and genetic features of patients with limb girdle muscular dystrophy type 2C. *Turk Patoloji Derg* 2014;30:111-7.
- Yis U, Baydan F, Karakaya M, et al. Importance of skin changes in the differential diagnosis of congenital muscular dystrophies. *Biomed Res Int* 2016;2016:3128735.
- Bamborschke D, Pergande M, Becker K, et al. A novel mutation in sphingosine-1-phosphate lyase causing congenital brain malformation. *Brain Dev* 2018;40:480-3.
- Wunderlich G, Brunn A, Daimagüler HS, et al. Long term history of a congenital core-rod myopathy with compound heterozygous mutations in Nebulin gene. *Acta Myol* 2018;37:121-7.
- Topaloglu H. Epidemiology of muscular dystrophies in the Mediterranean area. *Acta Myol* 2013;32:138-41.
- Dincer P, Akcoren Z, Demir E, et al. A cross section of autosomal recessive limb-girdle muscular dystrophies in 38 families. *J Med Genet* 2000;37:361-7.
- Balci B, Uyanik G, Dincer P, et al. An autosomal recessive limb girdle muscular dystrophy (LGMD2) with mild mental retardation is allelic to Walker-Warburg syndrome (WWS) caused by a mutation in the *POMT1* gene. *Neuromuscul Disord* 2005;15:271-5.
- Harris E, Topf A, Vihola A, et al. A 'second truncation' in *TTN* causes early onset recessive muscular dystrophy. *Neuromuscul Disord* 2017;27:1009-17.
- Balci B, Aurino S, Haliloglu G, et al. Calpain-3 mutations in Turkey. *Eur J Pediatr* 2006;165:293-8.
- Angelini C, Fanin M. Calpainopathy. In: Adam MP, Ardinger HH, Pagon RA, et al., Eds. *GeneReviews*(R). Seattle (WA) 1993-2018. 2005 May 10 [updated 2017 Aug 3]
- Khadilkar SV, Faldu HD, Patil SB, et al. Limb-girdle muscular dystrophies in India: a review. *Ann Indian Acad Neurol* 2017;20:87-95.
- Dincer P, Leturcq F, Richard I, et al. A biochemical, genetic, and clinical survey of autosomal recessive limb girdle muscular dystrophies in Turkey. *Ann Neurol* 1997;42:222-9.
- Saenz A, Leturcq F, Cobo AM, et al. LGMD2A: genotype-phenotype correlations based on a large mutational survey on the calpain 3 gene. *Brain* 2005;128:732-42.
- Nigro V, Savarese M. Genetic basis of limb-girdle muscular dystrophies: the 2014 update. *Acta Myol* 2014;33:1-12.
- Alavi A, Esmaeili S, Nilipour Y, et al. LGMD2E is the most common type of sarcoglycanopathies in the Iranian population. *J Neurogenet* 2017;31:161-9.
- Giugliano T, Fanin M, Savarese M, et al. Identification of an intragenic deletion in the *SGCB* gene through a re-evaluation of negative next generation sequencing results. *Neuromuscul Disord* 2016;26:367-9.
- Sandona D, Betto R. Sarcoglycanopathies: molecular pathogenesis and therapeutic prospects. *Expert Rev Mol Med* 2009;11:e28.
- Trabelsi M, Kavian N, Daoud F, et al. Revised spectrum of mutations in sarcoglycanopathies. *Eur J Hum Genet* 2008;16:793-803.
- Reddy HM, Hamed SA, Lek M, et al. Homozygous nonsense mutation

- in *SGCA* is a common cause of limb-girdle muscular dystrophy in Assiut, Egypt. *Muscle Nerve* 2016;54:690-5.
21. Diniz G, Tosun Yildirim H, Akinci G, et al. Sarcolemmal alpha and gamma sarcoglycan protein deficiencies in Turkish siblings with a novel missense mutation in the alpha sarcoglycan gene. *Pediatr Neurol* 2014;50:640-7.
 22. Diniz G, Tosun Yildirim H, Gokben S, et al. Concomitant alpha- and gamma-sarcoglycan deficiencies in a Turkish boy with a novel deletion in the alpha-sarcoglycan gene. *Case Rep Genet* 2014;2014:248561.
 23. Stehlikova K, Skalova D, Zidkova J, et al. Autosomal recessive limb-girdle muscular dystrophies in the Czech Republic. *BMC Neurol* 2014;14:154.
 24. Ghafouri-Fard S, Hashemi-Gorji F, Fardaei M, et al. Limb girdle muscular dystrophy type 2E due to a novel large deletion in *SGCB* gene. *Iran J Child Neurol* 2017;11:57-60.
 25. Balci B, Wilichowski E, Haliloglu G, et al. Beta-sarcoglycan gene mutations in Turkey. *Acta Myol* 2004;23:154-8.
 26. Diniz G, Tekgul H, Hazan F, et al. Sarcolemmal deficiency of sarcoglycan complex in an 18-month-old Turkish boy with a large deletion in the beta sarcoglycan gene. *Balkan J Med Genet* 2015;18:71-6.
 27. Kirik S, Ozgur B, Isikay S, et al. Limb girdle 2E tanılı hastada *SGCB* geninde tanımlanan yeni mutasyon. 1.Ulusal Nöromuskuler Hastalıklar Kongresi Bildiri Kitabı, 2017, s28.
 28. Dincer P, Piccolo F, Leturcq F, et al. Prenatal diagnosis of limb-girdle muscular dystrophy type 2C. *Prenat Diagn* 1998;18:1300-3.
 29. Piccolo F, Jeanpierre M, Leturcq F, et al. A founder mutation in the gamma-sarcoglycan gene of gypsies possibly predating their migration out of India. *Hum Mol Genet* 1996;5:2019-22.
 30. Wu L, Xiang B, Zhang H, et al. Three novel recessive mutations in *LA-MA2*, *SYNE1*, and *TTN* are identified in a single case with congenital muscular dystrophy. *Neuromuscul Disord* 2017;27:1018-22.
 31. Hu P, Wu S, Yuan L, et al. Compound heterozygous *POMT1* mutations in a Chinese family with autosomal recessive muscular dystrophy-dystroglycanopathy C1. *J Cell Mol Med* 2017;21:1388-93.
 32. Wallace SE, Conta JH, Winder TL, et al. A novel missense mutation in *POMT1* modulates the severe congenital muscular dystrophy phenotype associated with *POMT1* nonsense mutations. *Neuromuscul Disord* 2014;24:312-20.
 33. Yis U, Uyanik G, Kurul S, et al. A case of Walker-Warburg syndrome resulting from a homozygous *POMT1* mutation. *Eur J Paediatr Neurol* 2007;11:46-9.
 34. Endo T, Many H, Seta N, et al. *POMGnT1*, *POMT1*, and *POMT2* mutations in congenital muscular dystrophies. *Methods Enzymol* 2010;479:343-52.
 35. Madej-Pilarczyk A, Niezgoda A, Janus M, et al. Limb-girdle muscular dystrophy with severe heart failure overlapping with lipodystrophy in a patient with *LMNA* mutation p.Ser334del. *J Appl Genet* 2017;58:87-91.
 36. Maggi L, Carboni N, Bernasconi P. Skeletal muscle laminopathies: a review of clinical and molecular features. *Cells* 2016;5.
 37. Garg A, Cogulu O, Ozkinay F, et al. A novel homozygous Ala529Val *LMNA* mutation in Turkish patients with mandibuloacral dysplasia. *J Clin Endocrinol Metab* 2005;90:5259-64.
 38. Demir T, Onay H, Savage DB, et al. Familial partial lipodystrophy linked to a novel peroxisome proliferator activator receptor -gamma (*PPARG*) mutation, H449L: a comparison of people with this mutation and those with classic codon 482 Lamin A/C (*LMNA*) mutations. *Diabet Med* 2016;33:1445-50.
 39. Kutbay NO, Yurekli BS, Onay H, et al. A case of familial partial lipodystrophy caused by a novel lamin A/C (*LMNA*) mutation in exon 1 (D47N). *Eur J Intern Med* 2016;29:37-9.
 40. Ozer L, Unsal E, Aktuna S, et al. Mandibuloacral dysplasia and *LMNA* A529V mutation in Turkish patients with severe skeletal changes and absent breast development. *Clin Dysmorphol* 2016;25:91-7.
 41. Karaoglu P, Quizon N, Pergande M, et al. Dropped head congenital muscular dystrophy caused by de novo mutations in *LMNA*. *Brain Dev* 2017;39:361-4.
 42. Akinci B, Onay H, Demir T, et al. Clinical presentations, metabolic abnormalities and end-organ complications in patients with familial partial lipodystrophy. *Metabolism* 2017;72:109-19.
 43. Celebi HBG, Ayca S, Polat M, et al. A novel de novo missense *LMNA* mutation in a Turkish patient with laminopathies. *Eur J Paediatr Neurol* 2017;21:227.
 44. Selcen D, Engel AG. Myofibrillar Myopathy. In: Adam MP, Ardinger HH, Pagon RA, et al., Eds. *GeneReviews* (R). Seattle (WA)1993-2018. 2005 Jan 28 [updated 2012 Oct 29].
 45. Hauser MA, Conde CB, Kowaljow V, et al. Myotilin mutation found in second pedigree with *LGMD1A*. *Am J Hum Genet* 2002;71:1428-32.
 46. Gundesli H, Talim B, Korkusuz P, et al. Mutation in exon 1f of *PLEC*, leading to disruption of plectin isoform 1f, causes autosomal-recessive limb-girdle muscular dystrophy. *Am J Hum Genet* 2010;87:834-41.
 47. Ardicli D, Gocmen R, Talim B, et al. Congenital mirror movements in a patient with alpha-dystroglycanopathy due to a novel *POMK* mutation. *Neuromuscul Disord* 2017;27:239-42.
 48. Koehler K, Milev MP, Prematilake K, et al. A novel *TRAPPC11* mutation in two Turkish families associated with cerebral atrophy, global retardation, scoliosis, achalasia and alacrima. *J Med Genet* 2017;54:176-85.
 49. Ghaoui R, Cooper ST, Lek M, et al. Use of whole-exome sequencing for diagnosis of limb-girdle muscular dystrophy: outcomes and lessons learned. *JAMA Neurol* 2015;72:1424-32.
 50. Harris E, Topf A, Barresi R, et al. Exome sequences versus sequential gene testing in the UK highly specialised Service for Limb Girdle Muscular Dystrophy. *Orphanet J Rare Dis* 2017;12:151.

LGMD1D myopathy with cytoplasmic and nuclear inclusions in a Saudi family due to DNAJB6 mutation

SAEED A. BOHLEGA¹, SARAH ALFAWAZ¹, HUSSAM ABOU-AL-SHAAR², HINDI N. AL-HINDI³, HATEM N. MURAD¹, MOHAMED S. BOHLEGA¹, BRIAN F. MEYER^{4,5} AND DOROTA MONIES^{4,5}

¹ Division of Neurology, Department of Neurosciences, King Faisal Specialist Hospital and Research Centre, Riyadh, Saudi Arabia; ² Department of Neurosurgery, Hofstra Northwell School of Medicine, Manhasset, New York, USA; ³ Department of Pathology & Laboratory Medicine, King Faisal Specialist Hospital & Research Centre, Riyadh, Saudi Arabia; ⁴ Department of Genetics, King Faisal Specialist Hospital & Research Centre, Riyadh, Saudi Arabia; ⁵ Saudi Human Genome Program, King Abdulaziz City for Science and Technology, Riyadh, Saudi Arabia

Autosomal dominant LGMD1D has been described in multiple families in Asia, Europe, and USA. However, to the best of our knowledge, no cases of LGMD1D have been reported among native Bedouin Saudi families. Fifty Saudi families with LGMD were analyzed and the causative underlying genes were studied utilizing genome wide linkage, homozygosity mapping, and neurological gene panel. We identified one family of a Bedouin origin with LGMD1D. Two patients had progressive proximal and distal weakness, dysphagia, and respiratory symptoms. Creatinine kinase was normal. Muscle biopsy showed marked variation in myofibers size with scattered angular atrophic fiber, necrotic fibers, and myophagocytosis, with red-rimmed vacuoles depicting a sarcoplasmic body. Heterozygous c.C287T (p.P96L) variant in exon 5 of *DNAJB6* (NM_005494) gene was found. This change is localized within glycine and phenylalanine rich domain and alter an amino acid residue. Our findings will expand on the existing genotypic and phenotypic spectrum of this disorder and aid in elucidating hidden mechanisms implicated in LGMD1D.

Key words: DNAJB6, LGMD1D, LGMD, Saudi Arabia, cytoplasmic inclusion, muscular dystrophy

Introduction

Limb girdle muscular dystrophies (LGMD) are not commonly encountered in clinical practice. Only scarce reports of LGMD originated from the Middle East or Arabic countries have been described in the literature (1, 2). LGMD has been classified to different subtypes based on the genetic mutations responsible for the disease, encompassing a genetically

and phenotypically heterogeneous group of disorders. Autosomal dominant LGMD1D is relatively rare, accounting for only 5-10% of all LGMD cases (3). Recently, mutations in the DnaJ homolog, subfamily B, member 6 (*DNAJB6*) gene have been described in patients with LGMD1D (OMIM 603511) (4-15). Patients with LGMD1D typically present with progressive proximal muscle weakness manifesting as slow exercise pace and capacity in late teens. A few patients may have additional features of distal weakness, dysphagia, and respiratory weakness (8, 10, 12-15).

Autosomal dominant LGMD1D has been described in multiple families in Asia, Europe, and USA (4-15). However, to the best of our knowledge, no cases of LGMD1D have been reported among native Bedouin Saudi families. Utilization of next generation sequencing technology might lead to an accurate estimation of the true prevalence of this disease in Saudi Arabia by potentially classifying more cases of undiagnosed muscular dystrophies (2). Herein, we report the first identified native Saudi Bedouin family with LGMD1D due to heterozygous mutation in *DNAJB6* gene (NM_005494:c.C287T;p.P96L).

Materials and methods

Patients inclusion

The Institutional Review Board granted approval of this study and informed consent was obtained from all par-

Address for correspondence: Saeed A. Bohlega, MD, FRCPC, FAAN, Division of Neurology, Department of Neurosciences, King Faisal Specialist Hospital and Research Centre, P.O. Box: 3354; Riyadh 11211, Saudi Arabia. Tel. +966-11-464-7272, Ext: 32819. Fax +966-11-442-4763. E-mail: boholega@kfshrc.edu.sa

ticipants. The study was approved by Hospital Research Advisory Council and Ethical Committee. A cohort of 50 Saudi Arabian families with LGMD were enrolled for this study under an IRB-approved protocol (RAC# 2070005). All patients were examined at the Neuromuscular Clinic in the Department of Neurosciences, King Faisal Specialist Hospital and Research Center (KFSH&RC) over a period of 12 years and recruited for this study to identify the causative underlying genes utilizing a genome wide linkage, homozygosity mapping, and neurological gene panel. We performed a retrospective review of the electronic medical records and charts of this Arabian family and obtained patient demographic and clinical data from the medical records for the entire family. History was taken, and clinical examination was performed on the affected cases and their family members. Magnetic resonance imaging (MRI) was obtained for the affected patients.

Neurological gene panel sequencing & analysis

Ten nanograms of DNA sample was treated to obtain the Ion Proton AmpliSeq library. DNA amplification required two pools of primers to cover all 768 known OMIM genes associated with neurological disorders. The library was further used in a batch of 24 normalized to 100pM samples which were pooled in equal ratios for emulsion PCR (ePCR) on Ion OneTouch™ System followed by the enrichment process using the Ion OneTouch™ ES, both procedures following the manufacturer's instructions (Thermo Fisher, Carlsbad, CA, USA). The template-positive Ion PI Ion Sphere particles were processed for sequencing on the Ion Proton instrument (Thermo Fisher, Carlsbad, CA, USA). Reads were mapped to UCSC hg19 (<http://genome.ucsc.edu/>) and variants identified using the Ion Torrent pipeline (Thermo Fisher, Carlsbad, CA, USA). The resultant variant caller file (vcf) was filtered using the Saudi Human Genome Program pipeline (16). Causative variant was validated by Sanger sequencing and further vetted for familial segregation based upon autosomal dominant inheritance.

Results

Clinical data

The family reported in this paper is a native Bedouin Arab originated from Northern Province of Saudi Arabia. The parents were first cousins and the sibships consisted only of 1 male.

Case 1: The proband is a 25-year-old male with a history of exertional dyspnea and proximal muscle weakness was referred to our service for further investigation and management. The patient noted that he was a slow runner

in his teens, which progressed to difficulty climbing stairs at the age 20. This was also associated with difficulty getting up from a sitting position with complete Gower maneuver at age 23. He also complained of dysphagia to both solids and liquids with frequent choking episodes and a nasal speech character. His symptoms were slowly progressive initially; however, they progressed more rapidly during the past 2 years, mainly with worsening lower limb weakness and noticeable involvement of the distal upper limbs and atrophy of the hands and forearms. Currently the patient is ambulating without assistance and able to perform activities of daily living independently.

Hypernasality was noticed on examination. Upper limb examination demonstrated wasting of the small muscles of the hands (i.e. the dorsal interossei and the thenar and hypothenar muscles) (Figs. 1A-B). Motor examination revealed bilateral proximal muscle power of 4/5 and distal power of 3/5 in the Medical Research Council (MRC) scale. No significant atrophy was present in the lower limbs. His lower limbs' proximal power was 4/5 and distal power was 3/5. Notably, the patient had difficulty squatting. The patient was unable to walk on his heels or his toes; however, he was able to bear weight during these positions. The rest of his examination was unremarkable.

Creatinine kinase (CK) level was up to 195 IU and pulmonary function test was within normal limits. Electrophysiologic studies including nerve conduction study (NCS) and electromyography (EMG) showed clear myopathic features of motor units. T1-weighted MRI of the lower extremities depicted chronic atrophic changes in the gastrocnemius and peroneous muscles. T2-weighted images with fat saturation demonstrated symmetrical involvement of the posterior compartment (i.e. soleus, tibialis posterior, flexor digitorum longus, and flexor Hallusis longus muscles) with high signal intensity. Right-sided tibialis anterior showed myoedema and was characteristically more involved than its left-sided counterpart (Figs. 1C-D-E).

A muscle biopsy showed moderate to marked variation in myofiber size with scattered atrophic fibers having elongated and angular contours (Fig. 2A). There was also a rare necrotic fiber, mild endomysial (interstitial) fibrosis, and fatty infiltration. Scattered fibers with eosinophilic cytoplasmic inclusions and rimmed vacuoles were noted. These vacuoles stained negatively with acid phosphatase and congo red stains. The vacuoles were rimmed with the modified Gomori trichrome stain (Fig. 2B). The NADH-TR reaction revealed a disorganized intermyofibrillar network resulting in a "moth-eaten" appearance (Fig. 2C). Immunohistochemical staining for the slow and fast myosin heavy chains isoforms revealed predominance of slow (type 1) myofibers. No selective myofiber type atrophy was noted.

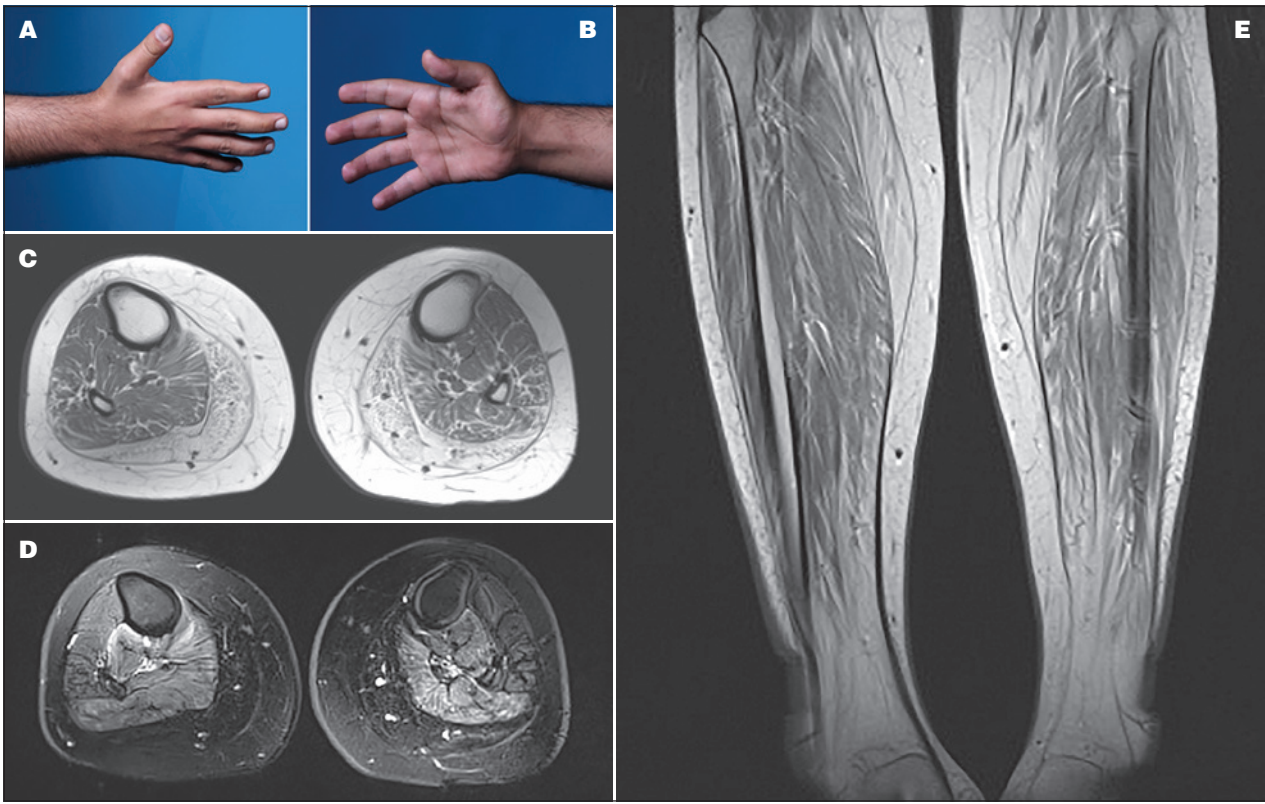


Figure 1. (A-B) A photograph of the proband's hand showing atrophy in the interossei (left) and thenar (right) muscle groups. (C) Axial T1-weighted MRI of the proximal leg showing selective involvement of the medial and posterior muscle groups with fatty infiltration. (D) Axial T2-weighted MRI of the mid-thigh depicting fiber changes in the posterior and medial muscle compartment. (E) Coronal STIR MRI of the proximal thighs demonstrating marked bilateral symmetrical increase signal intensity in the lateral compartment of the thigh consistent with fatty changes.

Case 2: The proband's father, a 58-year-old male who developed difficulty walking at age 18 with slow running pace and capacity. He noted that he walked on the medial aspect of his heels to support his weight; however, he had frequent falls, developed difficulty getting up from sitting position, and complete Gower at age 30. His symptoms progressed and needed a cane for ambulation at age 32 and became wheelchair bound at age 35. At the age 38, he had difficulty changing positions while seated, developed head drop, and later could not turn while in bed rendering him to sleep in a sitting position. At age 48, the patient developed recurrent chest infections and dysphagia to solids. He had a prolonged hospitalization course that ended up with respiratory failure, CO₂ narcosis, and eventually a coma for 2 weeks. Subsequently, the patient underwent tracheostomy and was put on a ventilator due to respiratory weakness, as well as a percutaneous endoscopic gastrostomy tube for feeding. Currently, the patient is bedbound and ventilator dependent with tube feeding. He can communicate via a speaking valve and has normal cognition.

Neurological examination showed normal cranial nerves except for a weak tongue and a gag reflex. There was a moderate degree of atrophy in the small muscles of the hand. Neck flexion power was 3/5 and 4/5 for neck dorsiflexion. His power was 1/5 in deltoids, 0/5 in biceps and triceps, 2/5 in wrist flexion, and 2/5 in wrist extension and finger flexion bilaterally. His ankle dorsiflexion power was 2/5 bilaterally. The remainder of his lower limb muscle power was 0/5. The patient also had scoliosis to the right side with winging of the scapulae. The power in the subscapularis and infrascapularis muscles was 1/5, and pectoralis muscle power was 2/5. Reflexes were depressed except for normal planter reflexes. The rest of his examination was unremarkable. CK level was normal, while NSC and EMG showed severe myopathic changes. His muscle and biopsy and MRI findings were similar to the proband.

Genetic analysis

Neurological gene pane in the index case identified 2714 variants relative to the UCSC hg19 (<http://genome>).

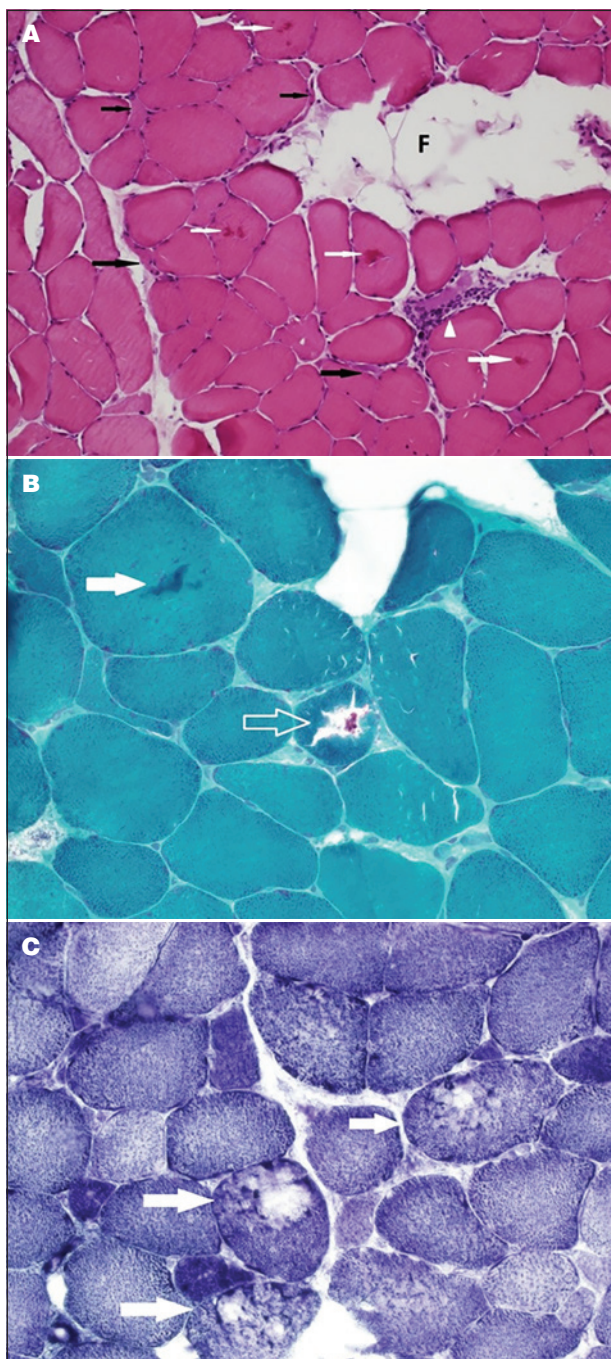


Figure 2. (A) Cross-section of a freshly frozen skeletal muscle showing moderate to marked variation in myofiber size with scattered elongated and angular atrophic fibers (black arrows). A necrotic fiber with myophagocytosis (arrowhead) and eosinophilic cytoplasmic inclusions (white arrows) are seen. Note the focal fatty infiltration (F). (B) Magnification of a trichrome-stained section depicting a cytoplasmic inclusions (solid arrow and open arrow). Note the atrophic fibers and the interstitial fibrosis. (C) A cryostat section stained with NADH-TR reaction showing several fibers (arrows) with disruption of the intermyofibrillar network giving a “moth-eaten” appearance.

ucsc.edu/) reference sequence. Variants were annotated using in-house programs that extend the public Annovar package with other commercial datasets such as HGMD, and in-house databases made up of a collection of disease-causing and polymorphic variants observed in individuals of Arab ethnicity. These were further filtered to exclude previously reported variants (present in dbSNP, 1000 genomes and 2000 Arab exomes), the list was narrowed to 59. Non-relevant variants were filtered out based on their quality, 5 variants survived. By only focusing on exonic and splice site variants we decreased the number to 1. (Fig. 3). It was a heterozygous variant in exon 5 of *DNAJB6* (NM_005494:c. C287T;p.P96L). The gene has been associated with muscular dystrophy, limb-girdle, type 1D. This mutation localizes within glycine and phenylalanine rich domain and alter an amino acid residue. This heterozygous change was confirmed by Sanger sequencing, and the mutation segregated dominantly with disease in the family studied

Discussion

There is an existing confusion in the LGMD1D nomenclature. The 7q36 locus has been designated as the site of gene defect for LGMD1E initially or LGMD1D/1E (5,17). However, according to the HUGO Gene Nomenclature Committee, the current nomenclature for LGMD associated with *DNAJB6* mutations is LGMD1D. The first identification of a pathogenic locus on chromosome 7 linked to LGMD1 was in 1995 by Speer et al. (18) in 2 American families. The disease was further described in a Finnish family where it was further localized to a possible genetic mutation on the same locus (4). Subsequently, Harms et al. (5) identified mutations within the G/F domain of the *DNAJB6* gene, of the LGMD1 locus on chromosome 7q36, thereby classifying *DNAJB6* dystrophy as a novel cause of autosomal dominant inherited myopathy (1-3, 5, 6).

Further studies described American, Canadian, Italian, French, Finnish, Japanese, and Taiwanese families with LGMD1D have also identified the causative gene to be *DNAJB6* (4-15). Missense mutations and deletions have been identified in this gene, including p.Phe89Ile, p.Phe93Leu, p.Asn95Ile, p.Phe96Arg, p.Phe96Ile, p.Phe96Leu, and p.Asp98del (4-15). It appears that the loss of phenylalanine from the protein domain is more important in the pathophysiology of the disease than the type of amino acid substitution (6). Given that most of the reported mutations occur in or in a close proximity to the p.Phe93Leu region, this suggests that this area could be a mutational hot spot within the *DNAJB6* gene (6, 7, 10). Both of our patients harbored a P96L mutation in the *DNAJB6* gene with additional phenotypic features expanding the previously described phenotypes. This P96L

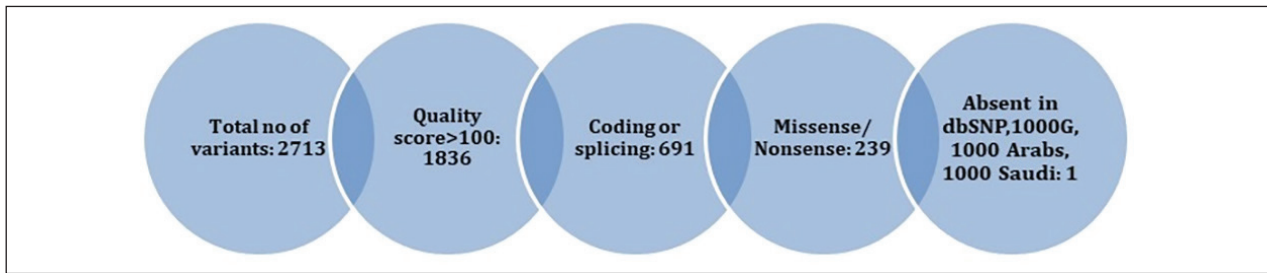


Figure 3. Filtration process of neurological gene panel results.

mutation has been previously described in a Taiwanese family (14). Tentative genotype-phenotype correlation indicate that p.Phe91 mutations in G/F domain are associated with a severe disease, while p.Phe89, p.Pro96, and p.Phe100 mutations were linked to an intermediate severity. Interestingly, p.Phe93 mutations were associated with the least severe phenotype (6, 10, 12, 13).

The DNAJB6 protein (encoded by the *DNAJB6* gene) is a member of the heat shock protein family (heat shock protein 40) a class of co-chaperones that is ubiquitously expressed in all tissues, with a higher expression rate in the brain than other tissues (19). The protein has a multitude of functions including suppressing protein aggregation and toxicity of polyglutamine proteins (19-21). The DNAJB6 protein has three domains: an N-terminal J domain, a variable C-terminal domain, and a G/F domain (13, 22). All the described LGMD1D mutations lead to amino acid substitutions or deletion in the G/F domain (4-15). The DNAJB6 protein has two isoforms a and b, which are produced by alternative splicing of its mRNA. DNAJB6a is located in the nucleus, while DNAJB6b is located in the cytosol (13, 22). Mutations in the isoform b are responsible for LGMD1D.

The mechanism by which mutant DNAJB6b causes muscular dystrophy is complex and not fully understood. In vitro studies suggest defective anti-aggregation properties by mutant DNAJB6b leading to toxic protein accumulation, interaction with the CASA complex, and BAG3 co-chaperones, which collectively cause altered protein degradation system and defective protein quality control (6, 19-21, 23). Pathologically, LGMD1D is characterized by the presence of rimmed vacuoles, cytoplasmic inclusions, and disintegrated myofibrils as shown in Figure 2 (5, 12). EMG and NC neurophysiological studies generally show myopathic changes and CK levels are typically normal or moderately elevated (4-15). All of these findings were also observed in our patients.

The MRI findings of LGMD1D have been studied by Sandell et al. (24) The authors found a typical pattern of involvement, showing fatty degeneration of multiple

muscles across the course of the disease. The MRI findings in our patients were also similar to what Sandell et al. (24) observed in their cohort along with chronic atrophic changes in the gastrocnemius and peroneus muscles.

As the number of reports continues to increase, there has been phenotypic expansion in LGMD1D clinical presentation. The age of onset varies from teenage to middle age years, with the youngest reported case in a 14-year-old (11). The initial symptoms are those related to proximal myopathy, involving predominantly the lower extremities presenting as difficulty running, climbing stairs, or rising up from a sitting position. Some patients have a concurrent distal muscle weakness and may present with muscle atrophy either proximally or distally (4-15). Other uncommonly encountered symptoms include dysphagia, dysarthria, myalgia, conduction defects in the heart, and respiratory symptoms (8, 10, 12-15). Interestingly, both of our patients had distal muscle weakness, dysphagia, and respiratory symptoms.

The natural history of LGMD1D is variable. The majority of patients have a slowly progressive disease and remain ambulatory till their early 50's. However, a relentlessly aggressive form may occur, particularly among patients with a young onset (6, 11-13). Unfortunately, one of our patients was rendered wheelchair bound in his 30's. Our two cases lie within the phenotypic spectrum of previously reported LGMD1D phenotypes. Additionally, our native Saudi Bedouin patients harbored a mutation c.C287T (p.P96L) in the *DNAJB6* gene. Exome-sequencing technology had aided us to discover this LGMD1D family among 50 other LGMD Saudi families (16). Utilization of this technology may further help us unleash more families with LGMD1D and provide a more accurate estimate of the true prevalence of this rare entity by classifying more cases of undiagnosed muscular dystrophies. Our study will therefore expand on the existing genotypic and phenotypic spectrum of this disorder and aid in elucidating hidden mechanisms implicated in LGMD1D.

References

1. Boyden SE, Salih MA, Duncan AR, et al. Efficient identification of novel mutations in patients with limb girdle muscular dystrophy. *Neurogenetics* 2010;11:449-55.
2. Monies D, Alhindi HN, Almuhaizea MA, et al. A first-line diagnostic assay for limb-girdle muscular dystrophy and other myopathies. *Hum Genomics* 2016;10:32.
3. Straub V, Murphy A Udd B. 229th ENMC international workshop: Limb girdle muscular dystrophies – Nomenclature and reformed classification Naarden, the Netherlands, 17-19 March 2017. *Neuromuscul Disord* 2018;28:702-10.
4. Hackman P, Sandell S, Sarparanta J, et al. Four new Finnish families with LGMD1D; refinement of the clinical phenotype and the linked 7q36 locus. *Neuromuscul Disord* 2011;21:338-44.
5. Harms MB, Sommerville RB, Allred P, et al. Exome sequencing reveals DNAJB6 mutations in dominantly-inherited myopathy. *Ann Neurol* 2012;71:407-16.
6. Sarparanta J, Jonson PH, Golzio C, et al. Mutations affecting the cytoplasmic functions of the co-chaperone DNAJB6 cause limb-girdle muscular dystrophy. *Nat Genet* 2012;44:450-5, S1-2.
7. Sato T, Hayashi YK, Oya Y, et al. DNAJB6 myopathy in an Asian cohort and cytoplasmic/nuclear inclusions. *Neuromuscul Disord* 2013;23:269-76.
8. Couthouis J, Raphael AR, Siskind C, et al. Exome sequencing identifies a DNAJB6 mutation in a family with dominantly-inherited limb-girdle muscular dystrophy. *Neuromuscul Disord* 2014;24:431-5.
9. Nam TS, Li W, Heo SH, et al. A novel mutation in DNAJB6, p.(Phe91Leu), in childhood-onset LGMD1D with a severe phenotype. *Neuromuscul Disord* 2015;25:843-51.
10. Ruggieri A, Brancati F, Zanotti S, et al. Complete loss of the DNAJB6 G/F domain and novel missense mutations cause distal-onset DNAJB6 myopathy. *Acta Neuropathol Commun* 2015;3:44.
11. Palmio J, Jonson PH, Evilä A, et al. Novel mutations in DNAJB6 gene cause a very severe early-onset limb-girdle muscular dystrophy 1D disease. *Neuromuscul Disord* 2015;25:835-42.
12. Sandell S, Huovinen S, Palmio J, et al. Diagnostically important muscle pathology in DNAJB6 mutated LGMD1D. *Acta Neuropathol Commun* 2016;4:9.
13. Ruggieri A, Saredi S, Zanotti S, et al. DNAJB6 myopathies: focused review on an Emerging and Expanding Group of Myopathies. *Front Mol Biosci* 2016;3:63. eCollection 2016.
14. Tsai PC, Tsai YS, Soong BW, et al. A novel DNAJB6 mutation causes dominantly inherited distal-onset myopathy and compromises DNAJB6 function. *Clin Genet* 2017;92:150-7.
15. Jonson PH, Palmio J, Johari M, et al. Novel mutations in DNAJB6 cause LGMD1D and distal myopathy in French families. *Eur J Neurol* 2018;25:790-4.
16. Monies D, Abouelhoda M, AlSayed M, et al. The landscape of genetic diseases in Saudi Arabia based on the first 1000 diagnostic panels and exomes. *Hum Genet* 2017;136:921-39.
17. Sandell S, Huovinen S, Sarparanta J, et al. The enigma of 7q36 linked autosomal dominant limb girdle muscular dystrophy. *J Neurol Neurosurg Psychiatry* 2010;81:834-9.
18. Speer MC, Gilchrist JM, Chutkow JG, et al. Evidence for locus heterogeneity in autosomal dominant limb-girdle muscular dystrophy. *Am J Hum Genet* 1995;57:1371-6.
19. Hishiya A, Salman MN, Carra S, et al. BAG3 directly interacts with mutated alphaB-crystallin to suppress its aggregation and toxicity. *PLoS One* 2011;6:e16828.
20. Arai H, Atomi Y. Chaperone activity of alpha B-crystallin suppresses tubulin aggregation through complex formation. *Cell Struct Funct* 1997;22:539-44.
21. Arndt V, Dick N, Tawo R, et al. Chaperone-assisted selective autophagy is essential for muscle maintenance. *Curr Biol* 2010;20:143-8.
22. Fan CY, Lee S, Cyr DM. Mechanisms for regulation of Hsp70 function by Hsp40. *Cell Stress Chaperones* 2003;8:309-16.
23. Ding Y, Long PA, Bos JM, et al. A modifier screen identifies DNAJB6 as a cardiomyopathy susceptibility gene. *JCI Insight* 2017;2 pii: 94086.
24. Sandell SM, Mahjneh I, Palmio J, et al. Udd BA. 'Pathognomonic' muscle imaging findings in DNAJB6 mutated LGMD1D. *Eur J Neurol* 2013;20:1553-9.

CASE REPORT

Myotonic dystrophy type 1 and pulmonary embolism: successful thrombus resolution with dabigatran etexilate therapy

EMANUELE GALLINORO¹, ANDREA ANTONIO PAPA¹, ANNA RAGO¹,
SIMONA SPERLONGANO¹, ANTONIO CASSESE¹, NADIA DELLA CIOPPA²,
MARIA CRISTINA GIADA MAGLIOCCA³, GIOVANNI CIMMINO¹ AND PAOLO GOLINO¹

¹ Department of Cardiology, University of Campania "L. Vanvitelli", Monaldi Hospital, Naples, Italy; ² Department of Anesthesiology, Monaldi Hospital, Naples, Italy; ³ Anesthesia Department, Moscati Hospital, Aversa, Italy

Myotonic dystrophy type 1 (DM1) is the most common form of adult muscular dystrophy. It is an autosomal dominant inherited disease with multisystemic involvement. Respiratory function is often affected and respiratory failure is the most common cause of death. Pulmonary embolism is a rare cause of respiratory failure in DM1 patients, so that the best anticoagulation strategy in these patients is still unclear. We describe the case of pulmonary embolism in a DM1 patient, in which pulmonary thrombus was completely resolved with oral dabigatran etexilate therapy.

Key words: myotonic dystrophy, pulmonary embolism, dabigatran etexilate, pulmonary thrombus

Introduction

Myotonic dystrophy type 1 (DM1) is the most common muscular dystrophy in adults, affecting approximately 1 in 8000 people worldwide. It is a multisystem disorder with autosomal dominant inheritance. Clinical manifestations may vary from muscle symptoms such as myotonia, muscle weakness/atrophy and fatigue to cardiac arrhythmias, early cataracts, central/obstructive apnea, respiratory failure, insulin resistance, dysphagia and gastrointestinal dysmotility (1). Cardiac involvement is quite common, as in other muscular dystrophies (2), affecting about 80% of patients, and often precedes the skeletal muscle one. Cardiac involvement may include arrhythmias (3-6) atrioventricular block (7), ventricular premature contractions, atrial fibrillation (8-10), atrial flutter (11),

right/left bundle branch block and non-sustained ventricular tachycardia (12) which often lead to needs of cardiac devices such as pacemakers or implantable cardiac defibrillator (13-16). Left ventricular systolic dysfunction has also been reported (17-22). Respiratory failure is a common feature in almost all muscular dystrophies and, together with cardiac involvement is the main cause of death (23-24). Respiratory failure in DM1 patients is often the consequence of a combination of respiratory muscle weakness and degeneration, and lung elastic properties alterations (25). Pulmonary embolism is a rare event in DM1 patients (26). Moreover, the best antithrombotic strategy in this subset of patients is still debated, and novel oral anticoagulants (NOAC) have never been systematically tested in DM1 patients (27). We described the case of a pulmonary embolism in a DM1 patient treated for the first time with dabigatran etexilate, obtaining a complete resolution of the pulmonary thrombus.

Case report

We report the case of a 62-year-old female patient affected by DM1. She had no other cardiovascular risk factors excepted for systemic arterial hypertension. She was admitted to the Emergency Department because of dyspnea arising 7 days before and worsening in the last 6 hours. The recent clinical history was not relevant, as only an unilateral knee pain was reported which limited her daily activities. At admission the patient was conscious; physical examination showed heart rate (HR) 124 bpm, blood pressure (BP) 110/60 mmHg, breath-

ing rate (BR) 23/min, SpO₂ 85% (FiO₂ 21%). The ECG showed a new-onset incomplete right bundle branch block with S wave in DI, Q wave and inverted T wave in DIII (a combination known as S1Q3T3 pattern, suggestive for pulmonary embolism). The arterial blood gas analysis revealed hypoxemia with hypocapnia and respiratory alkalosis; the blood exams showed high levels of I-troponin and D-dimer. The echocardiogram showed normal structure and function of the left ventricle, while the right ventricle presented a reduced longitudinal contractile function (Tricuspid Annulus Plane Systolic Excursion, TAPSE 14 mm), with abnormal function of mid-basal free wall and apical hyper-contractility (McConnell's sign). The systolic pulmonary artery pressure – derived from the echocardiographic measurement of the tricuspid regurgitant jet velocity – was 60 mmHg. The Wells score was 6. A parasternal short axis view revealed the presence of a large thrombus inside pulmonary artery just on the level of main pulmonary artery bifurcation (Fig. 1). As the suspicious for pulmonary embolism (PE) was high, Computed Tomography Pulmonary Angiography (CTPA) was performed. CTPA images, acquired with the maximum intensity of radio-opaque contrast in the pulmonary arteries, showed the presence of a large thrombus on the pulmonary artery bifurcation extended to the central part of the lumen of both branches (Fig. 2). In the absence of hemodynamic instability, the patient – according to the current ESC guidelines on acute pulmonary embolism management (28) – was treated with fondaparinux 7.5 mg, subcutaneously once daily. As after 5 days of medical therapy, the echocardiographic re-evaluation still

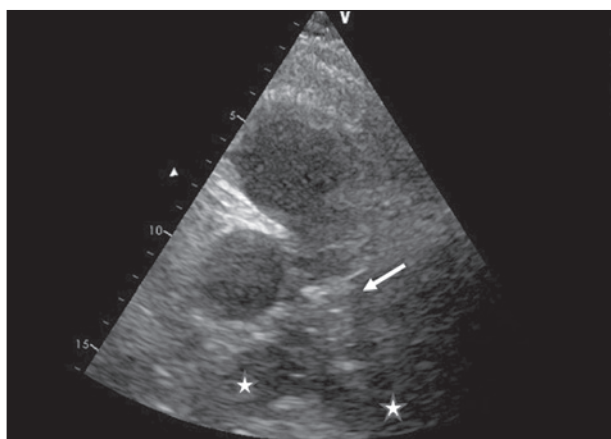


Figure 1. Parasternal short axis view of the pulmonary artery. The stars indicate the right and left pulmonary artery. The white arrow indicates the thrombus lying on the bifurcation of the pulmonary artery.

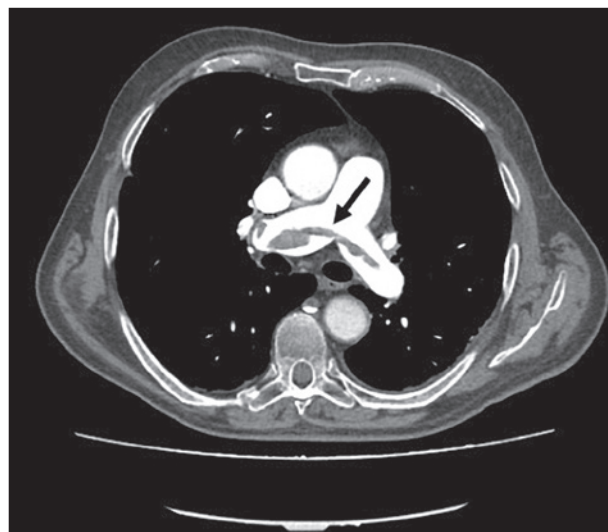


Figure 2. Computed tomography pulmonary angiography (CTPA) demonstrating saddle pulmonary embolism partially obstructing both main pulmonary arteries; the white area above the center is the pulmonary artery, opacified by radiocontrast; the black arrow indicates the pulmonary thrombus.

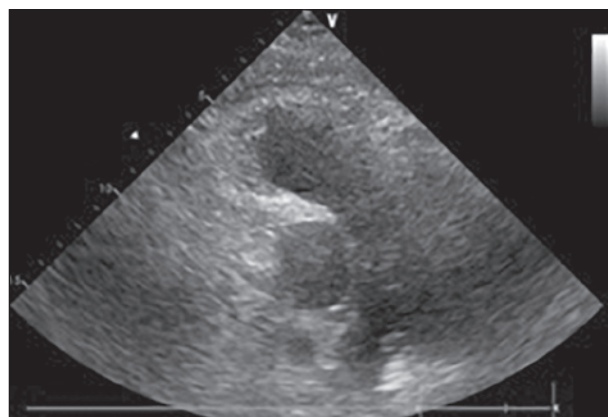


Figure 3. Parasternal short axis view of the pulmonary artery showing the complete resolution of the thrombus on the bifurcation of the pulmonary artery.

showed the thrombus in pulmonary artery, the treatment was stopped and dabigatran (a direct thrombin inhibitor, DTI) was administered at a dosage according to the patient's age and renal function (150 mg/bid). Seven days after, the cardiac ultrasound examination showed the complete resolution of the thrombus (Fig. 3). At the same time, the clinical and biochemical parameters returned within the normal ranges. Dabigatran was then prescribed as the long-life therapy according to the high thrombotic risk of the patient.

Discussion

Myotonic dystrophy type 1 is mainly characterized by skeletal muscle involvement, anyway cardiac involvement is quite common (29-31). Respiratory system is also affected with diaphragmatic weakness and/or recurrent pulmonary infections, which can lead to respiratory failure.

Recently it has been observed that dystrophic patients may have high thrombotic risk due to some predisposing factors. Firstly, they are affected by a myopathy that leads to mobility restriction and a sedentary lifestyle, which may increase their thromboembolic risk. The increasing age and a personal history of venous thrombo-embolism seem to be other predisposing factors. Compared with other inherited myopathies, patients with DM1 have a higher thromboembolic risk (32). Moreover, muscle degeneration can enhance coagulation and fibrinolysis processes as described in other forms of muscular dystrophies such as Duchenne muscular dystrophy (DMD), Becker muscular dystrophy (BMD) and Fukuyama congenital muscular dystrophy (FCMD). Hyper-coagulability state could be another predisposing factor for recurrent thrombotic events; however little is still known about the mechanisms underlying hypercoagulability state in these patients (33). In DMD and BMD a protein known as utrophin (a dystrophin-related protein), could play a role in hypercoagulability and recurrent thrombosis events. It seems that the upregulation of utrophin observed in these patients, leads to a lower expression of thrombomodulin, resulting in hypercoagulability state (34). However, none of these evidences is quite strong and referred to DM1. New perspective about incidence of venous thromboembolism and predicting factors of recurrent thrombosis specifically in the subset of DM1 patients may will rise from the results of a retrospective cohort study by Whabi et al. (NCT number: NCT03141749). What could be the best anticoagulation strategy in these patients is still debated. To date, Warfarin is still considered the first line treatment and the standard of care for DM1 patients requiring anticoagulation, as its safety and effectiveness has been established over the last decades (35). However, the difficulties in achieving an optimal anticoagulation with conventional warfarin therapy, likely related to several factors such as the slow onset of action, the variable pharmacologic effects, the interaction with several food and drug and the needs of periodic closely target INR monitoring, make the therapeutic management in clinical practice it difficult and reduce the real-life DM1 patient's compliance. All these challenges have prompted an extensive research on the use of NOACs in a subset of patients (36, 37). Unfortunately, none of the trials evaluating the use of NOACs (38) in clinical practice, included DM1 patients (39-41). Dabigatran etexilato is a thrombin direct

inhibitor whose safety and effectiveness in the treatment of venous thrombo-embolism and pulmonary embolism (PE) was tested in RE-COVER (42) and RE-COVER II (43) trials. Its efficacy was non-inferior to warfarin, with no significant differences in minor and major bleedings. No data are available about the use of this drug for the management of PE in DM1 patients. This case report is the first to report the use of Dabigatran etexilato for PE in a DM1 patient; using this drug the complete resolution of the pulmonary thrombus after an episode of pulmonary embolism was achieved. No major or minor bleedings were observed during treatment, and clinical and biochemical parameters returned within normal range 7 days after therapy.

Oral anticoagulation is an important issue in this subset of patients because they present a high prevalence of atrial fibrillation (44-47) requiring long-term anticoagulation to reduce the risk of thromboembolic events (48, 49).

Conclusions

The present case is the first to report the complete resolution of a pulmonary thrombus in a DM1 patient with pulmonary embolism, by using dabigatran etexilato. The use of dabigatran etexilate as anticoagulation treatment could be particularly useful in this subset of patients, for their variable cognitive impairment and consequent poor compliance with periodic INR monitoring.

References

1. Smith CA, Gutmann L. Myotonic dystrophy type 1 management and therapeutics. *Curr Treat Options Neurol* 2016;18:52.
2. Nigro G, Papa AA, Politano L. The heart and cardiac pacing in Steinert disease. *Acta Myol* 2012;31:110-6.
3. Nigro G, Russo V, Politano L, et al. Right atrial appendage versus Bachmann's bundle stimulation: a two-year comparative study of electrical parameters in myotonic dystrophy type-1 patients. *Pacing Clin Electrophysiol* 2009;32:1191-6.
4. Russo V, Papa AA, Rago A, et al. Arrhythmic risk evaluation in myotonic dystrophy: the importance of selection criteria and methodological approach. *Clin Auton Res* 2017;27:203-4.
5. Russo V, Rago A, Ciardiello C, et al. the role of the atrial electro-mechanical delay in predicting atrial fibrillation in myotonic dystrophy type 1 patients. *J Cardiovasc Electrophysiol* 2016;27:65-72.
6. Russo V, Papa AA, Rago A, et al. Increased heterogeneity of ventricular repolarization in myotonic dystrophy type 1 population. *Acta Myol* 2016;35:100-6.
7. Nigro G, Russo V, Vergara P, et al. Optimal site for atrial lead implantation in myotonic dystrophy patients: the role of Bachmann's Bundle stimulation. *Pacing Clin Electrophysiol* 2008;31:1463-6.

8. Russo V, Rago A, Politano L, et al. The effect of atrial preference pacing on paroxysmal atrial fibrillation incidence in myotonic dystrophy type 1 patients: a prospective, randomized, single-blind cross-over study. *Europace* 2012;14:486-9.
9. Russo V, Di Meo F, Rago A, et al. Paroxysmal atrial fibrillation in myotonic dystrophy type 1 patients: P wave duration and dispersion analysis. *Eur Rev Med Pharmacol Sci* 2015;19:1241-8.
10. Russo V, Papa AA, Rago A, et al. Which is the true epidemiology of atrial fibrillation in myotonic dystrophy type 1 patients? *Pacing Clin Electrophysiol* 2016;39:1418-9.
11. Russo V, Rago A, Papa AA, et al. Voltage-directed cavo-tricuspid isthmus ablation using a novel ablation catheter mapping technology in a myotonic dystrophy type I patient. *Acta Myol* 2016;35:109-13.
12. Russo V, Rago A, Di Meo F, et al. Ventricular fibrillation induced by coagulating mode bipolar electrocautery during pacemaker implantation in myotonic dystrophy type 1 patient. *Acta Myol* 2014;33:149-51.
13. Proietti R, Labos C, Davis M, et al. A systematic review and meta-analysis of the association between implantable cardioverter-defibrillator shocks and long-term mortality. *Can J Cardiol* 2015;31:270-7.
14. Russo V, Nigro G, Politano L. Role of electrophysiological evaluation for the best device choice to prevent sudden cardiac death in patients with myotonic dystrophy type 1 and Emery Dreifuss muscular dystrophy. *Trends Cardiovasc Med* 2017. pii: S1050-1738(17)30013-0.
15. Russo V, Rago A, Papa AA, et al. Bachmann bundle pacing reduces atrial electromechanical delay in type 1 myotonic dystrophy patients. *J Interv Card Electrophysiol* 2018;51:229-36.
16. Muto C, Solimene F, Russo V, et al. Optimal left ventricular lead placement for cardiac resynchronization therapy in postmyocardial infarction patients. *Future Cardiol* 2018;14:215-24.
17. Petri H, Witting N, Ersbøll MK, et al. High prevalence of cardiac involvement in patients with myotonic dystrophy type 1: a cross-sectional study. *Int J Cardiol* 2014;174:31-6.
18. Russo V, Di Meo F, Rago A, et al. Atrial electromechanical delay in myotonic dystrophy type 1 patients. *Eur Rev Med Pharmacol Sci* 2015;19:3991-2.
19. Russo V, Rago A, D'Andrea A, et al. Early onset "electrical" heart failure in myotonic dystrophy type 1 patient: the role of ICD biventricular pacing. *Anadolu Kardiyol Derg* 2012;12:517-9.
20. Russo V, Papa AA, Nigro G. The controversial epidemiology of left ventricular dysfunction in patients with myotonic dystrophy type 1. *JAMA Cardiol* 2017;2:1044.
21. Russo V, Rago A, Papa AA, et al. Which is the true epidemiology of left ventricular dysfunction in patients with myotonic dystrophy type 1? *J Chin Med Assoc* 2017;80:740-1.
22. Russo V, Papa AA, Williams EA, et al. ACE inhibition to slow progression of myocardial fibrosis in muscular dystrophies. *Trends Cardiovasc Med* 2018;28:330-7.
23. Nigro G, Russo V, Politano L, et al. Does Bachmann's bundle pacing prevent atrial fibrillation in myotonic dystrophy type 1 patients? A 12 months follow-up study. *Europace* 2010;12:1219-23.
24. Nigro G, Russo V, Rago A, et al. Right atrial preference pacing algorithm in the prevention of paroxysmal atrial fibrillation in myotonic dystrophy type 1 patients: a long term follow-up study. *Acta Myol* 2012;31:139-43.
25. Lo Mauro A, Aliverti A. Physiology of respiratory disturbances in muscular dystrophies. *Breathe (Sheff)* 2016;12:318-27.
26. Cho JY, Seo SY, Cho YJ, et al. Pulmonary thromboembolism in a patient with myotonic dystrophy type 1. *Ann Indian Acad Neuro* 2012;15:317-9.
27. Rago A, Papa AA, Arena G, et al. Complete resolution of left atrial appendage thrombosis with oral dabigatran etexilate in a patient with myotonic dystrophy type 1 and atrial fibrillation. *Acta Myol* 2017;36:218-22.
28. Konstantinides SV, Torbicki A, Agnelli G, et al. 2014 ESC guidelines on the diagnosis and management of acute pulmonary embolism. *Eur Heart J* 2014;35:3033-69, 69a-69k.
29. Russo V, Rago A, Papa AA, et al. Cardiac resynchronization improves heart failure in one patient with myotonic dystrophy type 1. A case report. *Acta Myol* 2012;31:154-5.
30. Russo V, Nigro G, Rago A, et al. Atrial fibrillation burden in myotonic dystrophy type 1 patients implanted with dual chamber pacemaker: the efficacy of the overdrive atrial algorithm at 2 year follow-up. *Acta Myol* 2013;32:142-7.
31. Russo V, Rago A, Nigro G. Sudden cardiac death in neuromuscular disorders: time to establish shared protocols for cardiac pacing. *Int J Cardiol* 2016;207:284-5.
32. Wahbi K, Sochala M, Porcher R, et al. Venous thromboembolism in adult patients with inherited myopathies: a high-risk in myotonic dystrophy. *Neuromuscular Disorders* 2017;27:S179.
33. Saito Y, Komiya T, Kawai M. Hypercoagulable state in Duchenne muscular dystrophy. *Rinsho Shinkeigaku* 1997;37:374-8.
34. Higuchi I, Niiyama T, Uchida Y, et al. Multiple episodes of thrombosis in a patient with Becker muscular dystrophy with marked expression of utrophin on the muscle cell membrane. *Acta Neuropathol* 1999;98:313-6.
35. Bushby K, Muntoni F, Bourke JP. 107th ENMC International Workshop: the management of cardiac involvement in muscular dystrophy and myotonic dystrophy. 7th-9th June 2002, Naarden, the Netherlands. *Neuromuscular Disorders*. 2003;13:166-72.
36. Russo V, Bottino R, Rago A, et al. Atrial fibrillation and malignancy: the clinical performance of non-vitamin k oral anticoagulants—a systematic review. *Semin Thromb Hemost* 2018 Aug 17. doi: 10.1055/s-0038-1661386.
37. Russo V, Attena E, Mazzone C, et al. Nonvitamin k antagonist oral anticoagulants use in patients with atrial fibrillation and bioprosthetic heart valves/prior surgical valve repair: a multicenter clinical practice experience. *Semin Thromb Hemost* 2018;44:364-9.

38. Russo V, Rago A, Papa AA, et al. Use of non-vitamin k antagonist oral anticoagulants in atrial fibrillation patients with malignancy: clinical practice experience in a single institution and literature review. *Semin Thromb Hemost* 2018;44:370-6.
39. Russo V, Di Napoli L, Bianchi V, et al. A new integrated strategy for direct current cardioversion in non-valvular atrial fibrillation patients using short term rivaroxaban administration: the MonaldiVert real life experience. *Int J Cardiol* 2016;224:454-5.
40. Russo V, Rago A, D'Onofrio A, et al. The clinical performance of dabigatran in the Italian real-life experience. *J Cardiovasc Med (Hagerstown)* 2017;18:922-3.
41. Russo V, Rago A, Papa AA, et al. Budget impact analysis of rivaroxaban vs. warfarin anticoagulation strategy for direct current cardioversion in non-valvular atrial fibrillation patients: the MonaldiVert Economic Study. *Minerva Cardioangiol* 2018;66:1-5.
42. Schulman S, Kearon C, Kakkar AK, et al. Dabigatran versus warfarin in the treatment of acute venous thromboembolism. *N Engl J Med* 2009;361:2342-52.
43. Schulman S, Kakkar AK, Goldhaber SZ, et al. Treatment of acute venous thromboembolism with dabigatran or warfarin and pooled analysis. *Circulation* 2014;129:764-72.
44. Russo V, Papa AA, Rago A, et al. Interatrial block to predict atrial fibrillation in myotonic dystrophy type 1. *Neuromuscul Disord* 2018;28:327-33.
45. Russo V, Rago A, Papa AA, et al. Does a high percentage of right ventricular pacing influence the incidence of paroxysmal atrial fibrillation in myotonic dystrophy type 1 patients? *Kardiol Pol* 2013;71:1147-53.
46. Russo V, Papa AA, Rago A, et al. Effect of dual-chamber minimal ventricular pacing on paroxysmal atrial fibrillation incidence in myotonic dystrophy type 1 patients: a prospective, randomized, single-blind, crossover study. *Heart Rhythm* 2018;15:962-8.
47. Proietti R, Gonzini L, Pizzimenti G, et al. Glomerular filtration rate: a prognostic marker in atrial fibrillation. A Sub-analysis of the ataf. *Clin Cardiol* 2018 Aug 24. [Epub ahead of print]
48. Russo V, Rago A, Papa AA, et al. Efficacy and safety of dabigatran in patients with atrial fibrillation scheduled for transoesophageal echocardiogram-guided direct electrical current cardioversion: a prospective propensity score-matched cohort study. *J Thromb Thrombolysis* 2018;45:206-12.
49. Bertaglia E, Anselmino M, Zorzi A, et al. NOACs and atrial fibrillation: Incidence and predictors of left atrial thrombus in the real world. *Int J Cardiol* 2017;249:179-83.

OBITUARY

Professor Frank Lehmann-Horn (1948-2018)



Since 2006, Frank Lehmann-Horn, the Director of the Division of Neurophysiology at the University of Ulm, had been fighting against various forms of cancer. On May 8, 2018, after an apparently successful bone marrow transplantation, he passed away owing to the sequelae of leukemia. The community of German researchers into neuromuscular diseases has lost one of its most distinguished members. In particular his co-workers at the University of Ulm miss him as their pioneer and sincere friend.

Frank's life-long research interest was mainly devoted to the groups of hereditary myotonias and periodic paralyses. After thorough training in physiology and neurology at the Technical University of Munich (TUM) he started sophisticated voltage-clamp experiments on excised intact muscle fibers from patients with paramyotonia congenita and hypokalemic periodic paralysis. These studies led to the first definition of the defect ion channel proteins in these diseases. In 1982, when he was only 34 years of age, the German Association of neuromuscular patients (DGM) duly bestowed on him and his group its highest award, the Erb-Duchenne Preis. In the following years, after some time training with Prof. Andrew Engel at the Mayo Clinic, Rochester MN, Frank returned to the TUM to discover several new forms of what he dubbed "channelopathies" e.g. potassium-sensitive

myotonia, a severe form of disease caused by mutations in the gene coding for the muscular sodium channel. The numerous mutations of this gene that can cause myotonia congenita to varying degrees of severity, of paramyotonia congenita and of periodic paralysis, defined the volume of his work in the ensuing years. In 1992, by which time he had already been promoted to Professor of Neurology at the TUM, Frank was offered the Chair of Applied Physiology at the University of Ulm. He gladly accepted it because it released him from routine clinical duties. The Ulm Medical Faculty, however, additionally charged on him the direction of its new Interdisciplinary Center for Clinical Research. During his 6 years in this job, Frank nurtured the center to full fruition. Needless to say, muscle research was a substantial part of its program. This again helped Frank when he later became Chair of the Ulm Neuromuscular Center. In 1995, the City of Ulm bestowed its Scientific Award on him. From 1996 to 2006, Frank also coordinated two EU networks. His key role in this successful collaboration was acknowledged in 2003 by an honorary doctor's degree from the Hungarian University of Debrecen, and in 2004 by the award of the Gaetano Conte Academy of Naples. Together with his chief co-worker of many years, Karin Jurkat-Rott, Frank then turned to more research into the periodic paralyses. Particularly, he devoted much time to pushing forward treatment for these diseases. His "ability to listen to patients" was repeatedly acknowledged in the USA, i.e. by awards of the Patients' Associations of Las Vegas (2002), Orlando (2007) and Washington DC (2009). The Conference of American Periodic Paralysis Associations decorated him for "Excellence in Research" in 2011. Other activities directed to the benefit of patients were the foundation of a reference center for families concerned with malignant hyperthermia (1995) and a center for rare diseases in Southern Germany (2010).

At home, Frank Lehmann-Horn's scientific achievements were recognized in 2008 by membership of the Heidelberger Akademie der Wissenschaften, and in 2009 by the endowment of a Senior Research Professorship by the German Non-Profit Hertie Trust. His most recent interests were the investigation of the role of increased intracellular sodium in periodic paralysis and Duchenne muscular dystrophy. After he retired from his Chair of Applied Physiology in 2010, the University of Ulm established in his honor a Division of Neurophysiology, the directorship of which he retained until his death.

Em. Prof. Reinhardt Rüdell, Ulm, Germany

NEWS FROM AROUND THE WORLD

AIM

The 18th Congress of the Italian Association of Myology was held from the 6 to 9 June in Genova, the same location that hosted the first meeting in 2000, organised by the same person, Professor Carlo Minetti.

Nearly 400 people from both Italy and all over the world attended this meeting, that with its 70 speakers, over 200 contributions and, for the first time, a joined session with the French Association of Myology, was one of the most intense and valuable of the past editions.

The congress was anticipated by a one-day full teaching course on the diagnostic interpretation of muscle biopsy. Several experts from Italy and Europe such as Maurizio Moggio, Enrico Bertini, Marina Mora, Rita Barresi and Edoardo Malfatti intervened and shared their expertise with the audience of young myologists.

For the first time the Congress had a topic: *From Basic Muscle Science To Translational Myology*. In the workshop dedicated to the basic muscle science, Professor Musarò from Rome introduced some of the common patho-mechanisms causing muscular dystrophy and damage of muscle fibres; Doctor Messina from Milan, explained the role of the transcription factor Nfix in the pathogenesis of Muscle Diseases; Professor Sandri, who worked for years in Basel, showed the molecular pathways involved in correct and altered muscle contraction; and Doctor Tedesco, a young Italian researcher working in London, fascinated the audience with the potentiality of 3D artificial skeletal muscle derived from pluripotent stem cells.

In the session of *Experimental Therapy*, Professor

Malerba from London reported the results of a research on the genetic therapy for OPMD; Professor Desaphy explained the importance of the genetic background of congenital myotonia on the response to drug treatment; Doctor Gazzero, another Italian scientist from Genova currently working in Berlin, argued on the double face of the inflammatory system in the pathogenesis of muscular dystrophy, potentially acting as both protective and aggravating element; finally Professor Corti from Milan reported on her work on induced pluripotent stem cells for the treatment of Spinal Muscular Atrophies.

The therapy of SMA was further discussed in a dedicated symposium. Results of the new genetic therapy able to rescue the production of SMN2, the vicariant gene of SMN complex, were reported. Italy was not less, treating so far 120 SMA1 children with astonishing results.

A further topic was the *Diagnosis and Management of the Floppy Infant*, a common diagnostic challenge and typical onset of many different neuromuscular conditions starting in the paediatric age. Beside these exciting topics, many other were discussed including 2 *breakfast seminars*, one on *nutrition aspects in muscle diseases* coordinated by Doctor Pini from Bologna, and the other one on *the new molecular genetic technologies*, which saw Professor Tupler from Modena and Professor Vincenzo Nigro from Naples as speakers. To stay updated, early coffee for the Italian Myologists!

Four intense *Lectures* by national/international speakers enriched the congress. The opening one – in honour of the beloved Professor Giovanni Nigro who passes away in October 2017 – was made by Professor Politano, his pupil, who reinforced the role of Professor Nigro and the Italian school of



Cardiomyology to build up the story of myology in Italy, and recalled how many muscle diseases can present with underlying heart conditions. Professor Di Mauro, a leading scientist at the Columbia University, who taught all mitochondrial secrets to many Italian Doctors, introduced the *Mito-Lectures* made by two eminent scientists, Professor Hirano and Professor Zeviani. The fourth lecture was held by Jeffrey Chamberlain from Washington, who has recently shown, in a Nature Communications paper, how CRISPR/Cas9 repertoire is able to restore dystrophin levels and improve muscle function in mice.

The novelty of the 18th AIM congress was undoubtedly the Joined Session with the colleagues from the French Association of Myology. Three French experts: Guillaume Bassez, Pascale Laforet and Catherine Caraoult discussed with the Italian counterpart respectively on Myotonic Dystrophy, Pompe Disease and Laminopathies.

One-hundred-eighty posters and 32 oral presentations completed the congress program.

As it is tradition for many years, 2 prizes were awarded to young researchers for their innovative results, to Doctor Panicucci from the Genova University for his study on the antagonism of purinergic receptors to ameliorate muscle damage in mdx mice, and to Doctor Costa from the Bologna University for his study on the role of TNOP3 protein in myoblast myogenesis.

A third prize for the best oral communication, established by the *Gaetano Torre Association for Muscular Diseases of Naples* to honor the memory of Prof. Giovanni Nigro, was awarded to Dr. E. Malfatti for his studies on morphological features in patients with GYG1 mutations.

Finally, the social dinner inside the Aquarium of Genova, shocked the participants with a superb meal just between dolphins and turtles tanks. The next AIM congress will be held in Bergamo in June 2019. All the readers all welcome.

Congress report by Chiara Fiorillo, UOC Neurologia Pediatrica e Malattie Muscolari - Genova

MSM

The 13th Meeting of the Mediterranean Society of Myology (MSM) in connection with the 2nd Congress of the Neuromuscular Society of Turkey was held in Avanos, Cappadocia between 28-30 June. This was a special congress in honour of our late Professor Giovanni Nigro who was the founder of the MSM. He quoted in 2017 “thirty-six years ago, a group of researchers with interest in the field of muscular dystrophies felt the need to promote a mutual cooperation among the people of the Mediterranean area, and created the Mediterranean Society of Myology in 1993, in Ischia”.

The main theme of the congress was limb-girdle muscular dystrophies. A basic course on neuromuscular disorders in general was offered to the young scientists prior to the original conference. The whole area was covered by 38 invited

speakers from basic science to bed-side along with future expectations, planning and thoughts, particularly newer therapies. There were over 200 participants to include the local members. A total of 38 bursaries were given (whom 15 were medical students). The conference was well-attended by scientists coming from 13 countries, not only the Mediterranean but also from Asia and the US.

Congress report by Haluk Topaloglu, Hacettepe Children's Hospital 06100 Ankara, Turkey



WMS

The 23rd International WMS Congress will be held in Mendoza, Argentina from 2 to 6 October 2018. The symposium will follow the traditional format with 3 selected topics: new developments in genetic and acquired disorders of the neuromuscular junction; mitochondrial function and dysfunction in neuromuscular disorders: pathogenesis and therapies; advances in the treatment of neuromuscular disorders.

One day of the symposium will be dedicated to each of the selected topics. Invited keynote speakers will summarize the state of the art on the selected topics, covering clinical, molecular and other aspects. The sessions will comprise selected oral papers and poster presentations with guided discussions. Contributions will also be welcome on new advances across the neuromuscular field. The 16th WMS Pre-Congress Teaching Course will be held on 1-2 October 2018. Please note only 45 places are available. Early booking is advised.

FORTHCOMING MEETINGS

edited by L. Maggi and V. Russo

2018

October 2-6

23rd Congress of World Muscle Society. Mendoza, Argentina. Information: website: www.worldmusclesociety.org

October 16-20

ASHG Annual Meeting. San Diego, CA, USA. Information: website: www.ashg.org

October 17-21

Asia Pacific Heart Rhythm Society (APHRs). Taipei, Taiwan. Information: website: <http://www.aphrs.org>

October 24-25

9th World Congress on Targeting Mitochondria, Berlin, Germany. Information: website: <https://targeting-mitochondria.com>

October 3 - November 2

World Congress on Human Genetics. Valencia, Spain. Information: website: <http://humangenetics.conferenceseries.com>

November 2-4

TREAT-NMD Advisory Committee for Therapeutics (TACT) meeting, Chicago US. Information: website: <http://www.treat-nmd.eu/events/715/>

November 9-10

9th International Conference & Exhibition on Tissue Preservation and Biobanking at Atlanta, USA during, 2018. Information: website: <http://biobanking.conferenceseries.com>

November 9-11

Action Duchenne International Conference, Birmingham, UK. Information: website: <https://www.actionduchenne.org/conference-registration>

November 15-17

Portuguese Neurology Congress, Porto, Portugal. Information: ana.costa@norahsevents.pt

November 19-20

SMA masterclass, Rome, Italy
Information: website: <https://forms.ncl.ac.uk/view.php?id=2345860%20>

November 28-29

2nd EURO-NMD annual meeting, Prague, Czech Republic
Information: website: <https://ern-euro-nmd.eu/event/euro-nmd-annual-meeting>

November 30 - December 2

238th ENMC workshop on Cardiac dystrophinopathy. Naarden, NL. Information: website: www.enmc.org

2019

February 5-6

Biospecimen Research Symposium. Berlin, Germany. Information: website: www.isber.org

March 6-8

Advances in skeletal muscle biology in health and disease, University of Florida, Gainesville, FL, US. Information: website: <http://myology.institute.ufl.edu/conferences/muscle-biology-conference>

March 25-28

AFM-Téléthon Scientific Congress in Myology, Bordeaux, France. Information: website: <http://www.afm-telethon.com>

April 4-5

11th Annual Neuromuscular Translational Research Conference, Newcastle, UK. Information: website: <http://www.ucl.ac.uk/cnmd/events>

May 4-10

American Academy of Neurology, 71st Annual Meeting, Philadelphia, PA, US. Information: website: <https://www.aan.com/conferences-community/upcoming-conference-dates>

May 7-10

ISBER 2019. Shanghai, China. Information: website: www.isber.org

May 15-17

Annual Meeting of the French Society for Extracellular Matrix Biology. Reims, France. Information: www.univ-reims.eu; comnco@comnconews.com

May 2019

Heart Rhythm 40th Annual Scientific Sessions (HRS). Chicago, IL. Information: website: <http://www.hrssessions.org>

June 15-18

The European Human Genetics Conference 2019. Gothenburg, Sweden. Information: conference@eshg.org

June 29 - July 2

European Academy of Neurology, 5th Congress, Oslo, Norway. Information: website: <https://www.ean.org/oslo2019/5th-Congress-of-the-European-Academy-of-Neurology-Oslo-2019.3649.0.html>

September 24-28

24th Congress of World Muscle Society. Copenhagen, Denmark. Information: website: www.worldmusclesociety.org

October 22-26

ASHG Annual Meeting. Toronto, Canada. Information: website: www.ashg.org

November 13-15

Third International Conference on Genomic Medicine (GeneMed-2019) in Baltimore, USA

Information: website: <http://unitedscientificgroup.com/conferences/genemed>

To be announced

Asia Pacific Heart Rhythm Society (APHRS). Bangkok, Thailand. Information: website: <http://www.aphrs.org>

2020**April 25 - May 1**

American Academy of Neurology, 72nd Annual Meeting. Toronto, Ontario, Canada.

Information: website: <https://www.aan.com/conferences-community/upcoming-conference-dates/>

June 6-9

The European Human Genetics Conference 2020, Berlin, Germany. Information: conference@eshg.org

October 27-31

ASHG Annual Meeting. San Diego, CA, USA .Information: website: www.ashg.org

To be announced

25th Congress of World Muscle Society. Toronto, Canada. Information: website: www.worldmusclesociety.org

For application or renewal to MSM

MEDITERRANEAN SOCIETY OF MYOLOGY* (MSM)

V. Nigro, *President*
H. Topaloglu, *Past President*
L.T. Middleton, G. Siciliano, *Vice Presidents*
K. Christodoulou, *Secretary*
L. Politano, *Treasurer*

APPLICATION/RENEWAL FORM

Application/Renewal for **1yr** **2 yrs**

Prof. Luisa Politano, Cardiomiologia e Genetica Medica, Primo Policlinico, piazza Miraglia, 80138 Napoli, Italy
Fax: 39 081 5665101 E-mail: actamyologica@gmail.com • luisa.politano@unicampania.it
Fax or Mail to the above address. Type or print.

Name _____ Degree(s) _____
Last First

Department _____

Institution _____

Street Address _____

City, State, zip, country _____

Tel (_____) _____ Fax (_____) _____
Area code Area code

* Amount payable: 1 year Euro 100
2 years Euro 180



I enclose copy of the bank transfer to:

Bank name: Banca Prossima
Bank address: via Toledo 177/178
Account holder: MSM-Mediterranean Society of Myology
IBAN code: IT80J0335901600100000160879
BIC/SWIFT code (for foreign countries): BCITITMX



INSTRUCTIONS FOR AUTHORS

Acta Myologica publishes articles related to research in and the practice of primary myopathies, cardiomyopathies and neuromyopathies, including observational studies, clinical trials, epidemiology, health services and outcomes studies, and advances in applied (translational) and basic research.

Manuscripts are examined by the editorial staff and usually evaluated by expert reviewers assigned by the editors. Both clinical and basic articles will also be subject to statistical review, when appropriate. Provisional or final acceptance is based on originality, scientific content, and topical balance of the journal. Decisions are communicated by email, generally within eight weeks. All rebuttals must be submitted in writing to the editorial office.

On-line submission

Manuscript submission must be effected on line: **www.actamyologica.it** according to the following categories:

Original articles (maximum 5000 words, 8 figures or tables). A structured abstract of no more than 250 words should be included.

Reviews, Editorials (maximum 4000 words for Reviews and 1600 words for Editorials). These are usually commissioned by the Editors. Before spontaneously writing an Editorial or Review, it is advisable to contact the Editor to make sure that an article on the same or similar topic is not already in preparation.

Case Reports, Scientific Letters (maximum 1500 words, 10 references, 3 figures or tables, maximum 4 authors). A summary of 150 words may be included.

Letters to the Editor (maximum 600 words, 5 references). Letters commenting upon papers published in the journal during the previous year or concerning news in the myologic, cardio-myologic or neuro-myologic field, will be welcome. All Authors must sign the letter.

Rapid Reports (maximum 400 words, 5 references, 2 figures or tables). A letter should be included explaining why the author considers the paper justifies rapid processing.

Lectura. Invited formal discourse as a method of instruction. The structure will be suggested by the Editor.

Congress Proceedings either in the form of Selected Abstracts or Proceedings will be taken into consideration.

Information concerning new books, congresses and symposia, will be published if conforming to the policy of the Journal.

The manuscripts should be arranged as follows: 1) Title, authors, address institution, address for correspondence; 2) Repeat title, abstract, key words; 3) Text; 4) References; 5) Legends; 6) Figures or tables. Pages should be numbered (title page as page 1).

Title page. Check that it represents the content of the paper and is not misleading. Also suggest a short running title.

Key words. Supply up to three key words. Wherever possible, use terms from Index Medicus – Medical Subject Headings.

Text. Only international SI units and symbols must be used in the text. Tables and figures should be cited in numerical order as first mentioned in the text. Patients must be identified by numbers not initials.

Illustrations. Figures should be sent in .jpeg or .tiff format. Legends should be typed double-spaced and numbered with Arabic numerals corresponding to the illustrations. When symbols, arrows, numbers, or letters are used to identify parts of the illustrations, each should be explained clearly in the legend. For photomicrographs, the internal scale markers should be defined and the methods of staining should be given.

If the figure has been previously published a credit line should be included and permission in writing to reproduce should be supplied. Colour photographs can be accepted for publication, the cost to be covered by the authors.

PATIENTS IN PHOTOGRAPHS ARE NOT TO BE RECOGNISABLE

Tables. Tables should be self-explanatory, double spaced on separate sheets with the table number and title above the table and explanatory notes below. Arabic numbers should be used for tables and correspond with the order in which the table is first mentioned in the text.

References. Reference numbers in the text must be in brackets. References in the list must be numbered as they appear in the text.

Standard journal article: Figarella-Branger D, Bartoli C, Civatte M, et al. Cytokines, chemokines and cell adhesion molecules in idiopathic inflammatory myopathies. *Acta Myol* 2000;19:207-8.

Books and other monographs: Dubowitz V. *Muscle disorders in childhood*. London: WB Saunders Company Ltd; 1978.

Please check each item of the following checklist before mailing:

- Three index terms, short title for running head (no more than 40 letter spaces) on the title page.
Name(s) of the author(s) in full, name(s) of institution(s) in the original language, address for correspondence with telephone and fax numbers and email address on the second page.
- Summary (maximum 250 words).
- References, tables and figures cited consecutively as they appear in the text.
- Figures submitted actual size for publication (i.e., 1 column wide or 2 columns wide).
- Copyright assignment and authorship responsibility signed (with date) by all Authors.
- References prepared according to instructions.
- English style.
- Patients in photographs not recognisable.